VNIVERSITAT DE VALÈNCIA

FACULTY OF MEDICINE

DEPARTMENT OF BIOCHEMISTRY AND MOLECULAR BIOLOGY

DOCTORATE PROGRAM

030E CLINICAL-MEDICAL BIOCHEMISTRY AND IMMUNOLOGY

HETEROGENEITY OF HUMAN MELANOMA CELL LINES: A QUANTITATIVE STUDY OF PROTEIN AND mRNA EXPRESSION PROFILES USING FLOW CYTOMETRY AND REAL-TIME PCR

PHD THESIS PRESENT BY

SANDRA CRISTINA NORTE PINTO

DIRECTED BY

DR. ROBERT CALLAGHAN PITLIK

DR. JOSÉ ENRIQUE O'CONNOR BLASCO

VALENCIA, OCTOBER 2015

VNIVERSITAT DE VALÈNCIA

FACULTY OF MEDICINE

DEPARTMENT OF BIOCHEMISTRY AND MOLECULAR BIOLOGY

DOCTORATE PROGRAM

030E CLINICAL-MEDICAL BIOCHEMISTRY AND IMMUNOLOGY

HETEROGENEITY OF HUMAN MELANOMA CELL LINES: A QUANTITATIVE STUDY OF PROTEIN AND mRNA EXPRESSION PROFILES USING FLOW CYTOMETRY AND REAL-TIME PCR

PHD THESIS

ORIGINAL WORK PRESENT BY

SANDRA CRISTINA NORTE PINTO

VALENCIA, OCTOBER 2015

VNIVERSITAT DE VALÈNCIA

FACULTY OF MEDICINE

Dr. Robert Callaghan Pitlik (Professor at the University of Valencia) and **Dr. José Enrique O'Connor Blasco** (Professor at the University of Valencia),

CERTIFY:

This work has been carried out entirely by the PhD candidate **Sandra Cristina Norte Pinto** at the Cytomics Laboratory at Prince Felipe Research Centre (Valencia, Spain) under our supervision. Furthermore, we authorise that this PhD thesis is submitted and evaluated by an assigned jury.

Dr. Robert Callaghan Pitlik Dr. José Enrique O'Connor Blasco

Valencia, October 2015

This work was supported by a predoctoral fellowship from Fundação para a Ciência e a Tecnologia (SFRH/BD/40301/2007, Portugal) and financed by POPH – QREN.

Additional funding was provided by the *Fondo de Investigación en Salud* (Carlos III Health Institute, Spain): FIS 07/0805 and FIS 07/1203.

Acknowledgments

My acknowledgment goes to the numerous people that were involved and contributed in many ways to the completion of this thesis.

Firstly I would like to express my gratitude to Enrique and Robert, my scientific advisors, for their support and for sharing their knowledge and ideas with me.

I would like to thank all the people from the Cytomics Laboratory, at CIPF, for their help and friendship during the years we have worked together. A special acknowledgment to Alicia, who taught me almost everything I know in flow cytometry, and for all the helpful brainstorming during this thesis!

I would also like to thank the eco-people at CIDE for always welcoming me so warmly.

A very special thanks goes to all the friends I 've made during the years I've been in Valencia. You made me feel at home, you were (are!) part of my family and I will always carry you in my heart. Now I can only say that I have a lot of *saudades*!

To all of you: Muchas gracias! Moltes gracies!

I would also like to express my gratitude to my supervisor, colleagues and friends at my current lab, for their constant support and for pushing me to finish this thesis.

Finally I would also like to thank all my family, specially my mother Fernanda and my father Alcides for the support they provided me through my entire life and for understanding all my decisions.

Last but not least, I must acknowledge the two most important people in my life (for now, I hope!), Bruno and Nuno Afonso. I could not have done it with out you!!! Bruno, thank you for always showing me that what is essential in life is invisible to the eyes, and also for believing in me (more than I do). Nuno, my little prince, thank you for all your smiles, affections and constant happiness... you are my (our) rose. I must also apologise for all the time this thesis has stolen from us...

"O valor das coisas não está no tempo que elas duram, mas na intensidade com que acontecem. Por isso, existem momentos inesquecíveis, coisas inexplicáveis e pessoas incomparáveis." (Fernando Pessoa)

It always seems impossible until its done.

Nelson Mandela

Index

Abbreviations

FCM	Flow cytometry
FS	Forward scatter
SC	Side scatter
MFI	Mean fluorescence index
PE	Phycoerytrin
PI	Propidium iodide
RT-PCR	Real-time Polymerase chain reaction
RIN	RNA integrity number
MAA	Melanoma associated antigens
CSC	Cancer stem cells
MIC	Melanoma initiating cells
SP	Side population
EMT	Epithelial-to-mesenchymal transition
MET	Mesenchymal-to-epithelial transition

Table Index

Figure Index

Introduction

Melanoma skin cancer

The skin, the biggest human organ, is continuously self-renewing and covers the surface of the body, separating it from the outside world. It provides protection against external agents such as mechanical and chemical aggressions such as heat, infections, water, and electromagnetic radiation. Is divided into two main structural compartments: the epidermis or epithelial component coating on the surface, and the in-depth dermis or connective component of nutrition. Both skin compartments cooperate in the formation of a highly specialized matrix structure, the basement membrane, which physically separates the two compartments, providing a stabilizing and dynamic interface (Proksch *et al.* 2008).

Melanoma is the most aggressive type of skin cancer, which arises from melanocytes, melanin-producing cells located in the bottom layer (the stratum basale) of the skin's epidermis. The highest rates of incidence of melanoma can be found in North America, Australia and part of Europe. From the latest data of the International Agency for Cancer Research regarding 2012, 232.130 new cases of melanoma were detected and 24% of the diagnosed patients died (Ferlay *et al.* 2013).

Cancer can spread through tissue, the lymph system, and the blood. When it spreads through tissue, it starts growing into nearby areas. When cancer cells break away from where they began (the primary tumor) and travel through the lymph system or blood to other parts of the body where they start forming a metastatic tumor, it is called **metastasis**. As for other cancers, the main cause of death in melanoma is the widespread metastasis (Chambers *et*

al. 2002).

Different types of treatment are available for patients with melanoma. Surgery to remove the tumor is the primary treatment of all stages of melanoma. Wide local excision can be performed to remove the melanoma and some of the normal tissue around it. Normally, during surgery the sentinel lymph node (the first lymph node the cancer is likely to spread to from the tumor) is removed and biopsied. A marker (radioactive substance and/or blue dye) is injected near the tumor. The marker flows through the lymph ducts to the lymph nodes and the first lymph node to receive the substance or dye is removed. After evaluating the presence of cancer cells, the pathologist decides if is necessary to remove more lymph nodes or not. Skin grafting (taking skin from another part of the body to replace the skin that is removed) may be done to cover the wound caused by surgery (Essner *et al.* 2004).

Even if all the melanoma is removed in surgery, most patients are offered chemotherapy after surgery to kill any cancer cells that are left. Chemotherapy given after surgery, to lower the risk that the cancer will relapse, is called adjuvant therapy. When chemotherapy is taken by mouth or injected into a vein or muscle, the drugs enter the bloodstream and can reach cancer cells throughout the body (systemic chemotherapy). When chemotherapy is placed directly into the cerebrospinal fluid, an organ, or a body cavity such as the abdomen, the drugs mainly affect cancer cells in those areas (regional chemotherapy, Krementz *et al*. 1994).

Radiation therapy, using high-energy x-rays or other types of radiation to kill cancer cells or keep them from growing, may also be used. There are two types of radiation therapy: external radiation therapy uses a machine outside

the body to send radiation toward the cancer; and internal radiation therapy uses a radioactive substance sealed in needles, seeds, wires, or catheters that are placed directly into or near the cancer (Shuff *et al.* 2010).

Targeted therapy is a type of treatment that uses drugs or other substances to selectively attack cancer cells. Targeted therapies usually cause less harm to normal cells than chemotherapy or radiation therapy do. For example, Vemurafenib and Dabrafenib are signal transduction inhibitors used to treat some patients with advanced melanoma or tumors that cannot be removed by surgery. These drugs block the activity of proteins made by mutated BRAF genes. Angiogenesis inhibitors are also being used to block the growth of new blood vessels that tumors need to grow (Garbe *et al*. 2011)

Immunotherapy is a treatment that uses the patient's immune system to fight cancer. Substances produced by patient's body or made in a laboratory are used to boost, direct, or restore the body's natural defenses against cancer. Interferon, interleukin-2 (IL-2), tumor necrosis factor (TNF) and ipilimumab are commonly used in melanoma. Interferon and TNF affect the division of cancer cells and can slow tumor growth. IL-2 boosts the growth and activity of many immune cells, especially lymphocytes. Ipilimumab is a monoclonal antibody that increases the immune response against melanoma cells. It binds to cytotoxic T-lymphocyte-associated antigen 4 (CTLA-4) and blocks the interaction of CTLA-4 with its ligands, CD80 and CD86 (Garbe *et al.* 2011)

Immunotherapy is a type of systemic therapy used in the treatment of melanoma at high risk for recurrence and metastases; therefore, the characterization of **melanoma associated antigens (MAA)** is of great importance. MAA can be classified according to their expression pattern in

shared (i.e. expressed by different tumors and/or normal tissues) and unique (i.e., expressed only in particular melanomas). Shared MAA can be subdivided in three groups (Parmiani *et al*. 2003): differentiation antigens (proteins expressed both by melanoma cells and normal melanocytes), tumor-specific (proteins expressed by melanoma and other tumors, but not in normal tissues); and over-expressed antigens (generally expressed in normal tissues but over-expressed in melanoma and other tumors).

Examples of differentiation antigens are Melan-A (MART-1 or - Melanoma Antigen Recognized by T-cells), Pmel27 protein from melanocytes (or gp100), tyrosinase (TYR) and the microphthalmia-associated transcription factor (MITF). Although the role of Melan-A and gp100 is not completely understood, Melan-A has recently been found to localize to vesicles, including melanosomes, suggesting a role in melanosome biogenesis; while gp100 localizes to an early melanosome trafficking compartment and may function in melanosome structure, biosynthesis of the melanin intermediate 5,6-dihydroxyindole-2-carboxylic acid (DHICA), or morphogenesis of premelanosomes (Weinstein *et al.* 2014). TYR is involved in the reaction of melanin formation (Hearing 2011). MITF is essential for the development of the melanocyte lineage. Furthermore, it has been shown that transcription of the genes of Melan-A, gp-100 and TYR is regulated by MITF (Du *et al.*, 2003;. Urosevic *et al.*, 2005). Melastatin or TPRM1 is a member of the transient receptor potential superfamily of ion channel proteins, and is important in cell-cycle control and cell survival. It is expressed by nevi and *in situ* melanomas, and its expression is down-regulated in invasive and metastatic melanomas (Hammock *et al.* 2006).

Among the tumor-specific MAA are the members of the MAGE family, such as are MAGE-1 and MAGE-3, which are expressed in normal testis,

but its ectopic expression (i.e., in an abnormal local) is characteristic of malignant transformation (Urosevic *et al.* 2005).

Over-expressed antigens are equally important MAA, which are overexpressed in melanoma. These include the adhesion molecule CD146 (or MCAM - Melanoma cell adhesion molecule; Rapanotti *et al*., 2008) that is normally expressed in the endothelial lineage and Integrin beta-3 or CD61 which is normally expressed on platelets. (Fang *et al*. 2005). It has been shown that patients expressing CD61 are more likely to die or relapse than patients with CD61-negative tumors (Hieken *et al.* 1996) and that CD146 is associated with advanced stages of melanoma (Rapanotti *et al.* 2008). Metalotranferrin (p97) is also overexpressed in melanoma when compared to normal melanocytes (Smith *et al*. 2006). Additionally, the expression of p97 is correlated with tumor vascularization and progression, suggesting a proinvasive function associated with p97 in malignant tumors (Bertrand *et al.* 2006).

Melanoma initiation, growth and heterogeneity

Cancers arise via the acquisition of mutations that suppress senescence and promote cell division, but there are different models to explain cancer growth. The clonal or stochastic model (Nowell 1976) states that (epi)genetic changes occur over time in all tumor cells, and that cells gaining a selective advantage will generate clones that out-compete other clones. Stepwise natural selection of the fittest and most aggressive cells would

facilitate tumor progression in a linear stochastic manner (Nowell 1976). The cancer stem-cell model (Reya *et al.* 2011) suggests that only a subpopulation of cells within the tumor, the cancer stem cells (CSC) or **Melanoma-initiating cells (MIC)** in the case of melanoma, have the capacity to regenerate and maintain a tumor *in vivo*. The bulk of the heterogeneous tumor cell population does not share these properties and lacks the ability to be tumorigenic (Reya *et al.* 2011).

To the moment, MIC have been shown to express the stem cell markers CD133 (Frank *et al.* 2005, Klein *et al.* 2007, Monzani *et al.* 2007, Al Dhaybi *et al.* 2010), CD20 (Fang *et al*. 2005) and ABC transporters, like MDR1, ABCG2 and ABCB5 (Zabierowski and Herlyn 2008a, Monzani *et al.* 2007, Schatton *et al.* 2008, Keshet *et al.* 2008).

MIC also exhibit other stem-cell functional characteristics, like side-population (Zabierowski *et al.* 2008a) and sustain the stem-cell population while giving rise to progenitor cells that may or may not attain the capacity to self-renewing. These progenitor and trans-amplifying cells can give rise to differentiating clones of varying dominance that contribute to the overall tumor heterogeneity found in melanomas. MIC are also thought to play an important role in the cancer metastasis (Visvader *et al.* 2008). Therefore, understanding the biology of MIC is of great importance to the identification of possible molecular targets and development of novel therapies.

CD133 or prominin 1 is a glycoprotein which is found in the protrusions of the plasma membrane of epithelial cells, and is thought to play an important role as organizer of the plasma membrane topology and maintenance of its correct lipid composition (Mizrak *et al.* 2008). It is normally expressed in undifferentiated cells like endothelial progenitor cells, hematopoietic stem

cells and prostate epithelial stem cells, but also in tumor cells of numerous solid tumors like brain, prostate, pancreas and melanoma (Zabierowski and Herlyn 2008b, Al Dhaybi *et al.* 2010).

CD20 is an antigen specific of the mammalian immune system, which has an important function in the development and differentiation of B lymphocytes to plasma cells. It is expressed in B lymphocytes of sane individuals but it has also been found in numerous cancers, like lymphomas, leukemia and melanoma (Fang *et al.* 2005). A recent study, using mouse xenografts, demonstrated the importance of a small subpopulation of melanoma CD20+ cells. Engineered T cells produced to target specifically CD20+ melanoma cells were capable to eradicate established melanoma and significantly improved tumor-free survival (Schmidt *et al.* 2011).

CD34, a characteristic haematopoietic stem cell marker, has also been used, to a smaller extent, for the identification of MICs (Bongiorno *et al.* 2008).

CD90 or thymocyte differentiation antigen 1 (Thy-1) can normally be found in precursor of T cells in the thymus, on the surface of neurons, subsets of fibroblasts, endothelial cells, mesangial cells and some hematopoietic cells (Bradley *et al.* 2009). It plays an important role in the cell-cell and cell-matrix interactions and, in melanoma, also promotes the migration and adhesion of melanoma cells to endothelium (Rege *et al.* 2006). Its over-expression has also been associated to prostate cancer (True *et al.* 2010), hepatocellular carcinoma (Lu *et al.* 2011) and also in spindle cell melanoma (Winnepenninckx *et al*. 2003).

CD117, also known as tyrosine-protein kinase Kit or stem cell growth factor receptor, is normally expressed in subsets of hematopoietic stem cells, germ cells, cajal cells of the gastrointestinal tract, mast cells and melanocytes

(Miettinen *et al*. 2005). Furthermore, CD117-mediated pathways are of great importance in melanocyte physiology, influencing melanogenesis, proliferation, migration, and survival of these cells (Alexeev *et al.* 2006). Mutations in this gene are associated with some cancers like gastrointestinal stromal tumors, mast cell disease, acute myelogenous leukemia, piebaldism and also melanoma (Miettinen *et al.* 2005, Woodman *et al.* 2010).

Nerve growth factor receptor (NGFR) or CD271 was found on melanoma cells. The groups of Boiko and Civenni demonstrated, using different xenotransplantation models, preferential tumor formation by CD271+ melanoma cells isolated from patient samples (Boiko *et al.* 2010, Civenni *et al.* 2011). Furthermore, coexpression of ABCB5 and CD271 was found in clinical melanoma specimens (Frank *et al.* 2011).

Nestin, a class VI intermediate filament protein and TUJ1 (neuronal ßIII Tubulin), which are normally described as neural stem cell markers have also been found in melanoma. Nestin expression has been associated to poor prognosis in melanoma (Piras *et al.* 2009). Normal melanocytes robustly express TUJ1 protein, which tend to decrease with melanoma progression. A poor disease outcome was linked to high TUJ1 expression levels in some cancer types, such as ovary and lung (Akasaka *et al.* 2009).

ABC transporters are transmembrane proteins that use the energy of adenosine-5'-triphosphate (ATP) to translocate solutes through the plasma membrane (Higgins *et al.* 2001). When expressed in non-cancerigenous cells they facilitate the movement of endogenous compounds and contribute to cell detoxification, and when expressed in neoplastic cells they contribute to chemoresistance (Hatina *et al.* 2001, Gottesman *et al.* 2002, Chen *et al.* 2009). In melanoma, ABCB5 has been identified as an important mediator of

chemoresistance and tumor initiation (Frank *et al.* 2005, Schatton *et al*. 2008). Furthermore, it has also been described by the functional characterization of the *side population* (SP), that can be identified by flow cytometry for its capacity of pumping out fluorochromes like Hoechst 33342 (Grichnick *et al.* 2006, Hadnagy *et al.* 2006, Dou *et al.* 2009). The capacity to pump out fluorochromes like Hoechst 33342, which is a functional characteristic of the SP, seems to be correlated with the expression of ABC transporters, and it has been demonstrated that ABCG2 is the transporter which contributes the most for this phenotype (Scharenberg *et al.* 2002). This SP is thought to be enriched in cells with stem cell potential (Hadnagy *et al.* 2006) and it has been found in melanoma (Grichnick *et al*. 2006, Fukunaga-Kalabis *et al.* 2010).

Metastasis and melanoma aggressiveness

A major factor that drives metastasis is the **epithelial-to-mesenchymal transition (EMT),** a process seen in normal embryogenesis and adopted by epithelial cancers and resulting in a more aggressive phenotype (Lee *et al.* 2014). In EMT, polarized epithelial cells lose their associations to the surrounding environment and attain migratory properties of mesenchymal cells. The reversal of EMT, the mesenchymal-to-epithelial transition (MET), is the acquisition of an epithelial-like phenotype, a mechanism by which neoplastic cells colonize target tissues. Both EMT and MET involve differential regulation of cell adhesion and cytoskeletal proteins. EMT is

closely interrelated to the CSC model, as it may have a role in CSC-driven metastasis (Bao *et al.* 2012) For instance, EMT-induced breast cancer cells acquire a stem-like phenotype, and breast CSC isolated from patients have been found to express EMT-associated markers (Charpentier and Martin 2013). There is evidence that EMT may also be an important process underlying melanoma progression. By gene expression profiling, loss of E-cadherin with gain of N-cadherin and osteonectin (SPARC) was significantly associated with development of metastasis (Li *et al.* 2015). Also, overexpression of Snai2, a transcriptional repressor of proteins involved in cell-to-cell adhesion, was found to induce an EMT-like phenotype and promote melanoma cell migration. Likewise elevated levels of the transcription factor Snai1 as well as fibronectin, an expression profile consistent with a mesenchymal phenotype, were associated with increased melanoma metastases *in vivo* (Lee *et al*. 2014).

While normal melanocytes express few cell–cell adhesion receptors of the immunoglobulin gene superfamily of cell adhesion molecules (CAMs), melanoma cells show an increase in expression of melanoma cell adhesion molecule (MCAM/CD146, mentioned above), L1 cell adhesion molecule (L1-CAM, CD171), activated leukocyte cell adhesion molecule (ALCAM, CD166), vascular cell adhesion molecule 1 (VCAM-1, CD106) and intercellular cell adhesion molecule 1 (ICAM-1, CD54) (Haass *et al.* 2005). Casado and co-workers also show that melanoma cell lines express not only adhesion molecules that are likely to favour their interaction with cells of the immune system, but also their interaction with endothelial cells potentially increasing their invasiveness and metastatic capacity (Casado *et al.* 2009)

How the above described metastatic and migratory processes are influenced by chemokine–chemokine receptor engagement is not completely understood, though they may be the result of pleiotropic chemokine-related signaling acting on multiple cancer cell processes. One possible scenario is that chemokine receptor triggering controls selectin ligand and integrin activity on cancer cells in a manner analogous to the chemokine receptor-mediated control of homing receptors on leukocytes. For example, overexpression of CXCR4 or engagement by its ligand, CXCL12, was found to enhance adhesion of melanoma cells to the endothelium and to VCAM (Lee *et al.* 2014).

Chemokines are chemoattractant cytokines which were initially characterized by their important role in leukocyte recruitment during inflammatory and immune responses (Cyster 1999). They act through the interaction with a subfamily of G protein-coupled receptors (Allen *et al.* 2007) and the extent of the cellular response triggered by chemokines depends on the amount of receptor expressed at the plasma membrane, which is a consequence of the balance between endocytic and recycling pathways (Borroni *et al.* 2010). Several studies have shown that chemokines and their receptors are involved in different steps of tumorigenesis, including angiogenesis, tumor growth, invasion and metastasis of many human cancers (Kakinuma *et al.* 2006, Vandercappellen *et al.* 2008).

Chemokines and their receptors are of great importance in the melanoma tumor progression (Richmond *et al.* 2009). The expression of CXCR4 by melanoma cells in primary lesions is significantly associated with the presence of ulceration, increased tumor thickness and higher mortality rate (Longo-Imedio *et al*. 2005). The expression of CXCR3 has been observed in patients with primary invasive cutaneous melanomas and there is a

significant association of CXCR3-positive tumor cell immunostaining with tumor thickness >1 mm (Monteagudo *et al.* 2007).

They play an important role in the process of metastasis as they regulate organ selectivity (Ben-Baruch 2008). They are expressed at specific organs and act on tumor cells, which express the correspondent receptors, inducing their directed migration. Chemokines also improve tumor cell proliferation, survival and adhesion to microvessel walls, helping the process of extravasation into the target tissue (Kulbe *et al*. 2004, Ben-Baruch 2008). Indeed, it has been shown that mouse melanoma B16F10 cells constitutively express CXCR3, and its ligands CXCL9/Mig, CXCL10/IP-10, and CXCL11/I-TAC induce cellular responses in vitro, such as actin polymerization, migration, invasion, and cell survival (Kawada *et al.* 2004). Moreover, the expression of several chemokine receptors has been associated with a greater risk of developing regional and distant metastases (Longo-Imedio *et al.* 2005, Monteagudo *et al.* 2007) as lymph node metastasis (CCR7, Murakami *et al*. 2004; CCR10, Simonetti *et al*. 2006; CXCR3 and CXCR4, Robledo *et al.* 2001), pulmonary metastasis (CXCR4) or skin metastasis (CCR10, Murakami *et al.* 2004). The role in melanoma of the recently discovered CXCR7, which binds to CXCL11 and CXCL12 (Burns *et al*. 2006) is still not clear. However, it has been shown that CXCR7 is involved in tumor cell growth, survival, and metastasis in several tumor types (Sun *et al.* 2010).

Experimental models for melanoma

For most cancer types, including melanoma, **human cancer cell lines** have been one of the mostly used experimental models. They are pure, easily propagated and genetically manipulated while providing reproducible results when used with the same protocol and at the same stage (Staveren *et al.* 2009).

This model has been widely used as a disease-oriented screening model for new anticancer drugs as the need for high throughput and low cost means both for drug discovery and drug development makes human cell lines the most suitable model. Indeed, the panel of cell lines from the National Cancer Institute (NCI60), composed by 60 cancer cell lines established from different types of cancers, has been extensively used since it was developed in the late 1980s, contributing for great advances in cancer chemotherapy (Shoemaker 2006). Similarly, the Japanese Foundation for Cancer Research implemented a smaller panel of 39 cancer cell lines (JFCR39). This panel has 30 cell lines from the NCI60 together with 6 cell lines of stomach cancer for which the incidence is high in Japan, and 3 additional breast cancer cell lines (Kong and Yamori 2012).

Melanoma cell lines are broadly used in immunology and immunotherapy studies. Therefore, it was created a database and cell bank, called ESTDAB (http://www.ebi.ac.uk/ipd/estdab/), which provides a freely available and fully searchable database of highly characterized melanoma-derived cell lines, which have been extensively characterized for HLA genotype and surface expression, oncogene and tumor antigen expression, cytokine secretion, surface molecule expression, adhesion to extracellular matrix

components, cytokine gene polymorphisms and other factors, which allows the researchers to choose the most adequate cell line(s) for their work. (Robinson *et al.* 2009).

Although human cancer lines are so commonly used a major drawback is that often they do not resemble the original tumor from which they were established. This happens because cancer cells in tumors do not proliferate at the same rate as cultured cells. In fact, cultured cells are selected for rapid growth with doubling times much shorter than those of cancer cells in vivo. Most cancer cell lines have been maintained for decades in growth-promoting cocktails, in monolayer as opposed to three-dimensional culture, and in high oxygen tension (21%, whereas physiological oxygen tension ranges from 2% to 5%). These conditions undoubtedly affect the cells' characteristics and select for subpopulations of cells that differ dramatically from the predominant cells of a primary cancer (Gillet *et al.* 2013). Indeed, cell lines derived from metastases of the same melanoma has been shown to be genetically different (Sabatino *et al.* 2008). Thus cell lines derived from one clone cannot be representative of this diversity. Furthermore, the complexity of biological processes often requires *in vivo* analysis, specially in cancer where the microenvironment surrounding the malignant cells is of utmost importance.

To surpass some of these limitations, several mouse melanoma models have been developed which include: (i) xenotransplantation models; (ii) syngeneic transplantation models; and (iii) models involving genetically modified animals (Becker *et al.* 2010). The relevance of each particular model depends on how closely it represents the genetic and epigenetic aberrations, histology, physiological effects and metastatic pattern observed in human melanoma. Although genetically modified mice have been helpful in leading

to a better understanding of the molecular mechanisms involved in tumor initiation and are currently receiving most of the attention, they have been less successful in modeling advanced metastatic cancer (Larue and Beermann 2007).

Metastases are the main determinants of the clinical course of melanoma and patient survival, and are thus the target of systemic therapy. Human melanoma metastasizes preferentially into lymph nodes, lung, liver or brain. In this regard, xenotransplantation models, based on immunocompromised mice, are particularly successful in mimicking advanced, metastatic melanoma as their diminished ability to mount an effective immune response allows the growth of human melanomas and the expression of malignant properties (such as preferential colonization of certain organs, Zaidi *et al.* 2008). However, in these models, the role of the immune system, either fighting or promoting cancer, is not considered at all. Nevertheless, there are some types of immunocompromised mice, like the **athymic nude mice**, that are not severely immunocompromised, they lack T cells but the B cells, dendritic cells and granulocytes are all relatively intact, and there is a compensatory increase in both natural killer (NK)-cell activity and tumoricidal macrophages in these mice. Then, it is expectable that, by the time these metastatic lesions are surgically removed or biopsied, the tumor has already escaped immune surveillance and cell killing by the immune cells.

Tools for cell and molecular biology research

Flow cytometry (FCM) measures optical and fluorescence characteristics of single cells (or any other particle, including nuclei, microorganisms, chromosome preparations, and latex beads). Physical properties, such as size (represented by forward angle light scatter) and internal complexity (represented by right-angle scatter) can resolve certain cell populations. Fluorescent dyes may bind or intercalate with different cellular components such as DNA or RNA. Additionally, antibodies conjugated to fluorescent dyes can bind specific proteins on cell membranes or inside cells. When labeled cells are passed by a light source, the fluorescent molecules are excited to a higher energy state. Upon returning to their resting states, the fluorochromes emit light energy at higher wavelengths. The use of multiple fluorochromes, allows several cell properties to be measured simultaneously. Furthermore, FCM can be used in some systems (cell sorters) to physically separate individual cells or particles according to their properties. Consequently, FCM is unique in that multiple biological parameters can be quantified simultaneously on a single-particle basis, while up to thousands of events per second may be examined. As a result, large and heterogeneous cell populations are described based on the biometric properties of their individuals (O'Connor *et al.* 2001).

For all stated above, FCM has evident advantages over other conventional techniques of cellular biology and biochemical analysis methodologies (like western blot and immunocytochemistry techniques), specially for quantifying surface protein expression. Very importantly, FCM is a single cell based quantification and proteins located at the cell surface remain intact

as there is no need neither to lyse the cells to extract all the proteins, nor to fix and/or permeabilize the cells. This is of extreme importance to the study of characteristic surface markers in oncology research.

Polymerase chain reaction (PCR)-based techniques, namely real-time PCR, are also very powerful, sensitive and important for cancer research as they allow the acquisition of genetic information through the specific amplification of nucleic acid sequences starting with a very low number of target copies. This quantification of gene expression by malignant cells is of paramount importance to investigate gene patterns responsible for cancer development, progression and response/resistance to treatment but also to understand the heterogeneity of these complex systems (Mocellin *et al.* 2003).

Hypothesis and Objectives

Human melanoma is a highly heterogeneous cancer constituted by subpopulations of tumoral cells with distinct phenotypes. These subpopulations grant the biological complexity responsible for phenomena of self-renewal, tumor initiation, differentiation, progression and resistance to therapy. In this context we propose the following **hypothesis**:

- Human melanoma cell lines established from primary and metastatic tumors from different locations will allow us to determine the intra- and inter-tumoral heterogeneity of melanoma by profiling the protein and gene expression using the quantitative techniques of flow cytometry and real-time PCR.

- Xenotransplantation of human melanoma cell lines into athymic nude mice will allow us to obtain an *"in vivo culture"* and assess the dynamic variations of protein and gene expression after this selective pressure.

To validate these hypotheses, the following **objectives** are proposed:

- Characterize phenotypical and functionally human melanoma cell lines established from primary and metastatic tumors, through the quantification of protein and gene expression, of melanoma associated antigens, cancer stem cell markers, pluripotency stem markers, EMT markers and chemokines their receptors. using flow cytometry and real-time PCR.

- Understand the dynamic variations of the gene and protein expression profiles after xenotransplantion of the human melanoma cell lines into athymic nude mice.

- Correlate the data with the origin of the melanoma (primary or metastasis).

Methodology

1. Biological Samples

Established Melanoma Cell lines

Thirteen established human melanoma cell lines were used, five established from primary tumors and eight established from metastases at different locations (Table 1). In addition, the human T lymphoma Hut-78 cell line was also included in this study as it also expresses some of the chemokine receptors studied (Notohamiprodjo et al 2005).

Table 1. List of tested cell lines, tumor type, origin and source. DSMZ – German Resource Centre for Biological Material, ECACC – European Collection of Cell Cultures, ATCC - American Type Culture Collection, Dept. Pathology – Department of Pathology, University of Valencia, Valencia, Spain).

Tumor	*Cell line*	*Origin*	*Source*
Melanoma	IPC-298	Primary	DSMZ
	Mel-Juso	Primary	DSMZ
	Mel-HO	Primary	DSMZ
	IGR-39	Primary	DSMZ
	WM-115	Primary	ECACC
	A-375	Skin metastasis	ATCC
	MeWo	Lymph node metastasis	ATCC
	SK-Mel 28	Skin metastasis	ATCC
	Malme-3M	Lung metastasis	ATCC
	SK-Mel 2	Skin metastasis	ATCC
	WM-266.4	Skin metastasis(1)	ECACC
	IGR-37	Lymph node metastasis(2)	DSMZ
	Mel-RC08 §	Brain metastasis	Dept. Pathology
Human T-cell	Hut-78	Primary	ECACC

(1) Established from the same patient as cell line WM-115
(2) Established from the same patient as cell line IGR-39
§ Gil-Benso R. et al., Hum Cell. 2012 Jun;25(2):61-7.

Human tumor xenografts and derived cell lines

The primary WM-115 and the metastatic WM-266.4 cell lines, established from the same patient, were inoculated into 4-6 weeks old BALB/c athymic nude mice (Charles River, Spain). Each mouse was inoculated with 200 µl containing $2x10^6$ cells. Due to different growth rates of the tumors, the animals inoculated with WM-266.4 were sacrificed 35 days after inoculation and the ones inoculated with WM-115 were sacrificed 77 days after inoculation. Tumors were extracted and disaggregated using 0.02% collagenase type II (Sigma-Aldrich). Cells were resuspended in culture medium. A sub-sample was immediately used in the flow cytometry experiments (hereafter referred as xenografts WM-115-X and WM-266.4-X) and the remaining were maintained in culture, in order to establish new cell lines after xenotransplantation. Five cell lines were obtained from different xenografts of WM-115 and six cell lines were derived from distinct xenografts of WM-266.4. These modified cell lines were named WM-115-CX and WM-266.4-CX (CX stands for cultured xenografts). All the human tumor xenografts and derived cell lines were obtained from the Department of Pathology, University of Valencia.

Culture conditions

All melanoma cell lines grew as a monolayer, attached to a plastic substrate while Hut-78 grew in suspension. All cultures were grown and maintained in 75 cm^2 flasks, at 37ºC, in a humidified atmosphere with 5% CO2 using RPMI 1640 medium, supplemented with 10% fetal bovine serum inactivated by heat, 2 mM L-glutamine, 100 UI/mL penicillin and 100 µg/mL streptomycin sulfate (Invitrogen).

2. Flow Cytometry

Antibodies and fluorochromes

All monoclonal antibodies (mAbs) against chemokine receptors were conjugated to phycoerytrin (PE). mAbs against CXCR3, CXCR4, CCR7 and their corresponding isotypic controls were purchased from BD Biosciences. mAbs against CXCR7 and CCR10 and their corresponding isotypic isotypic controls were purchased from R&D Systems. All chemokine ligands (CXCL9, CXL10, CXCL11, CXCL12, CCL19, CCL21, CCL27 and CCL28) were detected using primary mouse-anti-human mAbs with a secondary goat anti-mouse antibody labeled with FITC (R&D Systems).

For the detection of melanoma biomarkers, mAbs against CD61, CD146 and the corresponding isotypic isotypic controls were purchased from Beckman-Coulter. Unconjugated antibody against Melan-A, purchased from Santa Cruz Biotechnology, was detected using a secondary goat-anti-mouse antibody labeled with FITC (R&D Systems).

For the detection of CSC and EMT biomarkers, mAbs against CD20, CD90, CD34, CD117 and their corresponding isotypic controls were purchased from Beckman-Coulter. mAbs against CD271, N-Cadherin, TUJ1 and their corresponding isotypic controls were purchased from BD Pharmingen. mAbs against ABCG2, E-Cadherin, Nestin and correspondent isotypic control were purchased from R&D Systems. mAb against CD133 and correspondent isotypic control were purchased from Mylteni Biotec. Unconjugated ABCB5, was purchased from Santa Cruz and was detected using a secondary donkey-anti-goat antibody labeled with FITC (R&D Systems).

The location of the studied proteins (i.e cell surface or intracellular) and the conditions used for their detection (type and volume of antibodies, time and temperature of incubation and cytometer settings) are described in Table 2A and B.

The DNA intercalating fluorochromes Hoechst 33342, propidium iodide (PI) and 7-Aminoactinomycin D (7-AAD) were purchased from Sigma-Aldrich.

Quantification of proteins with cell surface expression

Cells at subconfluency (50–70%) were detached either with 2 mM EDTA in PBS (for the detection of chemokine receptors) or with accutase solution (for the detection of melanoma, CSC and EMT biomarkers, Sigma-Aldrich), washed and resuspended in culture medium at 10^6 cells/ml. Subsequently, 100 µl of this cell suspension were incubated with each of the mAbs and correspondent isotypic controls and with the unconjugated primary antibody for ABCB5 (using secondary antibody alone as control), according to Tables 2A and 2B. After incubation, cells stained with conjugated antibodies were washed with ice-cold PBS and resuspended in 500 µl of culture medium for flow cytometric analysis. Cells stained with unconjugated ABCB5 were further stained with secondary antibody for 30 min, washed twice and resuspended in 500 µl of culture medium for flow cytometric analysis with a FC500 MCL flow cytometer (Beckman-Coulter). Additionally, when quantifying chemokine receptor expression, 3 µg/ml 7-AAD was added to the cell suspension in order to discriminate dead cells.

Table 2A Proteins detected by flow cytometry, their location in cells (Loc. - location in cells; CS – cell surface, I – intracellularly), and type of antibodies used for their detection.

Protein	***Type***	***Loc.***	***Antibodies for detection***
CXCR3	Chemokine receptors	CS/I	Mouse anti-human mAb-PE
CXCR4			
CXCR7			
CCR7			
CCR10			
CXCL9	Chemokines	I	Mouse anti-human mAb + Goat anti-mouse IgG - FITC
CXCL10			
CXCL11			
CXCL12			
CCL19			
CCL21			
CCL27			
CCL28			
Melan-A	Melanoma antigens	I	Mouse anti-human mAb + Goat anti-mouse IgG - FITC
CD61		CS	Mouse anti-human mAb-PE-Cy7
CD146			Mouse anti-human mAb-PE
CD20	CSC	CS	Mouse anti-human mAb-FITC
CD34			Mouse anti-human mAb-PE-Cy5
CD90			Mouse anti-human mAb-PE-Cy5
CD117			Mouse anti-human mAb-PE-Cy5
CD133			Mouse anti-human mAb-APC
CD271			Mouse anti-human mAb-Alexa647
ABCB1			Mouse anti-human mAb-PE
ABCB5			Goat anti-human mAb + Donkey anti-goat IgG - FITC
ABCG2			Mouse anti-human mAb-PE
Ecad			Mouse anti-human mAb-PE
Ncad			Mouse anti-human mAb-Alexa488
Nestin		I	Mouse anti-human mAb-PE
TUJ1			Mouse anti-human mAb-FITC

Table 2B. Proteins detected by flow cytometry and conditions for their detection (volume of antibodies used, time and temperature - Temp. of incubation, and cytometer setting for their detection). RT: room temperature.

Protein	***Antibody Volume (µl)***	***Incubation Conditions***		***Cytometry Settings***	
		Temp.	***Time (min)***	***Excitation (nm)***	***Emission (nm)***
CXCR3	5	Ice	30	488	575±20
CXCR4					
CXCR7					
CCR7					
CCR10					
CXCL9	1				525±20
CXCL10					
CXCL11					
CXCL12					
CCL19					
CCL21					
CCL27					
CCL28					
Melan-A	5	RT	60	488	525±20
CD61	5				785±20
CD146	4				575±20
CD20	10			488	525±20
CD34	10				675±20
CD90	10				675±20
CD117	2				675±20
CD133	2			633	675±20
CD271	5				
ABCB1	2			488	575±20
ABCB5	5				525±20
ABCG2	10				575±20
Ecad	5				575±20
Ncad	5				525±20
Nestin	5				575±20
TUJ1	5				525±20

Quantification of proteins with intracellular expression

Cells at subconfluency (50–70%) were detached either with 2 mM EDTA in PBS (for the detection of chemokine and their receptors) or with accutase solution (for the detection of melanoma and CSC biomarkers). Afterwards, cells were washed with PBS, fixed with 4% paraformaldehyde and permeabilized with 0.1% Triton/PBS adjusting cell suspension to 10^6 cells/ml. Then, 100 µl of this cell suspension was incubated with each of the conjugated mAbs and the correspondent isotypic controls and with the unconjugated primary antibodies (using secondary antibody alone as control), according to Tables 2A and 2B. After incubation, cells stained with conjugated antibodies were washed with ice-cold PBS and resuspended in 500 µl of ice-cold 1% BSA/PBS for flow cytometric analysis with a FC500 MCL flow cytometer. Cells stained with unconjugated antibodies were further stained with secondary antibodies for 30 min, washed twice and resuspended in 500 µl of ice-cold 1% BSA/PBS for flow cytometric analysis with a FC500 MCL flow cytometer (Beckman Coulter).

Chemokine secretion

The quantification of the secretion levels of chemokine was performed in cell culture medium collected after 24 h of sub-culturing the cells, using the commercial multiplex kits *MILLIPLEX™ Multi-Analyte Profiling (MAP)* (Millipore) according to manufacturer instructions (Table 3). Furthermore, the secretion of IL-8, Gro and MCP-1 was quantified, as a positive control of the melanocytic function (Payne and Cornelius, 2002). The samples were subsequently analyzed using Luminex 100™ System (Luminex Coorporation). Briefly, this multiplex technology uses 5.6 micron polystyrene microspheres which are internally dyed with red and infrared

fluorophores. The combination of different intensities of these dyes allows the generation of 100 different microsphere sets, each one of them characterized by a unique spectral signature determined by its red/infrared blend. Each set of microspheres is coated with a specific antibody against an analyte of interest (which in this case are different proteins). These allow the quantification of up to 100 analytes in a single reaction tube. After the sample has been incubated with the microspheres it is allowed to react with a biotinylated antibody against the analyte of interest, and finally, this is incubated with streptavidin conjugated to PE, whose fluorescence is measured to quantify the analyte of interest.

Table 3 *Milliplex*™ Multi-Analyte Profiling (MAP) kit and quantified analytes.

Milliplex™ MAP kit	***Quantified Analytes***
Human cytokine panel I	CXCL10/IP-10 CCL2/MCP-1 CXCL8/IL-8 CXCL1-3/GRO
Human cytokine panel II	CXCL12 CCL21 CCL27
Human cytokine panel III	CXCL9 CXCL11 CCL19

All protein quantifications (i.e. protein expression and secretion) were performed 24 h after sub-culturing, using cells with identical culture conditions. Furthermore, the quantification of cell surface expression of chemokine receptors and intracellular expression of chemokines and their receptors was performed in the same day.

Detection of the Side Population

Cells at subconfluency (50–70%) were detached with 2 mM EDTA in PBS, washed and resuspended at 10^6 cells/ml in culture medium supplemented with 10mM HEPES. Subsequently, cells were stained with 5 µg/ml Hoecsht 33342 for 90 min at 37ºC in the dark and constant agitation (in a water bath), in the presence or absence of 50 µM verapamil (ABCB1 inhibitor, Sigma-Aldrich) or 10 µM fumitremorgin C (ABCG2 inhibitor, Sigma-Aldrich). After incubation, cells were centrifuged at 4ºC and resuspended in cold culture medium supplemented with 10 mM HEPES. To exclude dead cells from the analysis, 5 µg/ml of PI was added prior to the analysis with a MoFlo Legacy high speed cell sorter (Beckman-Coulter).

Instrument settings

FC500 MCL Flow Cytometer

This standard instrument is equipped with an air-cooled argon ion laser (488 nm, 15mW) and a red Helium - Neon, laser (633nm, 20mW) for sample excitation. For detection the cytometer is equipped with two light scatter detectors that measure the forward scatter (FS, an estimation of cell size) and the side scatter (SC, an estimation of intracellular granularity/complexity), and five photomultiplier tubes that detect the appropriately filtered light. FITC and Alexa488 fluorescence were collected at emission values of 525±20nm, PE at 575±20nm, PE-Cy5, APC, Alexa647 and 7-AAD at 675±20nm, and PE-Cy7 at 785±20nm, all using a logarithmic amplification. When analyzing the cell surface expression of chemokine receptors all measurements were restricted to live cells by gating the cells that excluded 7-AAD whilst when analyzing the rest of the proteins the population was selected based on forward and side scatter parameters.

MoFlo high speed cell sorter

This cell sorter is equipped with a water cooled Enterprise II laser (488nm and 351nm, 30 mW). Cell morphology was analyzed with two light scatter detectors that measure the forward scatter (FS, estimation of cell size) and the side scatter (SC, estimation of intracellular granularity/complexity). Hoechst 33342 blue and red fluorescences were detected with the photomultipliers 405±30 nm and 670±20 nm, respectively, using a linear scale. PI was detected at 613±20 nm with logarithmic amplification.

A biparametric plot of FS and PI fluorescence was used to select live cells (PI negative). Then, gating in the live cells, a biparametric plot of Hoechst 33342 blue and red fluorescences was used to assess the dye efflux characteristic of the SP. For the correct identification of this subpopulation, cells were also analyzed in the presence of ABCB1 and ABCG2 inhibitors (verapamil and fumitremorgin C, respectively) to demonstrate that the SP disappeared by blocking Hoecsht 33342 efflux.

Luminex 100™ System

This instrument is equipped with two lasers, a classification laser (635 nm, 25 mW), to excite the red and infrared internal dyes of the microspheres allowing their identification/classification (i.e. which analyte is being measured), and a reporter laser (532 nm, nominal output 10-15 mW, maximun 500 mW,) to excite PE allowing the quantification of each analyte. For fluorescence detection, the instrument is equipped with a classification detector and doublet discriminator composed by avalanche photo diodes with temperature compensation, and a reporter detector composed by a photomultiplier tube, with a detection bandwidth of 565 – 585 nm.

3. Real-time PCR

RNA isolation

Established and tranfected cell lines. $2.5x10^5$ cells/well were seeded in 24 well plates and left in culture for 24 h. RNA was then extracted using RNeasy Micro kit (Qiagen) according to manufactures instructions.

Cultured xenografts cell lines. $2.5x10^5$ cells were detached, centrifuged and resuspended in 1000µl of RNAprotect cell reagent (Qiagen). Samples were kept at -20ºC until they were processed using RNeasy Micro Kit according to manufacture instructions.

After RNA isolation all samples were kept at -80ºC until used.

RNA quality control: yield, purity and integrity

Three quality controls were performed on isolated RNA to determine the quantity (i.e. yield), purity and integrity of RNA that had been isolated. RNA quantity and purity were determined using NanoDrop® ND-1000 UV-Vis Spectrophotometer (Thermo Fisher Scientific), which scans the absorbance from 200 nm to 350 nm, which is the relevant region for determining RNA concentration and purity. RNA has its absorption maximum at 260 nm and the ratio of the absorbance at 260 and 280 nm is a standard measurement to assess the RNA purity. RNA purity is considered acceptable when the ratio A260/A280 is within the range 1.8-2.0. To evaluate RNA integrity, samples were processed with Eukaryote RNA 6000 Nano Labchip kit and analysed with Agilent 2100 Bioanalyzer (Agilent Technologies). RNA samples were separated using electrophoretic separation on microfabricated chips and

subsequently detected via laser induced fluorescence detection. The bioanalyzer software generates an electropherogram and gel-like image that provides a detailed visual assessment of the RNA sample and displays results such as sample concentration and ribosomal ratio. Most importantly, the software provides a user independent measurement of RNA integrity, the RNA integrity number (RIN), which was employed to select RNA samples used in downstream applications. Although is common to accept a RIN above 5 (Derveaux et al 2010), in this study all RNAs were selected when samples had RIN>8 (Figure 1).

Two-step Real Time PCR

1. Reverse transcription

RNA was reverse transcribed using QuantiTec Reverse Transcription Kit (Qiagen) according to manufacture instructions (Table 4). Briefly, prior to reverse transcription, RNA was incubated for 2 min at 42ºC with a buffer to eliminate genomic DNA contamination. After this procedure, the RNA sample was ready for reverse transcription, which was done using a master mix prepared from Quantiscript Reverse Transcriptase, Quantiscript RT Buffer (containing dNTPs and Mg^{2+}), and RT Primer Mix (blend of oligo-dT and random primers). The entire reaction was performed at 42°C and afterwards inactivated at 95°C.

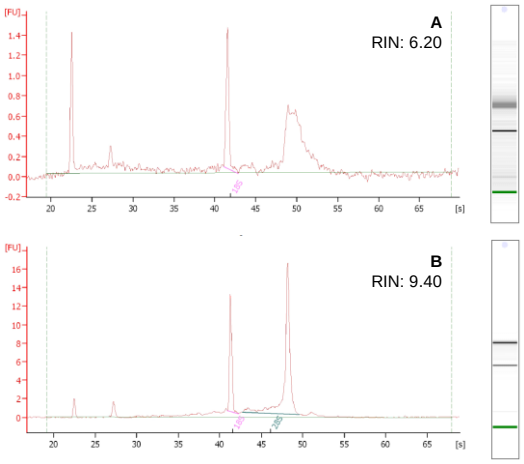

Figure 1. Examples of isolated RNA excluded and included in the gene expression study for having RIN<8 (A) and RIN>8 (B), respectively.

Table 4. cDNA synthesis with integrated removal of genomic DNA contamination: reverse transcription conditions using QuantiTec Reverse Transcription Kit (reaction components and incubations).

Step	Component	Volume (µl)/reaction	Incubation (Time, Temp)
I) Genomic DNA Elimination	gDNA Wipeout Buffer, 7x	2	2min, 42ºC
	Template RNA	Variable (1µg)	
	RNase-free water	Variable	
	Total volume	*14*	
II) Reverse Transcription	Quantiscript Reverse Transcriptase *	1	15min, 42ºC 3min, 95ºC
	Quantiscript RT Buffer, 5x §	4	
	RT primer mix ǂ	1	
	Template RNA	Entire reaction from step I (14)	
	Total volume	*20*	

* Contains RNase inhibitor; § Includes Mg2+ and dNTPs; ǂ Composed by a blend of oligo-dT and random primers

2. Relative quantification of gene expression by real time PCR (RT-PCR)

RT-PCR reactions were carried out with 50 ng template cDNA, QuantiTec primers specific for each gene quantified (Table 5) and 1X QuantiTect SYBR Green PCR Master Mix (Qiagen), according to Table 6. Non-template control reactions were performed for each gene, in order to evaluate unspecific amplification. Reactions were performed in a LightCycler® 480 Real-Time PCR System (Roche Applied Science) using the cycling conditions shown in Table 7. Melting curve analysis of the PCR products was performed in the end of each experiment to verify their specificity and identity, and discard the formation of primer dimers.

RT-PCR Analysis

RT-PCR results were analysed using LightCycler® 480 Software, release 1.5.0, v. 1.5.0.39 (Roche) and Ct values were extracted using the fit point analysis method.

A critical step for an accurate quantification of gene expression is the normalization of the results to a fixed reference; that is, one that is not affected by the experimental conditions. Although normalizing against one constitutively expressed housekeeping gene is the most common method, there is no universal reference gene that is constant in all experimental conditions. Therefore, we performed RT-PCR measurements of six different housekeeping genes, ACTB, B2M, GAPDH, PGK1, RPL13A and RRN18S, with all samples and then analysed the results with geNorm software (PrimerDesign). This software ranks the housekeeping genes according to their stability within the samples tested and recommends the optimal number of housekeeping genes to be used for optimal normalization (Vandesompele

et al 2002). For each data set analysed the most stable housekeeping genes were chosen. For comparison of relative gene expression of chemokine and chemokine receptors between the different melanoma cell lines and Hut-78, RPL13A, RRN18S, ACTB and PGK1 were used in the analysis (Figure 2); for the analysis of the transfected cell lines RRN18S, B2M and GAPDH were used; for the analysis of the xenotransplants RRN18S, PGK1, ACTB and RPL13A were used; and for all other analysis RRN18S, PGK1, ACTB, RPL13A and B2M were used.

For comparison of relative gene expression between the different melanoma cell lines, ΔCt was calculated as follows:

$$\Delta Ct_{(sampleA)} = [(\text{Mean } Ct_{[\text{gene of interest}]} - \text{GeometricMean } Ct_{[\text{HouseKeepings}]})_{(\text{sample A})}]$$

RNA from healthy skin (Agilent Technologies) was also quantified.

When analysing transfected cell lines or the cell lines obtained after xenotransplantation, the original cell line was used as calibrator sample, and therefore, $2^{-\Delta\Delta Ct}$ method was used (Livak & Schmittgen 2001), where:

$$\Delta\Delta Ct_{(sampleA)} = [(\text{Mean } Ct_{[\text{gene of interest}]} - \text{GeometricMean } Ct_{[\text{HouseKeepings}]})_{(\text{sample A})}] - [(\text{Mean } Ct_{[\text{gene of interest}]} - \text{GeometricMean } Ct_{[\text{HouseKeepings}]})_{(\text{calibrator sample})}]$$

Table 5. Genes quantified by RT-PCR using Quantitec Primer Assays (Qiagen).

Oficial Symbol	Oficial Gene Name	Catalog Number	Detected transcript (GenBank ID)
CXCR3	chemokine (C-X-C motif) receptor 3	QT00213493	NM_001504
CXCR4	chemokine (C-X-C motif) receptor 4	QT00223188	NM_001008540
CXCR7	chemokine (C-X-C motif) receptor 7	QT00069650	NM_020311
CCR7	chemokine (C-C motif) receptor 7	QT01666686	NM_001838
CCR10	chemokine (C-C motif) receptor 10	QT00034783	NM_016602
CXCL9	chemokine (C-X-C motif) ligand 9	QT00013461	NM_002416
CXCL10	chemokine (C-X-C motif) ligand 10	QT01003065	NM_001565
CXCL11	chemokine (C-X-C motif) ligand 11	QT02394644	NM_005409
CXCL12	chemokine (C-X-C motif) ligand 12	QT00087591	NM_000609
CCL19	chemokine (C-C motif) ligand 19	QT01157359	NM_006274
CCL21	chemokine (C-C motif) ligand 21	QT01157366	NM_002989
CCL27	chemokine (C-C motif) ligand 27	QT00231399	NM_006664
CCL28	chemokine (C-C motif) ligand 28	QT01673287	NM_019846
MITF	microphthalmia-associated transcription factor	QT00037737	NM_000248
PMEL	premelanosome protein	QT00016149	NM_006928
MLANA	melan-A	QT00028364	NM_005511
MCAM	melanoma cell adhesion molecule	QT00079842	NM_006500
TPRM1	transient receptor potential cation channel, subfamily M, member 1	QT00031087	NM_002420
MFI2	antigen p97 (melanoma associated)	QT00034174	NM_005929
MAGEA1	melanoma antigen family A, 1	QT01669430	NM_004988
MAGEA3	melanoma antigen family A, 3	QT01841224	NM_005362
ITGB3	integrin, beta 3 (platelet glycoprotein IIIa, antigen CD61)	QT00044590	NM_000212
TYR	tyrosinase (oculocutaneous albinism IA)	QT00080815	NM_000372

Oficial Symbol	Oficial Gene Name	Catalog Number	Detected transcript (GenBank ID)
ABCB1	ATP-binding cassette, sub-family B (MDR/TAP), member 1	QT00081928	NM_000927
ABCG2	ATP-binding cassette, sub-family G (WHITE), member 2	QT00073206	NM_004827
ABCB5	ATP-binding cassette, sub-family B (MDR/TAP), member 5	QT00049448	NM_178559
PROM1	prominin 1	QT00075586	NM_006017
CD44	CD44 molecule (Indian blood group)	QT00073549	NM_000610
KIT	v-kit Hardy-Zuckerman 4 feline sarcoma viral oncogene homolog	QT01679993	NM_000222
CD34	CD34 molecule	QT00056497	NM_001773
NES	nestin	QT01015301	NM_006617
TUBB3	tubulin, beta 3 class III	QT00083713	NM_006086
CDH1	cadherin 1, type 1, E-cadherin (epithelial)	QT00080143	NM_004360
CDH2	cadherin 2, type 1, N-cadherin (neuronal)	QT00063196	NM_001792
NGFR	nerve growth factor receptor	QT00056756	NM_002507
VIM	vimentin	QT00095795	NM_003380
THY1	Thy-1 cell surface antigen	QT00023569	NM_006288
NANOG	Nanog homeobox	QT01844808	NM_024865
CASP3	caspase 3, apoptosis-related cysteine peptidase	QT00023947	NM_004346
EPCAM	epithelial cell adhesion molecule	QT00000371	NM_002354
DPPA5	developmental pluripotency associated 5	QT00205968	NM_001025290
SOX2	SRY (sex determining region Y)-box 2	QT00237601	NM_003106
MYC	v-myc myelocytomatosis viral oncogene homolog (avian)	QT00035406	NM_002467
ALCAM	activated leukocyte cell adhesion molecule	QT00026824	NM_001627
KITLG	KIT ligand	QT00000693	NM_000899
TNC	Tenascin C	QT00024409	NM_002160
CTNNB1	catenin (cadherin-associated protein), beta 1, 88kDa	QT00077882	NM_001904

Oficial Symbol	Oficial Gene Name	Catalog Number	Detected transcript (GenBank ID)
VCAM1	vascular cell adhesion molecule 1	QT00018347	NM_001078
SPARC	secreted protein, acidic, cysteine-rich (osteonectin)	QT00018620	NM_003118
NCAM1	neural cell adhesion molecule 1	QT00071211	NM_000615
FN1	fibronectin 1	QT00038024	NM_212474
SPP1	secreted phosphoprotein 1	QT01008798	NM_000582
SNAI2	snail homolog 2 (Drosophila)	QT00044128	NM_003068
SNAI1	snail homolog 1 (Drosophila)	QT00010010	NM_005985
ACTB	actin, beta	QT01680476	NM_001101
B2M	beta-2-microglobulin	QT00088935	NM_004048
GAPDH	glyceraldehyde-3-phosphate dehydrogenase	QT01192646	NM_002046
PGK1	phosphoglycerate kinase 1	QT00013776	NM_000291
RPL13A	ribosomal protein L13a	QT00089915	NM_012423
RRN18S	18S ribosomal RNA	QT00199367	X03205

Table 6. Reaction setup for two-step RT-PCR using Quantitec Primer Assays and 50ng of template cDNA.

Component	***Volume (µl)***
2x QuantiTect SYBR Green PCR Master Mix*	12.5
10x QuantiTect Primer Assay	2.5
Template cDNA	1
RNase-free water	9
Total volume	*25*

* Provides a final concentration of 2.5 mM MgCl2.

Table 7. Cycling conditions for relative quantifications of gene expression using RT-PCR with LightCycler® 480 Real-Time PCR System.

Step	***Time***	***Temperature***	***Notes***
PCR initial activation step	15 min	95°C	This step activates HotStarTaq DNA Polymerase
3-step cycling:			
i. Denaturation	15 s	94°C	
ii. Annealing	30 s	55°C	
iii. Extension	30 s	72°C	Perform fluorescence data collection
Number of cycles	45 cycles		

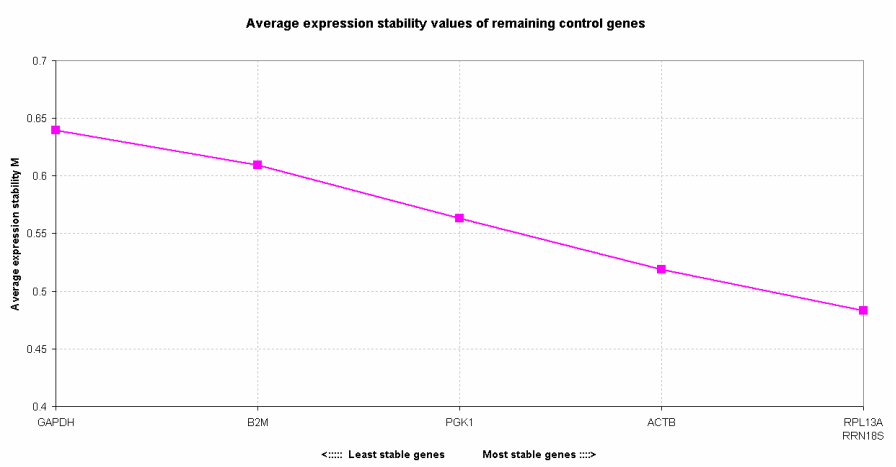

Figure 2. Example of the housekeeping genes expression stability determined by GeNorm analysis, for the analysis of chemokine and chemokine receptors in melanoma cell lines and Hut-78. For this data set the software recommended the use of the 4 most stable genes (RPL13A, RRN18S, ACTB and PGK1).

4. Transfected cell lines

Plasmids

cDNAs for CXCR3 and CXCR4 cloned into the vector pcDNA3.1+ were obtained from the cDNA Resource , University of Missouri (www.cdna.org), and the vector alone was obtained from Invitrogen. This vector contains the genes for ampicillin and neomycin resistance and can therefore, be propagated in *E. coli* strains and used for the production of stably transfected mammalian cell lines.

Bacterial transformation

One shot® TOP10 chemically competent *E. coli* (Invitrogen) were mixed with approximately 40ng of plasmid and submitted to a heat shock (30 min on ice, 42 s at 42ºC, in a thermoblock, and finally 2 min on ice). Afterwards, 1 ml of lysogeny broth (LB) medium was added to each tube and incubated for 1 h at 37ºC. Cells were then centrifuged, resuspended in 200 µl of LB containing 100 µg/ml ampicillin, plated in 100 mm culture dishes containing LB agar with ampicillin, and left overnight at 37ºC.

Plasmid "pre-amplification"

Isolated colonies were picked using a small sterile tip and incubated in 5 ml of LB with ampicillin at 37ºC with constant stirring. Prior to plasmid amplification the output of the transformation was evaluated. DNA of the transformed bacteria was extracted using High Pure Plasmid Isolation kit (Roche) according to the manufacture instructions and quantified using NanoDrop®. Afterwards, 100 ng of each DNA (pcDNA3.1+ alone, pcDNA3.1+/CXCR3 and pcDNA3.1+/CXCR4) was digested, for 1 h at 37ºC, with the restriction enzymes EcoRI and XhoI using the appropriate buffer (New England BioLabs, Inc). The products of the digestion were then analyzed by electrophoresis. For this purpose, they were mixed with Orange DNA loading dye (Fermentas Life Sciences) and loaded into a 1% agarose gel, using the ready-to-use O'GeneRuler 1kb DNA ladder (Fermentas Life Sciences) as reference.

Plasmid amplification

After confirming that transformed bacteria were propagating the corrected plasmids we proceeded with their amplification. For this, 250 µl of each bacteria culture (from the previous pre-amplification step) were inoculated in 250 ml of LB with ampicillin in a 1000 ml erlenmeyer flask to ensure a growth medium saturated with oxygen. This bacteria culture was then incubated overnight, at 37ºC, with constant stirring at 200rpm in an orbital incubator. Cells were harvested and DNA was extracted using Plasmid DNA Purification Nucleobond® Xtra Maxi kit (Macherey-Nagel), according to the manufacture instructions, and quantified using NanoDrop®.

Transfection of WM-115 and WM-266.4

Cell lines were transfected with pcDNA3.1+ alone, pcDNA3.1+/CXCR3 and pcDNA3.1+/CXCR4 using Lipofectamine® LTX and Plus Reagents (Invitrogen, Life Technologies) following the manufacture instructions. Optimization of transfection conditions, i.e. amount of plasmid, Lipofectamine® LTX and Plus Reagents, was performed using 24-well plates as the culture format, and the condition selected was the one that exhibited the higher percentage of CXCR3/CXCR4 surface expression (determined as explained in section II, Flow Cytometry) whilst maintaining a high cell viability. This condition was then scaled up in order to perform the stable transfection. For this reason, $2.5x10^6$ cells were seeded in 100 mm culture dishes with normal culture medium and left to grow as explained in section I (Culture conditions). After 24 h, culture medium was replaced by 20 ml of transfection medium (RPMI 1640 medium, supplemented with 1% fetal bovine serum inactivated by heat, 2 mM L-glutamine, without antibiotics).

Briefly, 40 µg of each plasmid were diluted in 4ml of transfection medium, containing 40 µl of Plus Reagent and incubated for 5min at RT, followed by the addition of 100 µl of Lipofectamine® LTX. This mixture was incubated for 30 min at RT, added to the culture dishes, and incubated at 37ºC in the CO_2 incubator. Six hours after transfection, medium was changed to fresh transfection medium and left to grow overnight. Twenty four hours after transfection, cells were switched to a selective medium which was supplemented with 800 µg/ml Geneticin (Invitrogen). Transfected cells were selected and maintained in this selective medium until stable cell lines were obtained.

Expression of CXCR3 and CXCR4

Gene expression and surface expression of CXCR3 and CXCR4 in the transfected cell lines were determined as explained in section III (RT-PCR) and section II (Flow Cytometry), respectively.

5. Data analysis

All measurements in cell lines were made in triplicate.

For the quantification of proteins in flow cytometry experiments, the number of positive cells stained with the different antibodies was compared with the number of positive cells in the correspondent negative controls (isotype or secondary antibody). Also, the mean fluorescence index (MFI), which is the ratio between the mean fluorescence of samples stained with the mAb against the protein of interest and correspondent control (isotype or secondary antibody), was calculated. The differences were analyzed using Student's t-test and considered significant when $p<0.05$. For chemokine secretion experiments, the concentration obtained in each sample was compared to the lowest standard concentration of the standard curve and the differences were analyzed using Student's t-test, and considered significant when $p<0.05$. The comparison between the expression of chemokines and their receptors in WM-115 and in WM-266.4 and the in the cell lines obtained after xenotransplantation (WM-115-X and WM-266.4-X) was analyzed using Student's t-test and considered significant when $p<0.05$.

Gene expression data was presented as heatmaps using ΔCts using R Software (package Heatmap3, Zhao *et al.* 2014). The similarity of gene expression patterns between different genes, to perform the Hierarchical Clustering, was assessed using the Euclidean distance as the distance method and complete linkage as the agglomeration method. In red are represented the genes that are more expressed (i.e. with lower ΔCts), while in green are represented the less expressed genes (i.e., with higher ΔCts). Genes that were not amplified are shown in white.

Spearman correlation between the data of gene expression and protein expression was performed using GraphPad Prim software, and considered significant when $p<0.05$.

Results and Discussion

1. Melanoma cell lines

Melanoma associated antigens (MAA)

As MAA are often used as diagnostic and prognostic markers (Weinstein *et al.* 2014), we have quantified CD61, CD146 and Melan-A by flow cytometry and CD61, CD146, Melan-A gp100, TYR, MITF, MAGE1, MAGE3, p97 and TPRM1 gene expression in our melanoma cell lines aiming to find patterns of expression that would allow us to group cell lines with similar profile and/or establish different patterns between primary and metastatic cell lines.

Previous studies using flow cytometry have reported a high variability in MAA expression levels between cell cultures originating from various patients (interindividual variability) as well as differences in MAA expression between various clones from the same patient (intraindividual variability). Additionally, they have demonstrated that during the course of the disease, MAA expression pattern changes resulting in either loss or gain of a particular antigen expression (temporal variability). The loss of melanoma antigen expression has been associated with immune escape and tumour progression (Urosevic *et al.* 2005).

In our study, using flow cytometry, most cell lines expressed MAA in a high percentage of their population. However, the level of this expression, represented by the mean fluorescence index (MFI), was different between the studied MAA and also between the studied cell lines (Table 8).

Table 8. Expression of Melanoma-associated antigens (MAA) in human melanoma cell lines. Mean percentage (%) of cells which significantly expressed ($p<0.05$) MAA; MFI represents the mean fluorescence index calculated as the ratio between the mean fluorescence of samples stained with the mAb anti-MAA and correspondent isotypic control (n =3, P – primary tumor, M – metastasis).

Origin	***Cell line***	***CD61***		***CD146***		***Melan-A***	
		%	***MFI***	***%***	***MFI***	***%***	***MFI***
P	IPC-298	98.91	64.86	99.23	67.38	95.63	9.85
P	Mel-Juso	98.80	15.96	98.76	124.1	96.26	14.79
P	Mel-HO	98.56	119.5	99.55	93.61	98.82	44.50
P	IGR-39	4.22	1.95	27.87	1.35	43.46	2.39
P	WM-115	99.22	129.7	95.85	74.39	82.10	11.08
M	A-375	99.41	33.46	99.48	68.93	93.52	8.34
M	MeWo	95.33	12.49	1.44	1.07	98.52	53.57
M	SK-Mel28	7.74	1.93	99.42	98.84	99.01	49.11
M	Malme-3M	98.97	34.99	99.19	65.96	97.36	11.88
M	SK-Mel 2	9.03	1.86	97.60	100.7	94.07	11.24
M	WM-266-4	98.78	165.7	98.73	117.2	87.40	4.74
M	IGR-37	4.59	1.63	78.01	17.37	97.27	27.57
M	Mel-RC08	95.54	29.31	99.58	49.42	96.91	21.61

The cell adhesion proteins CD61 and CD146 were, in general, expressed in a high percentage of the populations and also presented a high level of expression (high MFI). The cell lines IGR-39 and IGR-37 (established from the same donor) expressed both proteins in a smaller population and with a lower level of expression. Furthermore, SK-Mel-2 and SK-Mel-28 expressed CD61 in a smaller population with a lower level of expression. CD146, as an endothelial antigen, could affect angiogenesis and promote neoplastic progression from local invasive to metastatic disease, by upregulation of metalloproteinase MMP-2 and by cell interaction among extracellular matrix and vascular endothelial cells (Hass *et al.* 2005). The only cell lines

expressing CD146 in a small subpopulation were IGR-39 (27.7% CD146+ cells) and Mewo (1.44% CD146+ cells). Rappanoti and coworkers found that the presence of CD146 increases the probability of a patient being in an advanced stage of the disease (Rappanoti *et al.* 2009). If we compare the surface expression of CD146 in pimary and metastatic tumor cell lines from the same patient (IGR-39 and IGR-37, respectively) we can see an increase in the metastatic cell line. Comparative analysis of integrin expression in different stages of melanoma identified the beginning of CD61 expression as one of the most specific markers of the transition from radial growth phase to vertical growth phase of primary and is strongly expressed in metastatic melanoma (Kuphal 2005).

Melan-A was expressed in almost the entire population of all cell lines, with the exception of IGR-39 that expressed it in less than 50% of its population. However, the level of this protein expression was lower when compared to the level of expression of CD61 and CD146. Once more, an increase in the Melan-A expression was detected in metastatic cell line IGR-37 comparing with the primary cell line IGR-39.

In addition to Melan-A, CD146 and CD61, which were also studied at the protein level, we evaluated the gene expression of MAGE1, MAGE3, gp100, p97, TPRM1, TYR and MITF. For comparison of relative gene expression between the different melanoma cell lines (and healthy skin) ΔCts were calculated using RRN18S, PGK1, ACTB, RPL13A and B2M as housekeeping genes and presented in a heatmap clustering the genes (Figure 3).

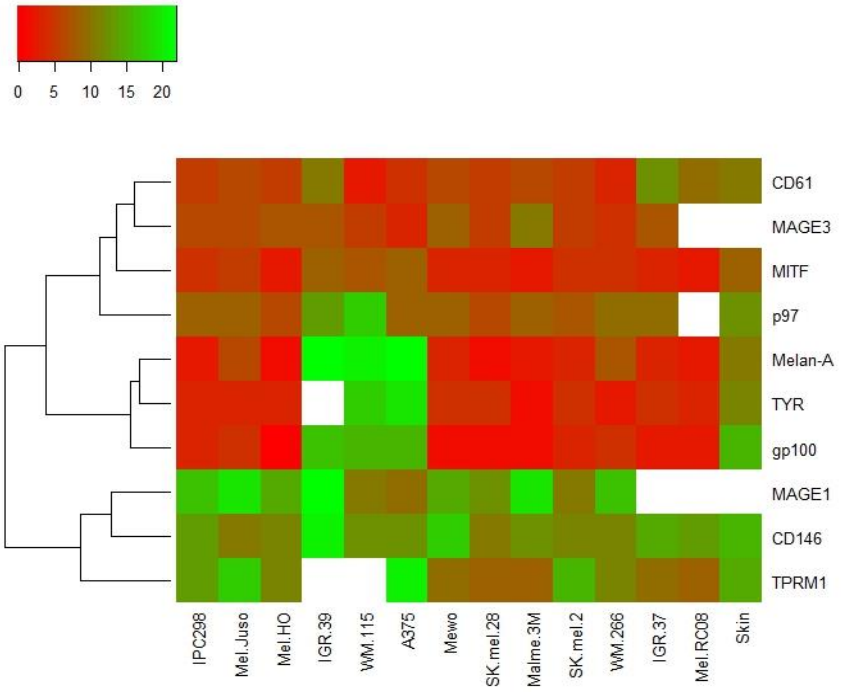

Figure 3. Gene expression of melanoma-associated antigens (MAA). Relative gene expression is presented in a heatmap with the ΔCts calculated using RRN18S, PGK1, ACTB, RPL13A and B2M as housekeeping genes. Red represent genes that are more expressed than those in green. Genes that were not amplified are shown in white.

Three main groups of genes were clustered into highly expressed in all cell lines (CD61, MAGE3, p97 and MITF), slightly expressed (MAGE1, CD146 and TPRM1) and genes that were highly expressed in most of the cell lines but slightly expressed in IGR-39, WM-115 and A375 (Melan-A, gp100 and TYR).

The members of the MAGE family are normally expressed in normal testis, but its ectopic expression is characteristic of malignant transformation, this explains why MAGE1 and MAGE3 are not detected in healthy skin.

Furthermore, they were both not detected in Mel-RC08 and MAGE1 was also not detected in IGR-37.

A similar pattern of expression can be observed in the expression of MITF and the genes this transcription factor is known to control (Melan-A, gp100, TPRM1 and TYR). For example, IGR-39, WM-115 and A375 are the cell lines expressing less MITF and also expressing less Melan-A, gp100, TPRM1 and TYR. On the contrary, Mel-HO, Malme-3M and Mel-RC08 are the cell lines expressing more MITF and also expressing more Melan-A, gp100, TPRM1 and TYR.

Finally, there are no significant differences in gene expression between primary and metastatic cell lines.

For all the MAA tested at the protein level, the level of protein expression (represented by the MFI) correlates positively with the level of gene expression (represented by $2^{-\Delta Ct}$). CD146 has the best correlation ($r = 0.9$, $p < 0.0001$, Figure 4).

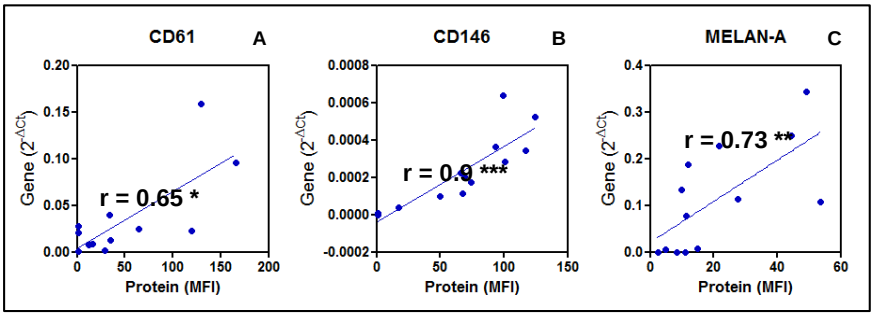

Figure 4. Spearman correlation between de gene and the protein expression of CD61 (A), CD146 (B), and Melan-A (C). (* $p<0.05$, ** $p<0.005$, *** $p<0.0005$).

Urosevic and coworkers found an increased expression of Melan-A, tyrosinase and MAGE-3 in cell cultures obtained from brain metastases, compared to that in other metastatic sites (Urosevic *et al.* 2005). However, Mel-RC08 that is a metastatic cell line derived from a brain metastasis, and is included in our study, does not express MAGE3. In fact, this is the only cell line where we could not detect the expression of this MAA. Similarly, this cell line does not express MAGE1 either. Our cell lines expressing the highest levels of Melan-A (i.e, higher MFI, Table 8) were the primary cell line Mel-HO and the metastatic cell lines Mewo (derived from lymph node) and SK-mel-28 (derived from skin).

SK-Mel-28 was the cell line with the highest relative gene expression of metalotransferrin (p97). It has been shown that gene expression knockdown of p97 using siRNA inhibits invasiveness of this cell line in nude mice (Bertrand *et al.* 2007). Using flow cytometry, Smith and coworkers found high levels of expression of p97 in SK-mel-28 and Malme-3M, moderate expression in A375, WM-15, IGR-37 and IGR-39, and low expression in IGR-39 and WM-115 (Smith *et al.* 2006), which is not totally in accordance to our results of gene expression.

Melanoma Cancer Stem Cells

The expression of a specific set of stem cell markers is a requisite for the isolation and characterization of the CSC population in melanoma (Fang *et al.* 2005, Frank *et al.* 2005, Klein *et al*. 2007, Mihic-Probst *et al*. 2007, Monzani et al. 2007, Schatton *et al.* 2008]. The purpose of our study was to

contribute to the characterization of these CSC in human melanoma cell lines. For this reason, we have analyzed, in our melanoma cell lines, the expression of the stem cell surface markers CD20, CD34, CD90, CD117 (ckit), CD133, CD271, TUJ1, Nestin and the ABC transporters ABCB1, ABCB5 and ABCG2. We have also analyzed the existence of the side population (SP) and quantified the gene expression of several genes that might be important in the characterization of melanoma cancer stem cells (Tables 9-11).

ABC transporters are transmembrane proteins that use the energy of adenosine-5'-triphosphate (ATP) to translocate solutes through the plasma membrane. They are often associated with CSC as when expressed in neoplasic cells they contribute to chemoresistance (Chen *et al*. 2009). The surface expression of these proteins is shown in Table 9.

ABCB1 was detected in all cell lines, although with variable expression. In Mel-Juso, Mel-HO, IGR-39, WM-115, SK-Mel-28, Malme-3M, SK-Mel-2, WM-266-4 and Mel-RC08 it was expressed in less than 40% of the population. In IPC-298, A375 and Mewo it was expressed in ca. 50% of the population and in IGR-37 was expressed in 82% of the population. Keshet and co-workers also found the expression of this marker in melanoma samples of 10 patients, although in lower percentages (1.3% - 9.7% ABCB1+ cells). These authors also detected an increase of three-fold in the expression of this marker when melanoma samples were grown in melanocytic stem cells enriched conditions. Furthermore, they found a ABCB1+/CD117+ subpopulation (Keshet *et al.* 2008).

ABCG2 was significantly expressed in almost all cell lines, with the exception of A375 and Mewo, but always in less than 10% of the population. The expression of this marker has been previously described in the WM-115 cell line (Monzani *et al*. 2007).

Table 9. Surface expression of ABC-transporters in human melanoma cell lines. Mean percentage (%) of cells which significantly expressed ($p<0.05$) ABC-transporters; MFI represents the mean fluorescence index calculated as the ratio between the mean fluorescence of samples stained with the mAb anti- ABC-transporter and correspondent isotypic control (n =3, P – primary tumor, M – metastasis).

Origin	***Cell line***	***ABCB1***		***ABCB5***		***ABCG2***	
		%	***MFI***	***%***	***MFI***	***%***	***MFI***
P	IPC-298	57.13	1.98	1.54	ns	3.23	1.15
P	Mel-Juso	35.74	2.00	2.57	1.17	5.37	1.50
P	Mel-HO	5.85	1.72	1.65	1.15	7.90	0.98
P	IGR-39	36.20	2.01	1.13	ns	1.65	1.10
P	WM-115	13.06	1.91	0.99	1.19	0.79	1.16
M	A-375	54.92	2.15	ns	ns	ns	ns
M	MeWo	50.27	2.00	ns	ns	ns	ns
M	SK-Mel28	5.18	6.93	1.06	1.09	0.98	1.08
M	Malme-3M	18.15	1.69	1.65	ns	1.96	ns
M	SK-Mel 2	19.58	1.98	1.28	ns	1.37	1.28
M	WM-266-4	31.39	1.60	ns	ns	4.76	ns
M	IGR-37	82.42	4.55	3.56	1.24	1.68	1.51
M	Mel-RC08	7.87	4.50	ns	ns	0.50	ns

ABCB5 was expressed in less than 5% of IPC-298, Mel-Juso, Mel-HO, IGR-39, WM-115, SK-Mel-28, Malme-3M, SK-Mel-2 and IGR-37. This marker has been previously detected in 2% to 10% of the melanoma cell line G3361 (Frank *et al.* 2005), and more recently in the WM-115 cell line (Fukunaga-Kalabis *et al.* 2010).

Furthermore, the level of expression of the genes encoding these proteins was also evaluated (Figure 5). ABCG2 is, of the 3 transporters tested, the

one with highest expression and is expressed in all cell lines, while ABCB1 was found to be expressed at lower levels. Interestingly, most of the cell lines which express more ABCB5 were metastatic (6 out of 8) although there was no statistically significant differences between the two types of cell lines (primary vs metastatic, t-student test). Furthermore, this transporter is only slightly expressed in healthy skin (while ABCG2 and ABCB1 are also expressed in healthy skin at comparable levels to the melanoma cell lines).

There is no correlation between the levels of gene and protein expression for these receptors.

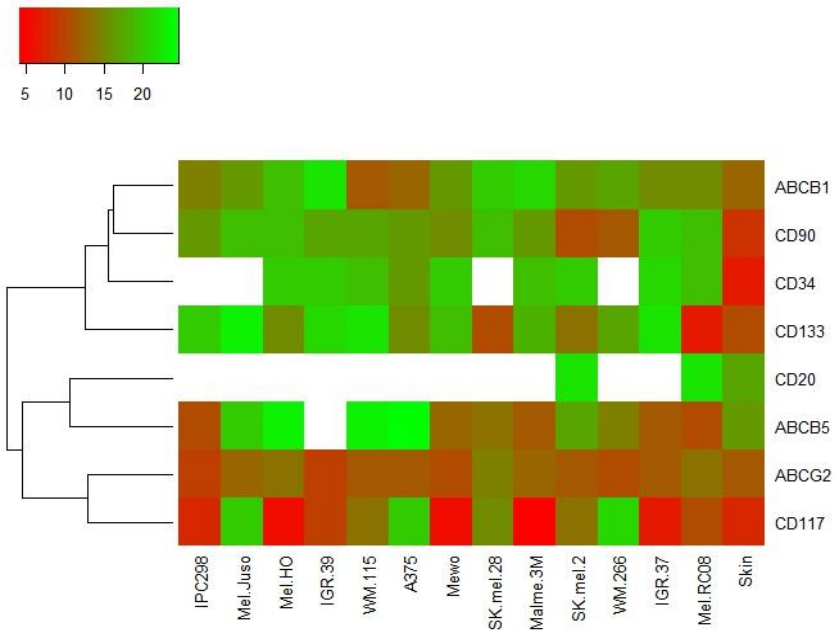

Figure 5. Gene expression of ABC-transporters and CSC markers in human melanoma cell lines. Relative gene expression is is presented in a heatmap with the ΔCts calculated using RRN18S, PGK1, ACTB, RPL13A and B2M as housekeeping genes. Red represent genes that are more expressed than green. Genes that were not amplified are shown in white.

Often associated with the ABC transporters is the existence of the SP (Hadnagy *et al.* 2006). Specifically, it has been shown that an increase in ABCB1 expression increases the SP (Bunting *et al.* 2000) and the importance of ABCG2 has also been highlighted (Scharenberg *et al*. 2002). Furthermore, an ABCB5 subpopulation has been recently described in melanoma cell lines within the SP (Fukunaga-Kalabis *et al*. 2010).

This population, easily identified by its capacity to pump out fluorochromes like Hoechst 33342, was present in seven of the 13 melanoma cell lines studied, four with primary tumor origin and three with metastatic origin (not significant, Fisher exact test). Although SP was identified in a greatest number of primary cell lines, the average size of this subpopulation was highest in metastatic cell lines. In Figure 6 are representative examples of the SP detected in the melanoma cell lines.

In accordance with what was previously stated regarding the correlation between ABC transporters and SP, in the present study, the SP+ melanoma cell lines with primary origin, Mel-Juso, Mel-HO, IGR-39 and WM-115, are also ABCB1+/ABCG2+/ABCB5+, and from the SP+ metastic melanoma cell lines, Mewo is ABCB1+, Malme-3M is ABCB1+/ABCB5+ and Mel-RC08 is ABCB1+/ABCG2+. Furthermore, in accordance with our results, SP has been previously found in lymph node metastatic melanoma cell lines (Gricknick *et al.* 2006) and more recently in WM-115 cell line (Fukunaga-Kalabis *et al*. 2010).

The identification of SP, although being an easy method to obtain an enriched stem cell population, has limitations. Hoescht 33342 toxicity compromises the comparison of the biological properties between the SP and the main population. Still, not all cells with SP phenotype are stem cells; therefore, this functional characterization of the stem cells should be done with the simultaneous stem cell markers staining (Hadnagy *et al*. 2006).

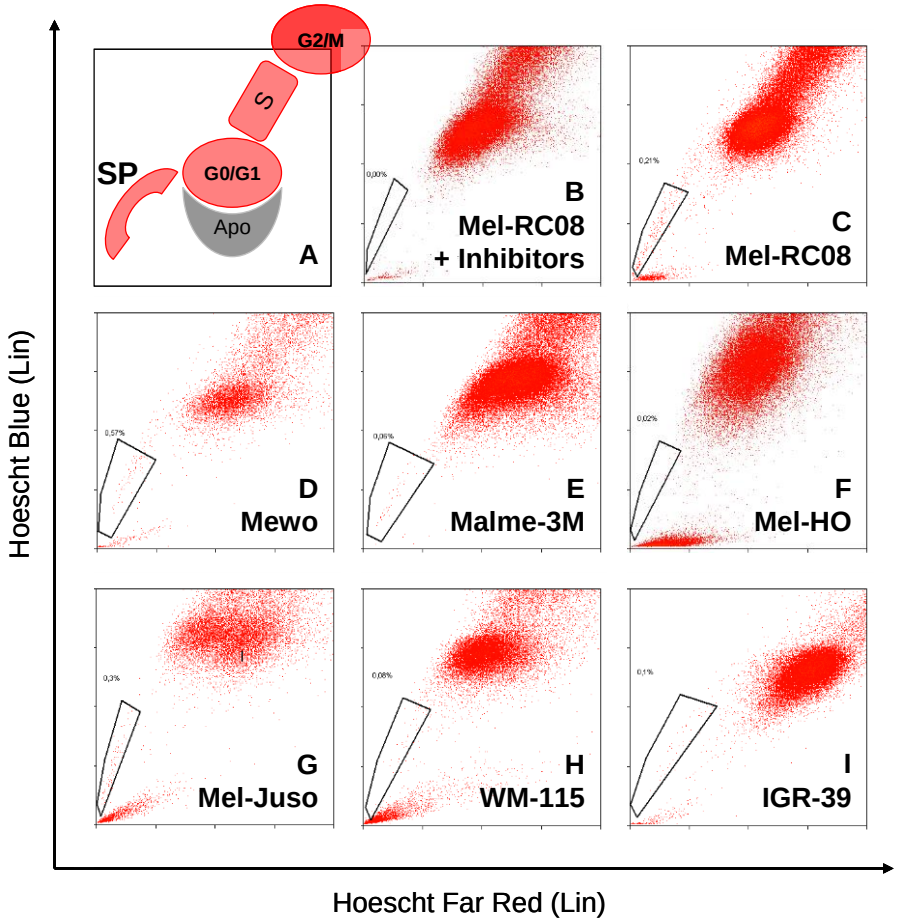

Figure 6. Side Population found in human melanoma cell lines. In A is a schematic dot plot showing the distribution of all the events. In B is an example of Hoecsht 33342 extrusion blockage by verapamil and fumitremorgin C (ABCB1 and ABCG2 inhibitors respectively) in Mel-RC08 cell line, which is an essential control for the correct identification of the SP phenotype and was performed for all cell lines. In C-I are representative biparametric dot-plots of the SP found in the human melanoma cell lines.

We also analysed the expression, both at protein (Table 10) and gene (Figure 5) level of some of the most commonly used biomarkers for CSC, namely CD20, CD34, CD90, CD117 and CD133.

Table 10. Surface expression of commonly used CSC markers in human melanoma cell lines. Mean percentage (%) of cells which significantly expressed ($p<0.05$) CSC markers; MFI represents the mean fluorescence index calculated as the ratio between the mean fluorescence of samples stained with the mAb anti-CSC marker and correspondent isotypic control (n =3, O - origin: P – primary tumor, M – metastasis).

O	***Cell line***	***CD20***		***CD34***		***CD90***		***CD117***		***CD133***	
		%	***MFI***	***%***	***MFI***	***%***	***MFI***	***%***	***MFI***	***%***	***MFI***
P	IPC-298	ns	ns	ns	ns	ns	ns	59.9	3.95	ns	ns
P	Mel-Juso	ns	ns	1.48	1.25	ns	ns	ns	ns	ns	ns
P	Mel-HO	ns	ns	ns	ns	ns	ns	91.5	14.2	ns	ns
P	IGR-39	ns	ns	ns	ns	0.89	ns	29.1	2.09	ns	ns
P	WM-115	ns	ns	2.75	0.98	ns	ns	ns	ns	ns	ns
M	A-375	ns	ns	ns	ns	ns	ns	ns	ns	ns	ns
M	MeWo	ns	ns	ns	ns	ns	ns	81.5	7.75	ns	ns
M	SK-Mel28	ns	ns	ns	ns	ns	ns	ns	ns	12.2	1.57
M	Malme-3M	ns	ns	ns	ns	ns	ns	90.6	11.3	ns	ns
M	SK-Mel 2	ns	ns	0.80	1.02	1.11	ns	ns	ns	10.7	1.76
M	WM-266-4	ns	ns	0.32	ns	ns	ns	ns	ns	ns	ns
M	IGR-37	ns	ns	0.94	ns	ns	ns	67.1	8.84	ns	ns
M	Mel-RC08	ns	ns	1.37	1.23	ns	ns	3.17	1.20	82.0	6.28

CD20 was not found in the surface of any of our cell lines and its gene expression was only detected very slightly in SK-Mel-2 and Mel-RC08. This marker was previously detected in WM-115, both grown as melanospheres in embryonary stem cell medium (10.10% CD20+) or as a monolayer in normal culture medium (0.06%; Fang *et al*. 2005). We found

0.12% of CD20+ WM-115 cells but without differing significantly from the control.

CD34 and CD90 were found at the surface of very few cell lines and in very small subpopulations (<3%) although a slight gene expression was detected in most of the cell lines (but always at lower levels that what was detected in healthy skin). The cell lines with the biggest subpopulations expressing CD34 protein were Mel-Juso, WM-115 and Mel-RC08 (1.48%, 2.75 and 1.37, respectively) while the cell lines SK-Mel-2, WM-266-4 and IGR-37 have a subpopulation smaller than 1% (0.80%, 0.32% and 0.9%, respectively). CD90 was only detected in IGR-39 and SK-Mel-2 (0.89% and 1.11%, respectively).

CD133 protein was found only in metastatic cell lines, in of SK-Mel-2 (10.67%) and SK-Mel-28 (12.23%) and in a large subpopulation of Mel-RC08 (82.02%). However, its gene expression has also been detected in the other cell lines. Previously, the expression of CD133 has been described as being more than 80% of the cell population in the cell lines WM-115 and IGR39 (Monzani *et al.* 2007). However, we have not found CD133+ populations in these cell lines, in agreement with the results obtained by others (Zimmerer *et al.* 2013).

Finally, CD117 was detected at the cell surface of 8 of the studied cell lines, although its gene expression was detected in cell lines that did not show protein expression. The expression of this marker has been previously detected in samples from melanoma patients (Keshet *et al.* 2008). Also, for this CSC marker there is a positive correlation between the level of protein expression (represented by the MFI) and the level of gene expression (represented by $2^{-\Delta Ct}$, Figure 7).

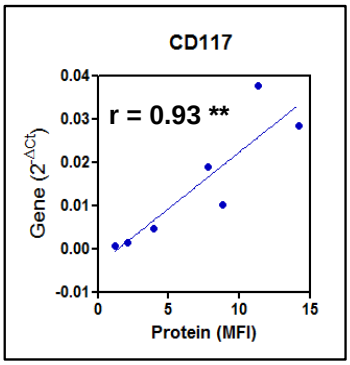

Figure 7. Spearman correlation between de gene and the protein expression of CD117, ** p<0.005.

Other stem cell markers like TUJ1, nestin and CD271, normally used as neuronal stem cell markers, were analyzed (Table 11 and Figure 8).

Although nestin was found in almost 100% of the population of the all cell lines, its expression was not detected in SK-Mel-28 and a low level of expression was found in Mel-RC08, IGR-39 and Mel-HO.

All cell lines expressed CD271 although the size of the subpopulation was variable, being that Mel-HO and IGR-37 were <1% CD271+ while Mel-Juso was 97.90% CD271+. Nevertheless its gene expression was found in all cell lines.

The protein of TUJ1 was found in the primary cell lines IPC-298 and Mel-Juso and in the metastatic A-375, Malme-3M and SK-mel-2, although the subpopulation of the former was much smaller (<5%) than the latter (>70%). However, all cell lines highly expressed this gene.

For CD271 and Nestin, the level of protein expression (represented by the MFI) correlates positively with the level of gene expression (represented by $2^{-\Delta Ct}$, Figure 9).

Table 11. Surface expression of neuronal stem cell markers in human melanoma cell lines. Mean percentage (%) of cells which significantly expressed ($p<0.05$) these CSC markers; MFI represents the mean fluorescence index calculated as the ratio between the mean fluorescence of samples stained with the mAb anti-CSC marker and correspondent isotypic control (n =3, P – primary tumor, M – metastasis).

Origin	*Cell line*	*TUJ1*		*Nestin*		*CD271*	
		%	*MFI*	*%*	*MFI*	*%*	*MFI*
P	IPC-298	4.77	0.80	98.71	1.27	36.86	4.86
P	Mel-Juso	1.55	1.15	99.26	190	97.90	39.87
P	Mel-HO	ns	ns	96.94	30.03	0.46	0.95
P	IGR-39	ns	ns	98.39	35.26	4.61	1.22
P	WM-115	ns	ns	98.58	320	70.84	17.56
M	A-375	97.81	7.63	98.33	368	13.57	1.54
M	MeWo	ns	ns	98.54	215	55.66	7.27
M	SK-Mel28	1.39	ns	99.49	92.43	4.68	1.34
M	Malme-3M	97.49	10.77	97.23	148	4.81	1.67
M	SK-Mel 2	72.84	5.23	94.57	108.8	58.56	16.73
M	WM-266-4	ns	ns	98.32	169	55.50	7.72
M	IGR-37	ns	ns	98.10	33.03	0.46	1.05
M	Mel-RC08	ns	ns	98.65	225.	8.45	2.85

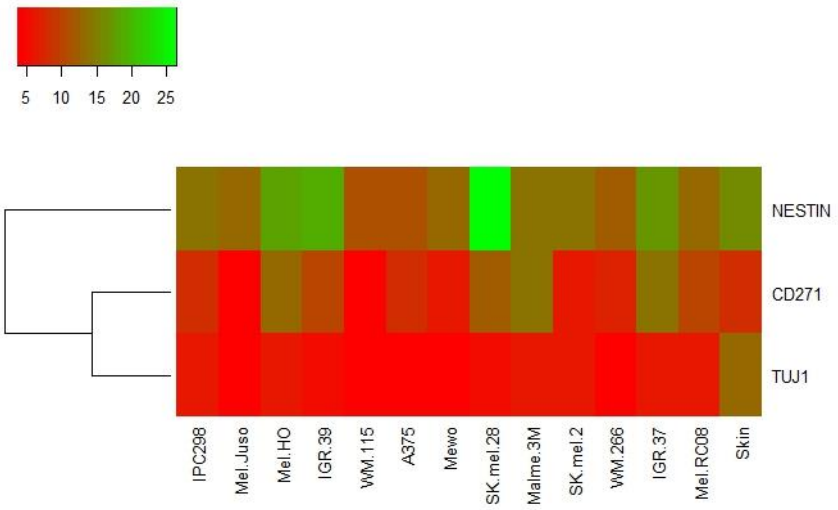

Figure 8. Gene expression of neuronal stem cell markers in human melanoma cell lines. Relative gene expression is is presented in a heatmap with the ΔCts calculated using RRN18S, PGK1, ACTB, RPL13A and B2M as housekeeping genes. Red represent genes that are more expressed than green. Genes that were not amplified are shown in white.

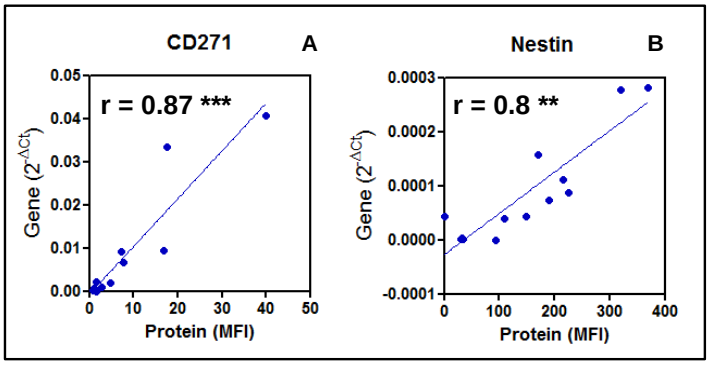

Figure 9. Spearman correlation between de gene and the protein expression of CD271 (A) and Nestin (B). ** p<0.005, ***<0.0005.

Finally, the gene expression of traditional pluripotency stem cell markers like OCT-4, NANOG and SOX-2, and other associated genes was also evaluated (Figure 10).

OCT4, NANOG, and SOX2 are three pluripotency transcription factors that are well known to contribute to the reprogramming of somatic cells into an embryonic stem cell-like state and there is evidence that the overexpression of these three genes occurs in human malignancies and is relevant to tumor transformation, tumorigenicity, tumor metastasis (Perego *et al.* 2010) These genes are moderately expressed in melanoma cell lines. They are clustered together in the heatmap but SOX-2 seems to be most expressed of them 3.

DPPA5, which has been proposed to contribute to early embryogenesis and may be specific marker of embryonic stem cells (Lagarkova *et al.* 2006), was the least expressed gene. In fact, it was not detected in 6 of the cell lines and the highest level of its expression was observed in healthy skin.

Although caspase 3 main role is associated with apoptosis it has been referenced as inductive cue for stem cell differentiation (Janzen *et al*. 2008) so it was also analyzed. It was the most expressed gene although the levels were comparable to healthy skin.

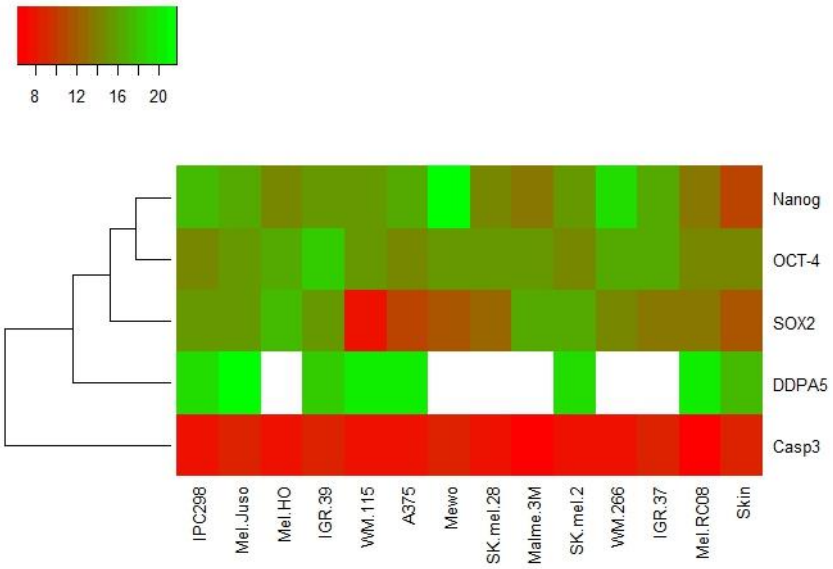

Figure 10. Gene expression of pluripotency stem cell markers in human melanoma cell lines. Relative gene expression is is presented in a heatmap with the ΔCts calculated using RRN18S, PGK1, ACTB, RPL13A and B2M as housekeeping genes. Red represent genes that are more expressed than green. Genes that were not amplified are shown in white.

Further studies need to be done in order to fully characterize and understand the melanoma CSC. The co-expression of the above mentioned cell surface markers together with the identification of the side population along with other functional studies (e.g., culturing subpopulations as melanospheres) will, for sure, help to achieve this goal.

Epethelial-Mesenquimal Transition (EMT)

To evaluate the EMT potential of these melanoma cell lines we quantified the expression of N-cadherin and E-cadherin, both at the protein (Table 12) and gene (Figure 11) level. Both cadherins are expressed in the surface of most of the cell lines with the exception of Mel-HO and Malme-3M that do not express N-cadherin and WM-266 that does not express E-cadherin. Nevertheless, both the size of the subpopulations expressing these cadherins and the level of their expression is variable.

Table 12. Surface expression of EMT markers in human melanoma cell lines. Mean percentage (%) of cells which significantly expressed ($p<0.05$) these EMT markers; MFI represents the mean fluorescence index calculated as the ratio between the mean fluorescence of samples stained with the mAb anti-EMT marker and correspondent isotypic control (n =3, P – primary tumor, M – metastasis).

Origin	*Cell line*	*Ncad*		*Ecad*	
		%	*MFI*	*%*	*MFI*
P	IPC-298	64.68	2.72	1.21	ns
P	Mel-Juso	23.57	2.21	1.12	1.33
P	Mel-HO	ns	ns	98.68	25.50
P	IGR-39	1.05	1.18	6.74	2.15
P	WM-115	39.34	3.66	0.65	1.18
M	A-375	47.72	8.94	6.14	2.21
M	MeWo	46.72	3.33	4.03	1.71
M	SK-Mel28	7.36	1.35	10.92	3.10
M	Malme-3M	ns	ns	99.16	42.05
M	SK-Mel 2	1.05	1.17	5.74	2.29
M	WM-266-4	79.79	3.88	ns	ns
M	IGR-37	2.71	1.25	42.22	4.02
M	Mel-RC08	61.28	2.50	16.84	2.57

Associated with the EMT phenotype is a shift in the cadherin expression profile, characterized by a decrease in E-cadherin expression (which leads to a decrease in keratinocytes attachment) and increase in N-cadherin expression (which allows the attachment to fibroblasts and endothelial cells in the tumor stroma, Haass *et al.* 2005) This is in accordance to our data where the only two cell lines that do not express N-cadherin are almost 100% for E-cadherine positive. Furthermore, most of the cell lines express more N-cadherin than E-cadherin.

Regarding the gene expression study, we found that N-cadherin is generally highly expressed in most of the cell lines, being detected in lower levels in Mel-HO, Malme-3M and SK-Mel-2, which are cells lines where the protein was not detected or detected in a very small population. This lower levels are comparable to the level of expression detected in healthy skin.

E-cadherin is highly expressed in almost all metastatic cell lines and in Mel-HO, at levels comparable to the healthy skin, while it is slightly expressed in most primary cell lines.

Only for N-cadherin there is a positive correlation between the level of protein expression (represented by the MFI) and the level of gene expression (represented by $2^{-\Delta Ct}$, Figure 12). The fact that a high gene expression of E-cadherin does not translate in protein expression is in accordance with previous studies stating that melanoma cell express non functional E-cadherin (Haass et al 2005).

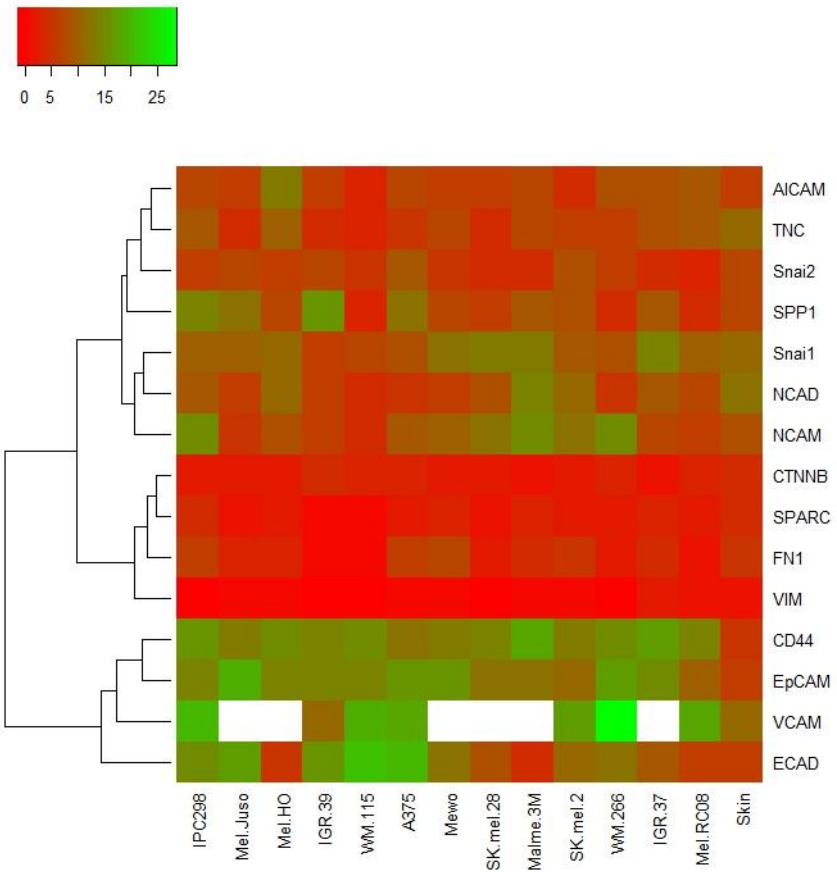

Figure 11. Gene expression of EMT markers in human melanoma cell lines. Relative gene expression is is presented in a heatmap with the ΔCts calculated using RRN18S, PGK1, ACTB, RPL13A and B2M as housekeeping genes. Red represent genes that are more expressed than green. Genes that were not amplified are shown in white.

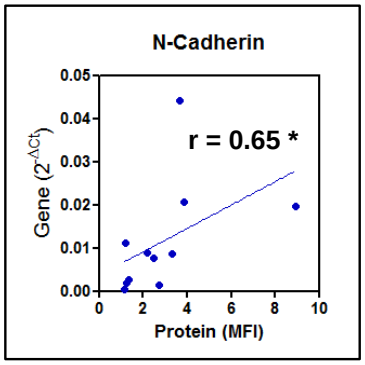

Figure 12. Spearman correlation between de gene and the protein expression of N-cadherin (A) and E-cadherin (B). * $p<0.05$, ***<0.0005.

We also evaluated the gene expression of the adhesion molecules EpCam, AlCam, VCam and Ncam, and other key players in EMT, like FN1, SPARC, SPP1, Snai1, Snai2, TNC, CTNNB, VIM and CD44 (Figure 11).

VIM, FN1, SPARC and CTNNB are clustered together in the heatmap as being the most expressed gene in all cell lines (and in healthy skin).

On the contrary, EpCam and VCam are clustered together as being the least expressed genes (together with E-cadherin).

All other genes are clustered in the third main group of genes, which are the genes with more variable levels of expression between the different cell lines.

Although there is no statistical significance, it seems that E-cadherin and NCAM are differently expressed between primary and metastatic cell lines, being E-cadherin more expressed in primary cell lines while NCAM is more expressed in metastatic cell lines (Figure 13).

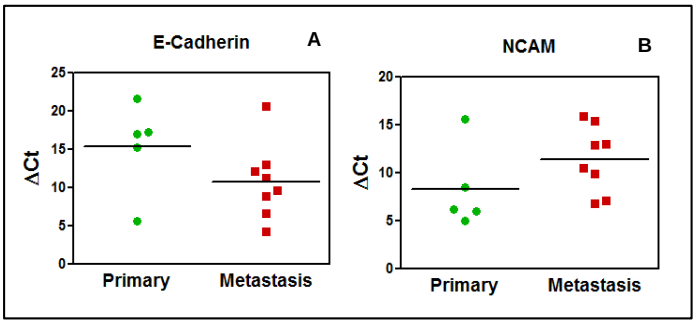

Figure 13. Gene expression of E-cadherin (A) and NCAM (B). Differences between primary and metastatic cell lines were evaluated using unpaired t-student test.

Chemokine and Chemokine Receptors Expression

Surface expression of chemokine receptors CXCR3, CXCR4, CXCR7, CCR7 and CCR10

We found that melanoma cell lines did not express or express in a low degree (less than 2% of the population; Table 13) the chemokine receptors on their cell surface. The control cell line (Hut-78) showed surface expression of CXCR3 (63.1%), CXCR4 (5.9%), CCR7 (3.36%) and CCR10 (1.23%). Representative flow cytometry plots are shown in Figure 14.

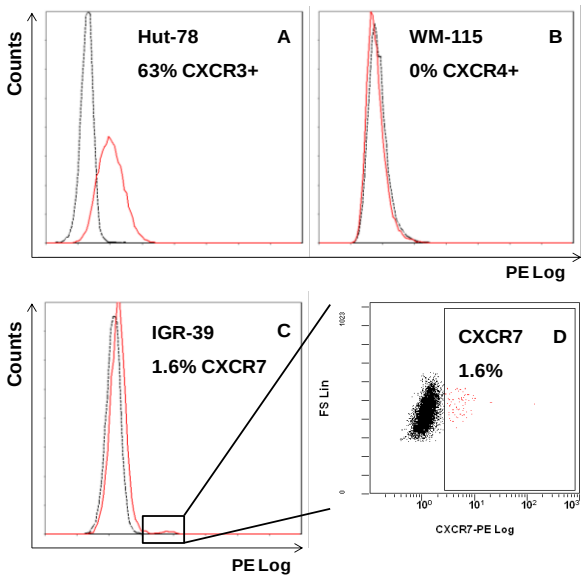

Figure 14. Surface expression of chemokine receptors in human melanoma cell lines. Representative examples for the quantification of chemokine receptors surface expression by flow cytometry are shown. Overlaid histograms of PE fluorescence of specific anti-receptor monoclonal antibody (continuous red line) and correspondent isotypic control (discontinuous black line) are shown to represent Hut-78 with high percentage of CXCR3+ subpopulation (A), WM-115 with no expression of CXCR4 (B) and IGR-39 with a small subpopulation of CXCR7+ cells (C), which is further illustrated in a biparametric dotplot of FS vs PE fluorescence (D).

Table 13. Surface expression of chemokine receptors in human melanoma cell lines. Mean percentage (%) of cells which significantly expressed ($p<0.05$) chemokine receptors at the cell surface; MFI represents the mean fluorescence index calculated as the ratio between the mean fluorescence of the positive population in the samples stained with the mAb anti-receptor and correspondent isotypic control (n =3, ns – not significant, O - origin: P – primary tumor, M – metastasis).

O	*Cell line*	*CXCR3*		*CXCR4*		*CXCR7*		*CCR7*		*CCR10*	
		%	*MFI*	*%*	*MFI*	*%*	*MFI*	*%*	*MFI*	*%*	*MFI*
P	IPC-298	0.16	3.10	ns	-	ns	-	ns	-	0.23	11.4
P	Mel-Juso	ns	-	ns	-	0.43	27.7	ns	-	0.43	12.8
P	Mel-HO	0.07	4.83	ns	-	0.36	4.91	ns	-	ns	-
P	IGR-39	0.83	8.31	ns	-	1.59	7.09	ns	-	1.79	4.05
P	WM-115	0.15	5.91	ns	-	ns	-	ns	-	0.11	5.09
M	A-375	ns	-	ns	-	ns	-	ns	-	ns	-
M	MeWo	ns	-	ns	-	ns	-	ns	-	ns	-
M	SK-Mel28	ns	-	ns	-	ns	-	ns	-	ns	-
M	Malme-3M	ns	-	ns	-	ns	-	ns	-	ns	-
M	SK-Mel 2	0.44	3.16	ns	-	0.35	10.3	ns	-	0.35	3.84
M	WM-266-4	ns	-	ns	-	ns	-	ns	-	ns	-
M	IGR-37	0.13	3.47	ns	-	0.22	14.8	ns	-	ns	-
M	Mel-RC08	ns	-	ns	-	ns	-	ns	-	ns	-
P	Hut-78	63.1	3.37	5.9	6.9	ns	-	3.36	7.66	1.23	8.36

Intracellular expression of chemokine receptors CXCR3, CXCR4, CXCR7, CCR7 and CCR10 in human melanoma cell lines

All cell lines significantly expressed all chemokine receptors intracellularly (Table 14). However a great variability was found in the pattern of expression, depending on the cell line and receptor studied. Some receptors were expressed in almost the entire population of all cell lines (e.g., CXCR4)

while other receptors were expressed in a large subpopulation of some cell lines and in a small subpopulation of other cell lines (e.g. CXCR7; Table 14). Representative histograms are shown in Figures 15A and 15B. Furthermore, the level of protein expression also varied between receptors and cell lines. In general, CXCR4 seems to be the receptor which is more expressed, as can be shown by its higher values of MFI, while CCR7 appears to be the receptor which is expressed at lower levels, having the lowers MFI values (Table 14).

Table 14. Intracellular expression of chemokine receptors in human melanoma cell lines. Mean percentage (%) of cells which significantly expressed ($p<0.05$) chemokine receptors intracellularly; MFI represents the mean fluorescence index calculated as the ratio between the mean fluorescence of samples stained with the mAb anti-receptor and correspondent isotypic control (n =3, ns – not significant, O - Origin: P – primary tumor, M – metastasis).

O	*Cell line*	*CXCR3*		*CXCR4*		*CXCR7*		*CCR7*		*CCR10*	
		%	*MFI*	*%*	*MFI*	*%*	*MFI*	*%*	*MFI*	*%*	*MFI*
P	IPC-298	99.45	7.34	99.41	6.29	21.26	1.48	58.30	1.92	45.67	1.86
P	Mel-Juso	53.74	3.27	62.50	4.16	3.58	1.18	39.58	2.51	18.64	1.78
P	Mel-HO	96.71	5.28	98.99	7.82	53.07	2.21	82.49	3.13	56.36	2.26
P	IGR-39	95.73	3.73	95.76	4.04	81.82	2.59	87.87	2.43	37.51	1.70
P	WM-115	88.59	5.40	92.45	3.95	4.97	1.57	20.16	1.70	13.67	1.57
M	A-375	43.61	2.51	94.44	14.10	63.20	3.45	12.70	1.59	45.45	2.89
M	MeWo	25.02	2.21	80.60	5.98	80.65	6.59	2.58	1.32	61.27	3.53
M	SK-Mel28	56.56	2.43	93.22	8.63	73.86	5.02	1.20	1.20	65.81	2.59
M	Malme-3M	64.99	2.07	92.84	2.66	97.78	5.66	64.86	1.99	71.88	2.37
M	SK-Mel 2	96.43	6.92	98.33	15.73	33.52	2.04	78.23	2.08	96.34	4.68
M	WM-266-4	74.08	2.22	96.26	3.39	21.53	1.68	40.16	1.69	24.00	1.63
M	IGR-37	97.88	4.25	97.85	4.53	43.84	1.89	67.83	2.03	56.29	1.89
M	Mel-RC08	45.79	2.69	95.02	7.33	72.05	3.99	9.14	1.61	60.81	2.84
P	Hut-78	82.05	2.93	95.95	4.62	19.75	1.95	13.53	1.68	88.40	4.08

It seems that metastatic cell lines have a significant bigger subpopulation expressing CCR10 (p=0.0428, Figure 16A) with a higher level of expression (ns, Figure 16B), cells with significant higher level of CXCR7 expression (p=0.0430, Figure 16C), and cells with significant lower level of CCR7 expression (p=0.0217, Figure 16D), when comparing to the primary cell lines.

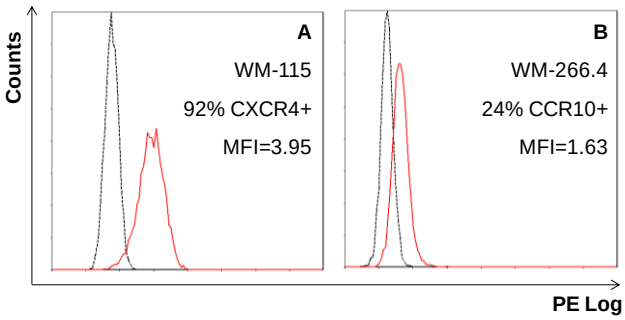

Figure 15. Intracellular expression of chemokine receptors in human melanoma cell lines. Representative examples for the quantification of intracellular chemokine receptor expression by flow cytometry are shown. Overlaid histograms of PE fluorescence of specific anti-receptor monoclonal antibody (continuous red line) and correspondent isotopic control (discontinuous black line) are shown to represent 92% CXCR4+ WM-115 subpopulation (A) and 24% CCR10+ WM-266.4 subpopulation (B).

Table 15. Intracellular chemokine expression in human melanoma cell lines. Mean percentage (%) of cells which significantly expressed ($p<0.05$) chemokine ligands intracellularly; MFI represents the mean fluorescence index calculated as the ratio between the mean fluorescence of samples stained with the mAb anti-receptor and correspondent isotypic control (n =3, ns – not significant, P – primary tumor, M – metastasis).

O	*Cell line*	*CXCL9*		*CXCL10*		*CXCL11*		*CXCL12*		*CCL19*		*CCL21*		*CCL27*		*CCL28*	
		%	*MFI*	*%*	*MFI*	*%*	*MFI*	*%*	*MFI*	*%*	*MFI*	*%*	*MFI*	*%*	*MFI*	*%*	*MFI*
P	IPC-298	95.39	3.69	0.93	1.11	7.00	1.36	97.93	5.34	99.02	16.86	53.98	1.94	98.71	7.39	ns	-
P	Mel-Juso	93.22	10.88	ns	-	12.90	2.10	89.57	5.80	99.04	70.62	6.12	1.60	98.75	17.36	ns	-
P	Mel-HO	96.59	8.39	7.32	1.32	65.87	5.83	97.86	8.12	98.62	60.07	82.62	3.72	98.65	23.48	ns	-
P	IGR-39	14.05	1.52	ns	-	10.49	1.37	95.86	3.89	98.76	16.71	23.50	1.54	98.58	5.21	ns	-
P	WM-115	28.31	2.06	0.46	1.12	2.66	1.24	81.77	3.96	98.79	20.00	15.55	1.65	94.06	4.89	ns	-
M	A-375	84.56	6.18	0.42	1.07	88.71	7.46	10.89	1.67	92.34	71.31	32.60	3.42	89.92	25.21	1.14	1.29
M	MeWo	45.53	5.28	1.46	1.44	46.10	8.72	24.41	2.15	50.06	34.71	23.62	3.96	37.85	10.86	1.74	1.86
M	SK-Mel28	67.63	3.06	2.01	1.18	82.59	5.72	71.82	3.09	86.62	44.41	28.42	1.96	86.34	14.37	ns	-
M	Malme-3M	50.32	3.45	ns	-	71.62	3.45	77.48	3.37	98.02	34.57	5.45	1.70	97.90	11.06	ns	-
M	SK-Mel 2	81.72	3.18	ns	-	94.63	5.53	95.94	8.46	98.34	36.70	22.45	1.86	97.47	13.02	ns	-
M	WM-266-4	71.84	4.57	15.19	1.74	46.26	3.24	98.24	9.56	98.58	30.17	60.21	3.71	98.50	11.38	1.14	1.25
M	IGR-37	87.92	5.06	ns	-	36.32	1.88	92.76	3.78	98.83	47.66	38.71	2.44	98.96	21.35	ns	-
M	Mel-RC08	49.96	3.29	ns	-	80.84	6.87	16.64	1.68	86.38	55.25	22.94	2.19	82.77	15.33	1.56	1.22
P	Hut-78	1.90	1.69	ns	-	ns	-	ns	-	65.99	11.71	ns	-	39.11	3.81	ns	-

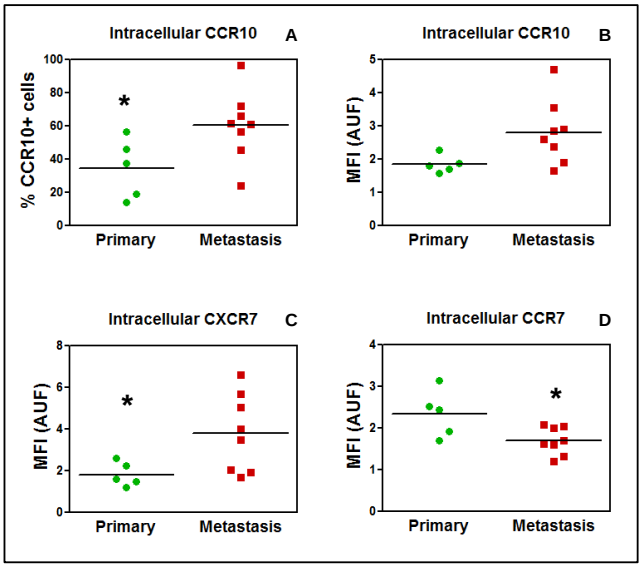

Figure 16. Intracellular expression of CCR10 (A and B), CXCR7 (C) and CCR7 (D). Differences between primary and metastatic cell lines were evaluated using unpaired t-student test (* $p<0.05$).

Intracellular expression of chemokines CXCL9, CXCL10, CXCL11, CXCL12, CCL19, CCL21, CCL27 and CCL28 in human melanoma cell lines

Most chemokines were expressed intracellularly in all melanoma cell lines (CXCL9, CXCL11, CXCL12, CCL19, CCL21 and CCL27). On the contrary, Hut-78 only expressed significantly CXCL9, CCL19 and CCL27 and in smaller subpopulations than the melanoma cell lines. CXCL10 and CCL28 were the chemokines expressed by fewer cells and with the lowest expression levels, whereas CCL19 was the chemokine with highest expression level (Table 15). Representative histograms are shown in Figure 17A and 17B.

When comparing metastatic and primary cells lines only CCL11 seems to have a significant difference in the pattern of expression being expressed in a bigger subpopulation of the metastatic cell lines (p=0.0042, Figure 18A) and higher level of expression (p=0.0375, Figure 18B).

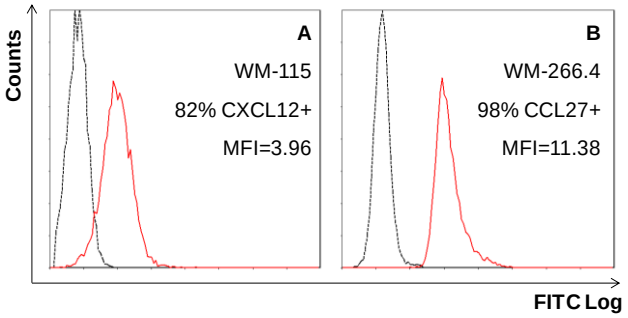

Figure 17. Intracellular expression of chemokines in human melanoma cell lines. Representative examples for the quantification of intracellular chemokine expression by flow cytometry are shown. Overlaid histograms of specific anti-chemokine policlonal antibody + FITC secondary antibody fluorescence (continuous red line) and correspondent control (cell with secondary antibody, discontinuous black line) are shown to represent 82% CXCL12+ WM-115 subpopulation (A) and 98% CCL27+ WM-266.4 subpopulation (B).

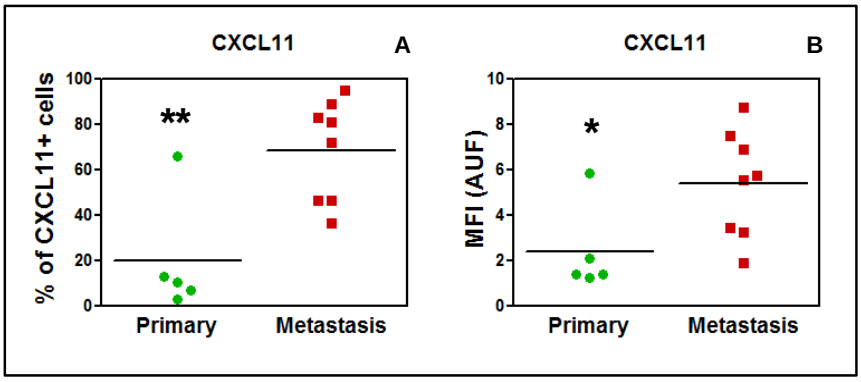

Figure 18. Intracellular expression of CXCL11 (A, percentage of positive cells, B, MFI). Differences between primary and metastatic cell lines were evaluated using unpaired t-student test (* $p<0.05$, ** $p<0.005$).

Gene expression of chemokines and their receptors

For comparison of relative gene expression between the different melanoma cell lines (and Hut-78) ΔCts were calculated using RPL13A, RRN18S, ACTB and PGK1 as housekeeping genes and presented in a heatmap clustering the genes (Figure 19).

The clustering identifies 2 main groups of genes. Most of the chemokines (with the exception of CXCL12 and CCL28) are grouped in the least expressed genes, while all the receptors are grouped in the most expressed genes, being, in most of the cell lines, CXCR4 the most expressed receptor. Interestingly CXCL12 is included in the later group along with the receptors. CXCL9 was not detected in any of the primary cell lines but is slightly expressed in most of the metastatic cell lines while CCL28, clustered independently in the heatmap, was not detected in most of the metastatic cell lines but is slightly expressed in most of the primary cell lines.

Both for chemokine and receptors there is no correlation between the protein level of expression (MFI) and the gene expression.

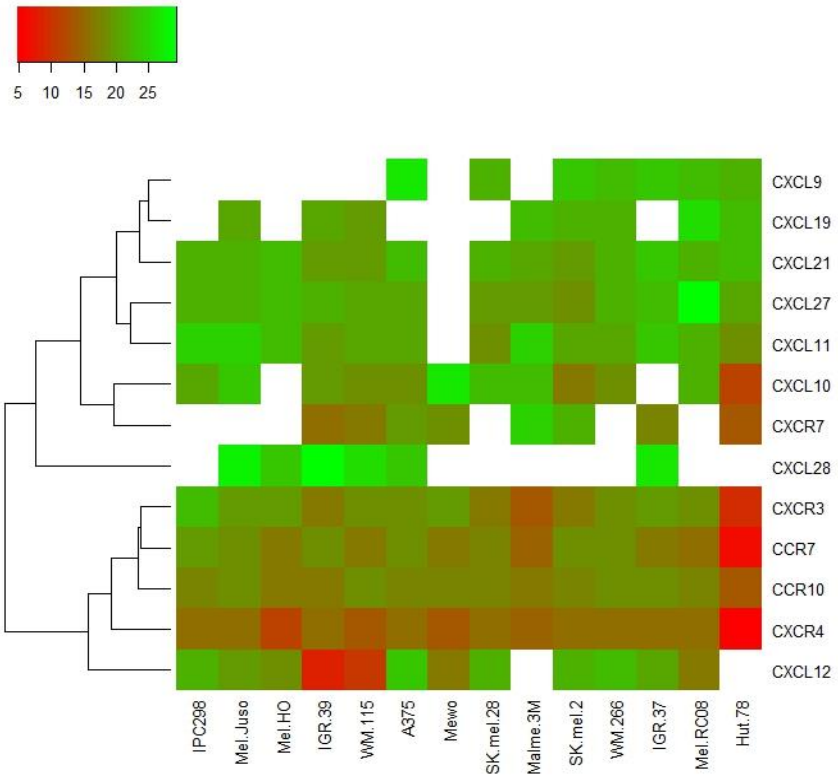

Figure 19. Gene expression of chemokines and their receptors in human melanoma cell lines. Relative gene expression is presented in a heatmap with the ΔCts calculated using RPL13A, RRN18S, ACTB and PGK1 as housekeeping genes. Red represent genes that are more expressed than green. Genes that were not amplified are shown in white.

Secretion of chemokines CXCL9, CXCL10, CXCL11, CXCL12, CCL19, CCL21, CCL27 and CCL28 in human melanoma cell lines

CXCL10 was the only chemokine secreted in the studied melanoma cell lines. This chemokine was secreted in low concentrations by A375 and SK-

Mel2 (40 pg/ml and 38 pg/ml, respectively). All melanoma cell lines secreted IL-8 and Gro (although in different amounts), which reassure us of their melanocytic function (Table 16).

Table 16. Secretion of chemokines in human melanoma cell lines. Mean concentration (pg/ml) of secreted chemokines (n =3, § concentration bellow the lower limit of detection, P – primary tumor, M – metastasis).

Origin	***Cell line***	**GRO**	**IL-8**	**CXCL10**
P	IPC-298	936	821	§
P	Mel-Juso	3939	6663	§
P	Mel-HO	439	274	§
P	IGR-39	117	787	§
P	WM-115	341	7614	§
M	A-375	4091	5234	40
M	MeWo	1234	235	§
M	SK-Mel28	197	212	§
M	Malme-3M	217	43	§
M	Sk-Mel2	1956	7457	38
M	WM-266-4	6419	346	§
M	IGR-37	2740	117	§
M	Mel-RC08	1921	4296	§

General discussion

It has been previously demonstrated that chemokine receptors allow the directed migration towards specific organs (Muller *et al.* 2001). Moreover, the receptors CXCR4, CCR7 and CCR10 have been implicated in the

process of metastasis in melanoma, based on studies with animals (Murakami *et al*. 2004). Some of them, namely CXCR4, were also associated with metastasis in other types of neoplasms like breast, prostate, ovarian, colon and lung cancers (Muller *et al.* 2001).

Flow cytometry is one of the methods available for immunophenotyping (i.e. cellular phenotyping using antibodies) which allows working with live cells and, therefore, to analyze cell surface expression of proteins like receptors (O'Connor *et al.* 2001). However, most studies that analyze chemokine receptors at the protein level have been performed using mainly immunohistochemistry and western blotting techniques, which do not permit the correct evaluation of cell surface expression. Gene expression studies have shown that melanoma cell lines express receptors CCR10 and CCR7, which could be implicated in the frequent metastasis of melanoma to skin and lymph nodes, respectively (Muller *et al*. 2001). However, these studies do not imply either the presence of functional receptors at the cell surface.

We detected surface expression of CXCR3 in the cell lines IPC-298, MEL-HO, IGR39, WM-115, SK-Mel 2, and IGR-37, surface expression of CXCR7 in the cell lines Mel-Juso, MEL-HO, MEL-HO, IGR-39, SK-Mel 2, and IGR-37, and surface expression of CCR10 in the cell lines IPC-298, Mel-Juso, IGR-39, WM-115 and SK-Mel2. However, in all cases this expression was only detected in a small subpopulation of cells (less than 2%). Our results differ from a study that describes functional plasma membrane CXCR4 in the cell lines MeWo and A375 (Robledo *et al*. 2001).

All cell lines significantly expressed all the receptors intracellularly, although there was significant variability in the pattern of expression between the different cell lines. As the extent of the cellular response triggered by chemokines depends on the amount of receptor expressed at the plasma membrane the intracellular localization could affect different steps of

tumorigenesis, including angiogenesis, tumor growth, invasion and metastasis (Kakinuma and Hwang 2006, Vandercappellen *et al*. 2008). The intracellular expression of chemokine receptors, in other tumors, has been shown to be correlated with metastasis directed to lymph nodes and with a bad prognosis (e.g., CXCR4 in breast cancer (Yasuoka *et al.* 2008); in lung cancer (Na *et al*. 2008); in colon cancer (Speetjens *et al*. 2009). In the case of hepatocellular carcinoma the intracellular expression of CXCR4 with lack of its expression at the cell surface and lack of response to its ligand CXCL12 has been reported (Kim *et al.* 2008).

In normal cells, human differentiated neurons CXCR7 protein expression is mostly limited to the intracellular compartment with little to no expression on the plasma membrane (Shimizu *et al.* 2011). In the case of multipotent mesenchymal stem cells (MSC) intracellular expression, at protein level, of chemokine receptors CCR1, CCR3, CXCR3, CXCR4 and CXCR6 has been found (Brooke et al. 2008). However, the surface expression of these chemokine receptors was much more restricted with only one of the chemokine receptors (CXCR6) displaying a strong signal.

A major feature of solid tumor microenvironment is hypoxia, i.e. decreased availability of oxygen (Finger and Giaccia 2010). Indeed, there are studies which show an increase of chemokine receptor expression in hypoxic conditions. For example, an increase in CXCR4 surface expression in the two human breast cancer cell lines, MDA-MB-231 and MCF7, following exposure to hypoxia resulted in a significant increase in migration and invasion in response to SDF1-alpha in vitro (Cronin *et al*. 2010). However, after submitting the primary cell lines WM-115 and IGR-39, and the metastatic cell lines WM-266.4 and IGR-37 to hypoxic conditions, we still failed to find an increase in cell surface expression of the chemokine receptors studied (results not shown).

Chemokine receptors form part of the family of G-protein coupled receptors. The appropriate delivery of chemokine receptors to the cell surface to allow receptor -ligand interactions, and their subsequent retrieval from the plasma membrane are of fundamental importance for the regulation of their activity (Borroni *et al.* 2010, Drake *et al.* 2006). Both during and subsequent to synthesis, chemokine receptors undergo a process of maturation before reaching the cell membrane. They must be properly inserted into the cell membrane, achieve their correct folding while still resident at the endoplasmic reticulum, traverse from the cis- to the trans-Golgi while undergoing modification, and finally be targeted to the plasma membrane where they attain residence as mature proteins. In order for a chemokine receptor to transduce an extracellular signal it must both traffic to and be retained at the cellular surface to allow for receptor- ligand interaction. Multiple proteins not involved in the signal transduction cascade have been identified which stabilize receptor surface expression (Tan *et al.* 2004). Post-translational modifications can also alter surface expression of the receptor. In neuroblastoma, CXCR4 surface expression requires ubiquination and oligomerization of the receptor (Carlisle *et al.* 2009). Finally, factors involved in the endocytic and recycling pathways could also affect the amount of receptor expressed at the plasma membrane (Borroni *et al.* 2010). For instance, CCR7 recycling to the cell surface has been found to be dependent on ubiquitination of the receptor (Schaeuble *et al*. 2012).

In this work we have also quantified by flow cytometry the intracellular protein expression of the chemokines which activate each of the receptors studied: CXCL9, CXCL10 (CXCR3), CXCL11 (CXCR3 and CXCR7), CXCL12 (CXCR4 and CXCR7), CCL19, CCL21 (CCR7) and CCL27, CCL28 (CCR10). Most chemokines were expressed in all cell lines, although with a heterogeneous pattern. However, chemokines CXCL10 and CCL28 had a low or null expression in most of the cell lines (Table 15).

We also analyzed the secretion of chemokines in the culture medium of all cell lines (Table 16). From all the chemokines studied, the only chemokine secreted by the melanoma cell lines was CXCL10. This chemokine was secreted only by the cell lines A375 and SK-Mel-2 in low concentrations. As a positive control we also quantified the secretion of the IL-8 and Gro chemokines that are produced by human melanoma (Lázár-Molnár *et al*. 2000).

There are few studies that analyze chemokine expression at protein level in melanoma. Using immunohistochemical techniques, a correlation has been found between T immunoreactive cells and the expression of CCR10 and its ligand CCL27 in cutaneous melanocytic lesions (Simonetti *et al.* 2006). Expression of both receptor and chemokine was found in melanoma cells. Their results suggest that in human melanomas CCR10 and CCL27 may act on the ability of neoplastic cells to grow, invade tissue, disseminate to lymph nodes and to escape the host immune response. Recently, immunohistochemical expression of CXCR4, CCR7 and CCR10 and their ligands has been described in tumor cells from primary and metastatic melanomas. The CXCL12-CXCR4 and CCL27-CCR10 ratios quantified by real time RT-PCR were found to be significantly higher in thin than in thick primary melanomas, and inversely associated with the development of distant metastasis (Monteagudo *et al.* 2012). There is evidence, based on experiments designed to avoid HIV-1 infection (Yang *et al.* 1997, Bai *et al.* 1998), that expression of genetically modified chemokines (intrakines) with an added endoplasmic reticulum retention signal are able to avoid surface expression of their chemokine receptors, by interacting with the nascent chemokine receptors and retaining them in the endoplasmic reticulum. This procedure has been extended to other chemokine receptors not involved in HIV infection (Onai *et al.* 2002, Meijer *et al.* 2006). The transfection with the native chemokine without the endoplasmic retention signal also inhibited

viral entry as demonstrated by the inhibitory effects on the syncytium formation (Yang *et al.* 1997), suggesting that the native chemokine can also prevent the transport of the receptor to the cell surface. This early interaction of chemokines with their chemokine receptors could alter post-translational processes, like glycosylations (Ludwig *et al.* 2000), or interactions with escort proteins that have been found necessary for trafficking to the plasma membrane and for expression of the proteins on the cell surface in other members of the family of G-protein-coupled receptors to which chemokine receptors belong (Dong and Wu 2007, Achour *et al*. 2008), therefore resulting in intracellular accumulation of chemokine receptors and interacting chemokines. Interestingly, the only chemokine that was found to be secreted in two cell lines in our study, CXCL10, shows a minimal or no intracellular expression in the melanoma cell lines a fact that could reflect that it does not interact intracellularly with its receptor and therefore is not accumulated within the cell.

Production of stable transfected cell lines with Chemokine Receptors expression

As we could not find a significant surface expression of the chemokine receptors in our melanoma cell lines we transfected WM-115 and WM-266.4. Stable cells lines expressing CXCR3 and CXCR4 were successfully produced, as shown by an increase in gene expression (Figure 20) and, most importantly, by a stable expression of the proteins on the cells surface (Figure 21). The percentage of the subpopulation with receptor expression was approximately 50% for WM-115-pCXCR3, WM-115-pCXCR4 and

WM-266-pCXCR4 and around 75% for WM-266-pCXCR3 (Figure 21). Furthermore, this expression was stable with cell passaging and after freeze/taw cycles.

Is important to point that the higher gene expression does not correlate with having a higher percentage of the subpopulation of cells expressing the corresponding protein (Figure 20 and 21).

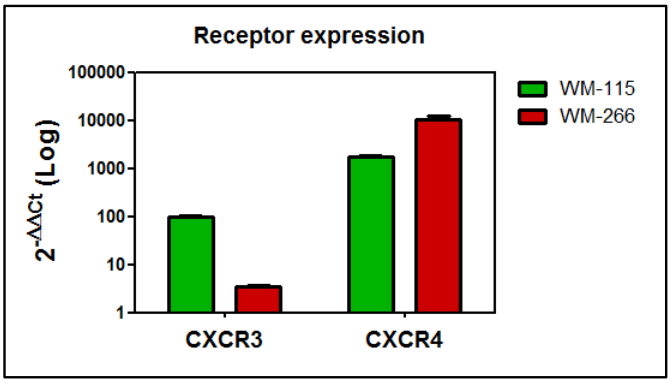

Figure 20. CXCR3 and CXCR4 gene expression in the stable cell lines produced. Transfected WM-115 is showed in green; transfected WM-266 is showed in red. Relative gene expression was calculated using $2^{-\Delta\Delta Ct}$ method is presented using RRN18S, B2M and GAPDH as housekeeping genes and the original cell line as a reference sample.

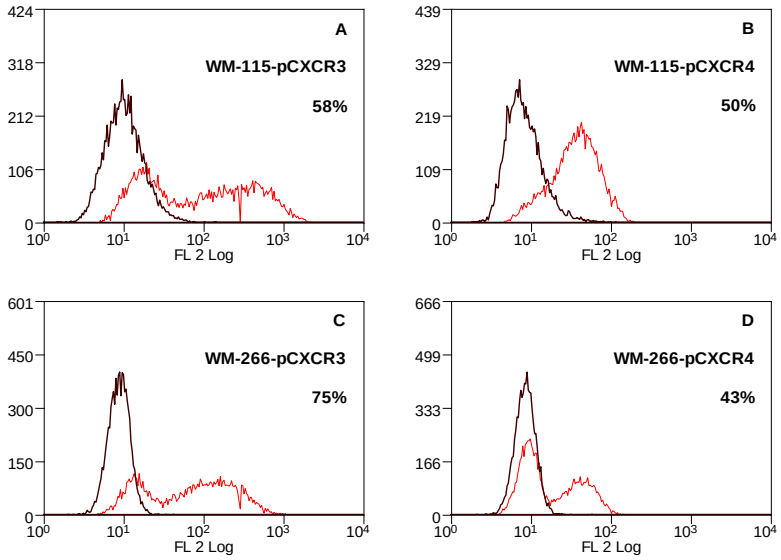

Figure 21. Subpopulations of WM-115 (A,B) and WM-266 (C, D) expressing CXCR3 (A, C) and CXCR4 (B, D). Overlaid histograms of PE fluorescence of specific anti-receptor monoclonal antibody (continuous red line) and correspondent isotopic control (discontinuous black line) are shown.

2. Xenografts and derived Cell lines

The development of human tumor xenograft models was a big step in obtaining more clinically relevant tumor models. In human tumor xenografts the malignant cells are human, although the stromal component of the tumors is rodent. Furthermore, these models have the advantage that the hosts are readily available and it is easy to have statistically valid numbers of mice (with its associated costs); also many of these models are quite reproducible and there are a wide variety of tumor lines available to xenograft. Nevertheless, the hosts are immunodeficient (specifically, in our study they are T-cell depleted) and the tumors are grown in a nonnatural sites (subcutaneously or intramuscularly, in our study).

Tumors from WM-266.4 grew faster than the ones from WM-115. The growth of the former was noticed after 10 days of inoculation while the growth of the latter was noticed after 30 days of inoculation.

After tumor disaggregation a subset of cells (WM-115-X and WM-266.4-X) was used directly for quantification of the expression of some CSC markers and of chemokines and their receptors by flow cytometry and another remaining was cultured for a few passages (WM-115-CX and WM-266.4-CX) for posterior quantification, in order to compare them with the original cell lines. When cultured, the cells exhibited some variability in the morphology and were slightly different from the original cell lines.

Furthermore, a more detailed studied was performed in 2 cell lines derived from WM-115 where all markers tested for melanoma cell lines (MAA, CSC, EMT and chemokines and receptors) were also evaluated.

i) Comparison with parental cell lines:

Changes in stem cell characteristics after xenotransplantation of WM-115 and WM-266.4 cell lines

Cell surface expression of CSC markers

When compared with the parental cell lines, the tumors WM-115-X and WM-266.6-X and the cell lines WM-115-CX and WM-266.6-CX obtained after xenotransplantation exhibited differences in the surface expression of the ABC transporters (Figures 22 and 23). The most drastic changes were observed in ABCB1 surface expression (Figure 22A,B). When compared with the parental cell line WM-115, there was more than 4-fold increase in its expression in all tumors and cells lines obtained after xenotransplantation (Figure 22A). As for WM-266.4, there was a significant decrease in tumors but a significant increase in cell lines obtained after xenotransplantation (Figure 22B). Regarding ABCG2 expression, there was an increase in its expression only in WM-115-CX but not on WM-115-X, when compared with the parental cell line (Figure 23A). As for WM-266.4, there was a sharp decrease in its expression in all tumors and cell lines obtained after transplantation (Figure 23B). Finnaly, ABCB5 was the ABC transporter that showed less variation. It was only observed a significant increase in its expression in WM-115-X when compared with the parental cell line (Figure 23A). There were no significant changes in its expression when compraing WM-266.4 parental cell line and its derived tumors and cell lines (Figure 23B).

Recent evidence indicates that WM-266.4 xenografts contain a cell subpopulation expressing ABCB5 endowed with intrinsic chemoresistance (Chartrain *et al.* 2012).

Side population

SP was analyzed in the parental cell lines and in cells cultured after xenotransplantation but not in tumors because of the reduced number of available cells. Taking into account the increase in ABCB1 expression it would be expectable to have an increase in the SP (Scharenberg *et al*. 2002). When compared with the parental cell line, there was a significant increase in the percentage of the SP in the WM-115-CX cell lines tested, which did not happen with the WM-266-CX cell lines. This might be due to the ABCG2 expression, which decreased in these cells lines when comparing to the parental cell line (Figure 23B).

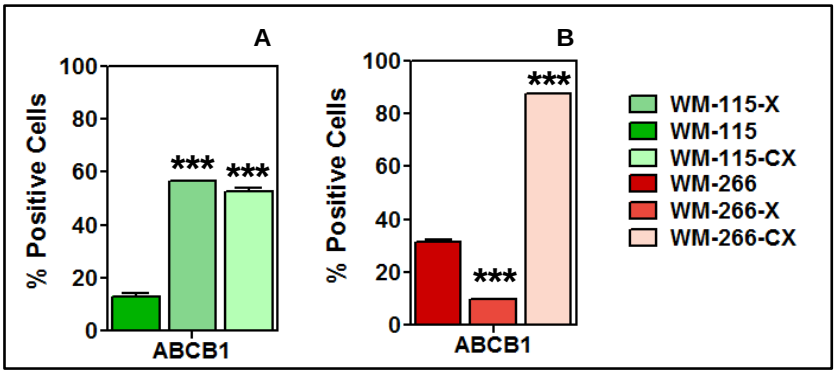

Figure 22. Surface expression of ABCB1 in WM-115 and WM-266.4 cell lines after xenotransplantation. Comparison between mean percentage of positive cells in the original melanoma cell lines WM-115 (A) and WM-266.4 (B) and the tumors and cell lines obtained after xenotransplantation. Bars refer to standard error (t-student test to compare with original cell line; ***p<0.001).

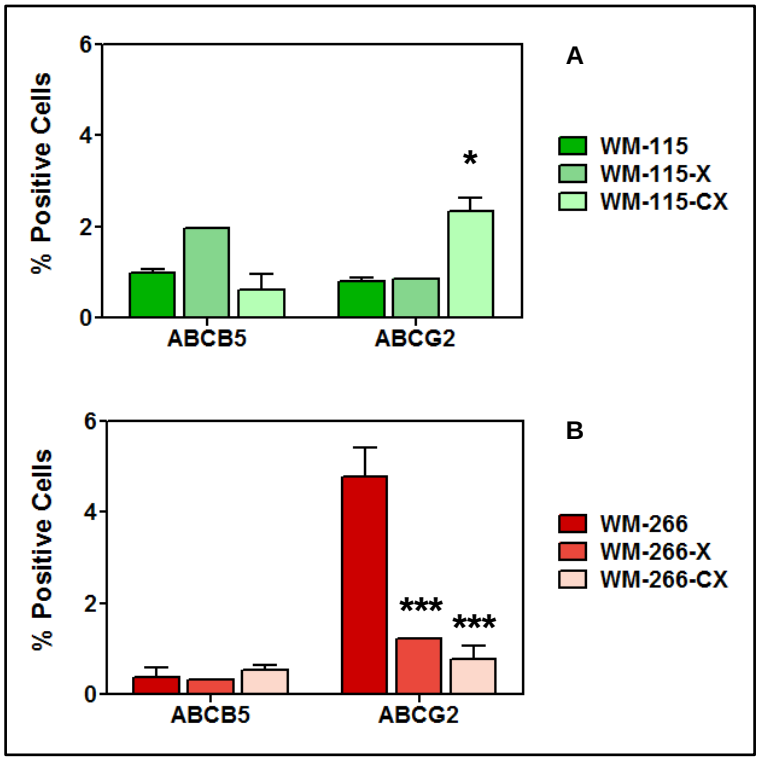

Figure 23. Surface expression of ABCB5 and ABCG2 in WM-115 and WM-266.4 cell lines after xenotransplantation. Comparison between mean percentage of positive cells in the original melanoma cell lines WM-115 (A) and WM-266.4 (B) and the tumors and cell lines obtained after xenotransplantation. Bars refer to standard error (t-student test to compare with original cell line; * $p<0.05$, ***$p<0.001$).

ii) Comparison with parental cell lines :

Surface and intracellular expression of chemokines and their receptors in WM-115 and WM-266.4 cell lines after xenotransplantation

Surface expression of chemokine receptors

We xenografted the primary cell line WM-115 and the metastatic cell line WM-266.4 in athymic nude mice expecting than an *in vivo* environment and stimuli to these established melanoma cell lines would lead to an increase in the chemokine receptors surface expression that was not detected in the cell lines tested.

When compared with the original cell lines, the WM-115-X and WM-266-X tumors obtained after xenotransplantation, as well as the cell lines derived from them (WM-115-CX and WM-266-CX) had similar patterns of cell surface expression of receptors, that is, minute or no expression was observed, without significant differences to the original cell lines.

WM-115-X and WM-266-X were obtained from collagenase treatment of these tumors so we can consider that the disaggregation procedure could influence the detection of the receptors at this level, as in the case of the cell lines these were detached solely using EDTA to avoid the effect of trypsin on the surface cell receptors.

Intracellular expression of chemokine receptors

When compared with the original cell line, the WM-115-X xenografts, as well as the derived WM-115-CX cell lines, showed a substantial increase in the expression of CCR7 and CCR10, a considerable decrease in the expression of CXCR4 and a slight but significant decrease in the expression of CXCR3. CXCR7 showed an increased expression in the WM-115-X

xenografts that was not observed in the derived WM-115-CX cell lines that were not significantly different from the original cell line. (Figure 24A, Table 17). WM-266-X xenografts showed a significant decrease of CXCR4 and significant increases of CXCR7 and CCR7, when compared with the original cell line, while the WM-266-CX derived cell lines presented increases of CXCR3, CCR7 and CCR10 with respect to the original cell line. (Figure 24B, Table 17).

Table 17. Intracellular expression of chemokine receptors after xenotransplantation. Mean percentage (%) of cells which significantly expressed ($p<0.05$) chemokine receptors intracellularly; MFI represents the mean fluorescence index calculated as the ratio between the mean fluorescence of samples stained with the mAb anti-receptor and correspondent isotypic control (WM-115-X and WM-266.4-X represent the xenografts; WM-115-CX and WM-266.4-CX represent the cell lines obtained after culturing the xenografts).

	CXCR3		***CXCR4***		***CXCR7***		***CCR7***		***CCR10***	
	%	***MFI***	***%***	***MFI***	***%***	***MFI***	***%***	***MFI***	***%***	***MFI***
WM-115	88.59	5.40	92.45	3.95	4.97	1.57	20.16	1.70	13.67	1.57
WM-115-X	59.84	3.46	14.10	1.62	58.89	4.14	75.32	4.10	66.90	3.47
WM-115-CX	76.11	3.95	12.14	1.65	5.44	1.34	82.03	3.44	81.90	3.44
WM-266	74.08	2.22	96.26	3.39	21.53	1.68	40.16	1.69	24.00	1.63
WM-266-X	28.19	2.24	6.71	1.26	13.96	2.08	56.31	2.50	28.54	1.83
WM-266-CX	91.65	4.41	94.17	3.74	53.67	2.34	72.95	32.77	88.62	4.60

Intracellular expression of chemokines

In WM-115-X xenografts a general decrease of chemokine expression is observed to levels similar to negative controls for most of the studied chemokines with respect to the initial WM-115 cell line, as can be detected by mean fluorescence index (Table 18). In WM-115-CX lines derived after xenotransplantation an increased expression of all chemokines is observed, when compared with the original cell line (Figure 25A, Table 18). In WM-266-X xenografts, a general decrease of chemokine expression is also observed when compared with WM-266.4 cell line, but that does not reach negative control values. The WM-266-CX cell lines derived from the xenografts only show significant increased expression of CXCL12 and CCL19 (Figure 25B, Table 18) with respect to the original cell line.

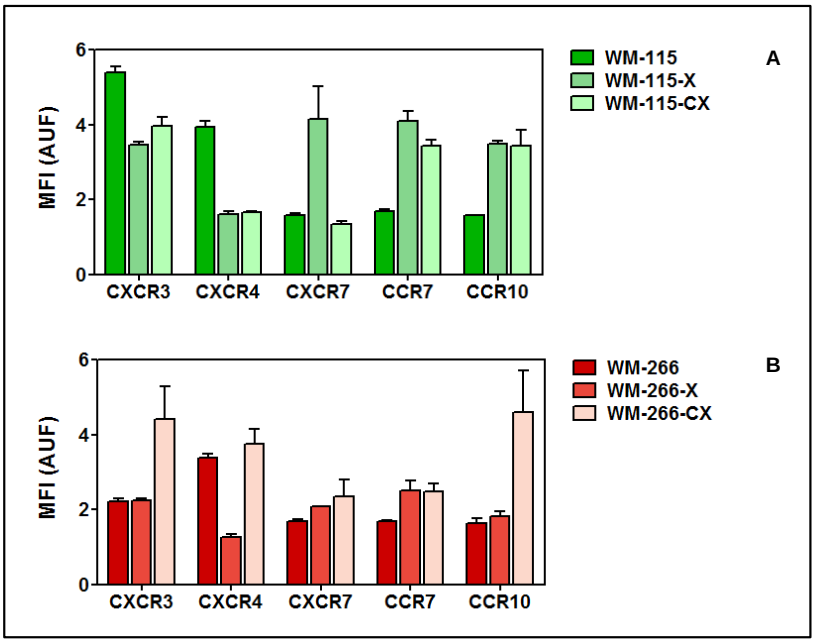

Figure 24. Intracellular expression of chemokine receptors in WM-115 and WM-266.4 cell lines after xenotransplantation. Comparison between mean intracellular expression of chemokine receptors in the original melanoma cell lines WM-115 (a) and WM-266.4 (b) and the tumors and cell lines obtained after xenotransplantation. Bars refer to standard error (* $p<0.05$).

Table 18. Intracellular chemokine expression after xenotransplantation. Mean percentage (%) of cells which significantly expressed ($p<0.05$) chemokine ligands intracellularly; MFI represents the mean fluorescence index calculated as the ratio between the mean fluorescence of samples stained with the mAb anti-receptor and correspondent isotypic control (WM-115-X and WM-266.4-X represent the xenografts; WM-115-CX and WM-266.4-CX represent the cell lines obtained after culturing the xenografts).

	CXCL9		***CXCL10***		***CXCL11***		***CXCL12***		***CCL19***		***CCL21***		***CCL27***		***CCL28***	
	%	***MFI***	***%***	***MFI***	***%***	***MFI***	***%***	***MFI***	***%***	***MFI***	***%***	***MFI***	***%***	***MFI***	***%***	***MFI***
WM-115	28.31	2.06	0.46	1.12	2.66	1.24	81.77	3.96	98.79	20.00	15.55	1.65	94.06	4.89	ns	0.94
WM-115-X	ns	1.10	ns	0.90	ns	0.96	0.30	0.94	50.38	3.80	ns	1.05	22.39	1.62	ns	0.97
WM-115-CX	50.39	5.36	4.33	2.54	15.24	5.25	79.83	5.08	98.64	36.76	14.46	4.24	98.17	13.36	3.51	2.98
WM-266	71.84	4.57	15.19	1.74	46.26	3.24	98.24	9.56	98.58	30.17	60.21	3.71	98.50	11.38	1.14	1.25
WM-266-X	2.12	1.46	2.53	1.28	22.73	1.93	3.81	1.42	81.95	10.43	2.38	1.33	54.41	3.39	1.25	1.19
WM-266-CX	67.84	7.02	3.72	1.41	37.75	4.98	95.52	14.66	98.10	43.82	50.06	4.00	97.12	12.36	0.29	0.97

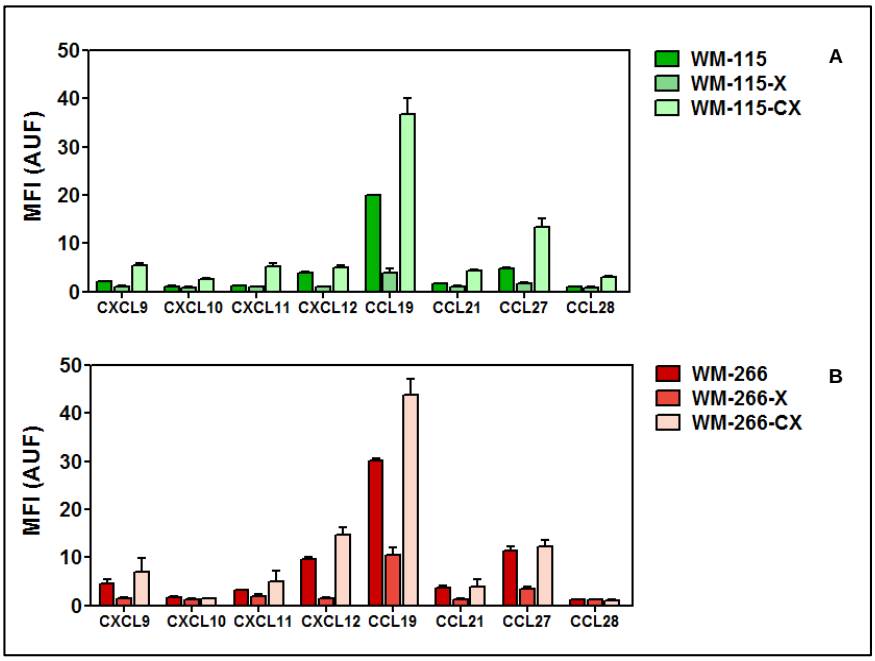

Figure 25. Intracellular expression of chemokines in WM-115 and WM-266.4 cell lines after xenotransplantation. Comparison between mean intracellular expression of chemokines in the original melanoma cell lines WM-115 (a) and WM-266.4 (b) and the tumors and cell lines obtained after xenotransplantation. Bars refer to standard error (* $p<0.05$).

In our study a selection process seems to take place within the tumoral population in the xenograft, especially in the case of WM-115 derived from a primary tumor where the changes observed in the intracellular chemokine receptors that have been involved in tumoral growth and progression are maintained in the derived cell lines in culture medium. However, intracellular chemokine levels show a general decrease in the xenografts, being more pronounced in WM-115-X than in WM-266-X and that seems to be due to environmental causes, as these changes are not maintained in the derived cell lines.

In summary, we find coexpression of chemokine receptors and their ligands in human melanoma cell lines. However, this expression is intracellular and receptors are not found at the cell membrane nor chemokines are secreted to the cell medium. The levels of intracellularly expressed chemokine receptors and their ligands show dynamic variations after xenotransplantation that differ depending on the origin of the cell line but we still cannot find surface expression of the receptor, as we expected. These changes could affect cell trafficking assays that correlate *in vitro* and *in vivo* data.

Our results could also have implications in the studies that analyze chemokines or chemokine receptors expression in melanomas that do not ascertain the cell membrane location of chemokine receptors or the secretion of chemokines to the extracellular medium.

iii) Detailed study of 2 cell lines established from WM-115 after xenotransplantation

WM115 vs WM115-CX-SC and WM115-CX-IM

Because of their great increase in the SP there were two cell lines derived from tumors of WM-115 cell line that were studied in more detail, especially at the CSC and EMT level. These cell lines were established from two tumors produced in the same animal, one which arise from sub-cutaneous inoculation of WM-115 (hereafter called WM-115-CX-SC) and the other which arise from its intra-muscular inoculation (hereafter called WM-115-CX-IM).

Regarding the surface expression of melanoma-associated antigens (Table 19) we could observe in both cell lines a decrease in the subpopulation $CD146^+$ (concomitant with a decrease in its gene expression) and an increase in the Melan-A^+. Also, genes like gp100, TPRM1 and MAGE1 were slightly augmented in both cell lines. Interestingly TYR was extremely overexpressed in WM-115-CX-SC but not in WM-115-CX-IM (Figure 26).

Table 19 Expression of Melanoma-associated antigens (MAA) after xenoransplantation. Mean percentage (%) of cells which significantly expressed ($p<0.05$) MAA; MFI represents the mean fluorescence index calculated as the ratio between the mean fluorescence of samples stained with the mAb anti-MAA and correspondent isotypic control (n =3).

Cell line	*CD61*		*CD146*		*Melan-A*	
	%	*MFI*	*%*	*MFI*	*%*	*MFI*
WM-115	99.22	129.71	95.85	74.39	82.10	11.08
WM-115-CX-SC	95.00	37.76	72.45	91.86	95.33	6.36
WM-115-CX-IM	97.08	37.03	74.26	98.26	98.43	38.01

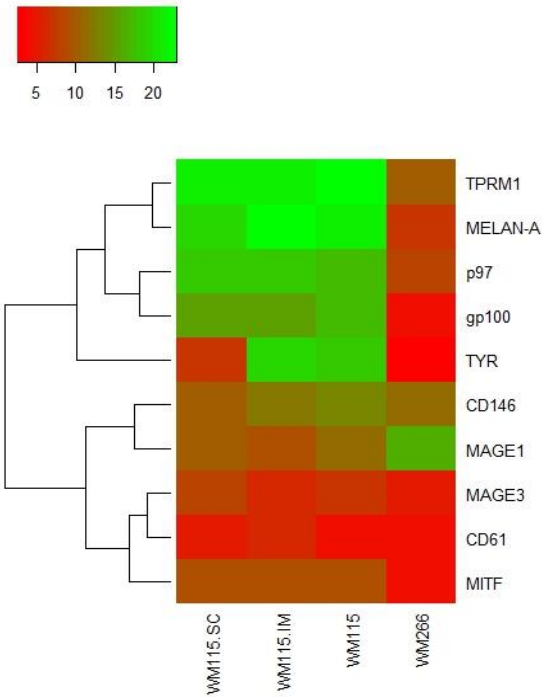

Figure 26. Gene expression of Melanoma-associated antigens (MAA) after xenotransplantation. Relative gene expression is presented in a heatmap with the ΔCts calculated using RRN18S, PGK1, ACTB and RPL13A as housekeeping genes. Red represent genes that are more expressed than green. Genes that were not amplified are shown in white.

The ABCB1+ subpopulation increased in both cell lines (Table 20) although this increase was not seen at the gene level (Figure 27). However, no changes were seen for the other ABC transporters tested. Regarding the SP, there was an increase in both cell lines although it was more pronounced on WM-115-CX-IM (Table 20). Nevertheless, the percentage of SP found in this cells line was highly variable between experiments. In Figure 28 can be seen an example where 12% of SP was analyzed.

Table 20. Surface expression of ABC-transporters and SP after xenotransplantation. Mean percentage (%) of cells which significantly expressed ($p<0.05$) ABC-transporters; MFI represents the mean fluorescence index calculated as the ratio between the mean fluorescence of samples stained with the mAb anti- ABC-transporter and correspondent isotypic control (n =3).

Cell line	*ABCB1*		*ABCB5*		*ABCG2*		*% of SP (Mean ± SE)*
	%	*MFI*	*%*	*MFI*	*%*	*MFI*	
WM-115	13.06	1.91	0.99	1.19	0.79	1.16	0.12 ± 0.04
WM-115-CX-SC	61.43	4.46	ns	ns	ns	ns	1.27 ± 0.36
WM-115-CX-IM	45.63	2.53	ns	ns	ns	ns	4.32 ± 0.88

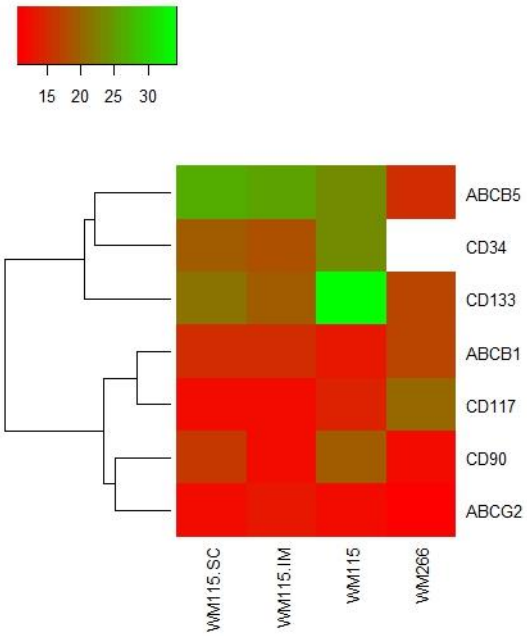

Figure 27. Gene expression of cancer stem cell markers after xenotransplantation. Relative gene expression is presented in a heatmap with the ΔCts calculated using RRN18S, PGK1, ACTB and RPL13A as housekeeping genes. Red represent genes that are more expressed than green. Genes that were not amplified are shown in white.

The importance of ABC transporters to the SP, discussed in the previous chapter, is corroborated by the increase in SP after xenotransplantation in both WM-115-X and WM-266.4-X cell lines. The increase in SP in WM-115-X cell lines might be related to the increase in ABCG2 gene expression as this is the only transporter whose expression increases significantly in WM-115-X-IM (ca. 3-fold) when compared with WM-115-X-SC, which in turn is reflected in a proportional increase in SP. As for WM-266.4, the slight increase in SP observed only in WM-266-X-IM might be related to the minor increase in ABCB5 expression, which is the only ABC transporter whose gene expression is simultaneously different between WM-266-X-IM and the SC and parental cell lines.

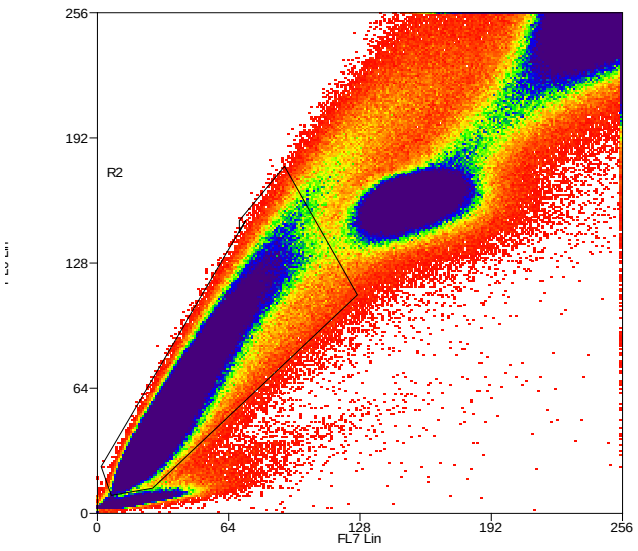

Figure 28. Side Population found in WM-115-CX-IM

The CD34+ subpopulation disappeared in both cell lines (Table 21) although an increase in its gene level expression was found (Figure 27). On the other hand, the parental cell line did not have a CD90+ subpopulation which appeared in both cell lines (Table 21, concomitant with an increased gene expression, Figure 27). Regarding CD117, although its gene expression was increased in both cell lines (Figure 27), only in WM-115-CX-SC showed a CD117+ subpopulation (Table 21). CD133 was highly overexpressed in both cell lines although this was not seen at the protein level as no CD133+ subpopulation was detected (Table 21, Figure 27).

Table 21. Surface expression of commonly used CSC markers after xenotransplantation. Mean percentage (%) of cells which significantly expressed ($p<0.05$) CSC markers; MFI represents the mean fluorescence index calculated as the ratio between the mean fluorescence of samples stained with the mAb anti-CSC marker and correspondent isotypic control (n =3).

Cell line	***CD34***		***CD90***		***CD117***		***CD133***	
	%	***MFI***	***%***	***MFI***	***%***	***MFI***	***%***	***MFI***
WM-115	2.75	0.98	ns	ns	ns	ns	ns	ns
WM-115-CX-SC	ns	ns	6.80	1.63	1.45	0.98	ns	ns
WM-115-CX-IM	ns	ns	10.44	2.24	ns	ns	ns	ns

Regarding the neuronal stem cell markers tested, changes were found in TUJ1 (Table 22, Figure 29). Although there was no increase at the gene level, a TUJ1+ subpopulation was found in WM-115-CX-SC. Also, CD271 gene expression slightly increased in WM-115-CX-SC.

Table 22. Expression of neuronal stem cell markers after xenotransplantation. Mean percentage (%) of cells which significantly expressed ($p<0.05$) these CSC markers; MFI represents the mean fluorescence index calculated as the ratio between the mean fluorescence of samples stained with the mAb anti-CSC marker and correspondent isotypic control (n =3).

Cell line	*TUJ1*		*Nestin*		*CD271*	
	%	*MFI*	*%*	*MFI*	*%*	*MFI*
WM-115	ns	ns	98.58	320.23	70.84	17.56
WM-115-CX-SC	6.39	1.47	98.34	146.11	58.31	18.55
WM-115-CX-IM	ns	ns	91.56	77.70	63.99	9.75

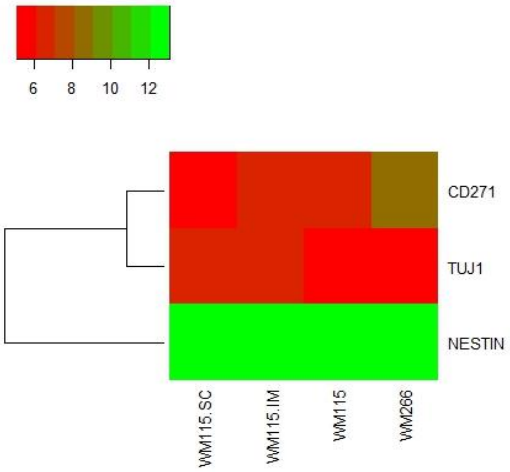

Figure 29. Gene expression of neuronal stem cell markers after xenotransplantation. Relative gene expression is presented in a heatmap with the ΔCts calculated using RRN18S, PGK1, ACTB and RPL13A as housekeeping genes. Red represent genes that are more expressed than green. Genes that were not amplified are shown in white.

As for gene expression of pluripotency stem cell markers, there is a slight increase in the gene expression of OCT-4, NANOG, SOX-2 and caspase-3 in WM-115-CX-IM, while DDPA5 was not detected in this cell line and had comparable level of expression in WM-115-CX-SC (Figure 30).

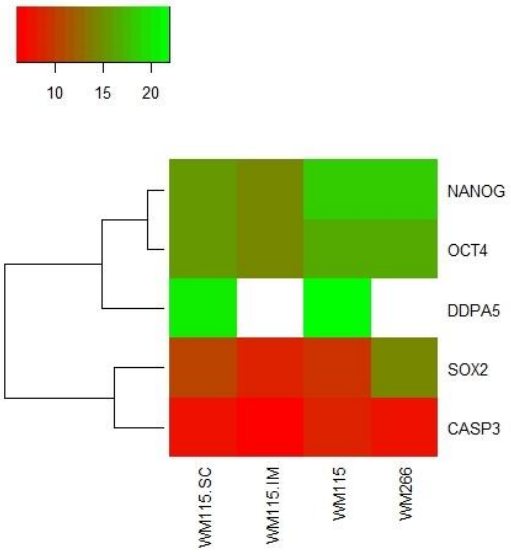

Figure 30. Gene expression of pluripotency stem cell markers after xenotransplantation. Relative gene expression is presented in a heatmap with the ΔCts calculated using RRN18S, PGK1, ACTB and RPL13A as housekeeping genes. Red represent genes that are more expressed than green. Genes that were not amplified are shown in white.

There was a slight decrease in the percentage of the N-cadherin+ subpopulation found in WM-115-CX-SC. As for E-cadherin, a small subpopulation was found in both cell lines, although no gene expression was detected (Table 23, Figure 31). Regarding the gene expression of the cell adhesion molecules, EpCAM slightly increased in both cell lines and VCAM was highly increased while NCAM and AlCAM were slightly overexpressed only in WM-115-CX-IM (Figure 20).

Table 23. Surface expression of EMT markers after xenotransplantation. Mean percentage (%) of cells which significantly expressed ($p<0.05$) these EMT markers; MFI represents the mean fluorescence index calculated as the ratio between the mean fluorescence of samples stained with the mAb anti-EMT marker and correspondent isotypic control (n =3).

Cell line	***Ncad***		***Ecad***	
	%	***MFI***	***%***	***MFI***
WM-115	39.34	3.66	0.65	1.18
WM-115-CX-SC	21.49	2.42	3.37	2.37
WM-115-CX-IM	36.76	2.16	3.62	1.70

It has been shown by others that E-cadherin loss is often associated with CD146 increases (Haass *et al.* 2005) which is in accordance with our gene expression data.

As can be seen in Figure 31 the rest of the genes related to EMT (SPARC, SPP1, SNAI1, SNAI2 and VIM) were slightly underexpressed when compared to the parental cell line with the exception of FN1 which was slightly overexpressed in WM-115-CX-SC.

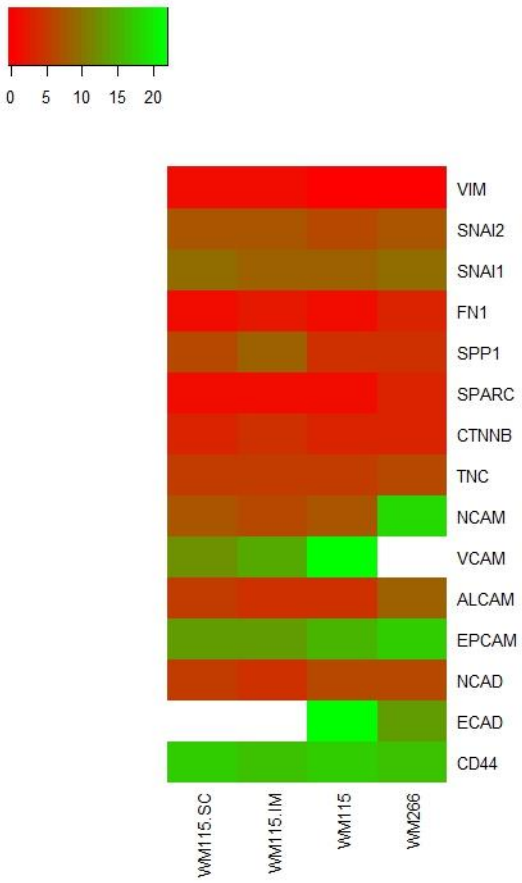

Figure 31. Gene expression of EMT markers after xenotransplantation. Relative gene expression is presented in a heatmap with the ΔCts calculated using RRN18S, PGK1, ACTB and RPL13A as housekeeping genes. Red represent genes that are more expressed than green. Genes that were not amplified are shown in white.

3. Xenografts versus human melanoma cell lines

The validity of a model used to study a biological question in the context of cancer, depends on how faithfully it reproduces the characteristic of the tumor. Although cancer cell lines are a common experimental model as they provide reproducible results (if used within the same range of passages and with the same protocol) they are limited because they have been established on the late time in the history of the original cancer they were derived from and, therefore, represent one time point of the tumor and not its dynamic evolution over time.

In this study we used thirteen established human melanoma cell lines, five established from primary tumors and eight established from metastases at different locations (skin, brain, lymph nodes and lung). In summary, if we analyse the gene expression of all the quantified genes in this study (Figure 32) it is obvious that there is no specific pattern of gene expression for primary and metastatic cell lines. On the contrary, we can appreciate the variability of the gene expression between all the cell lines.

Xenotransplantation models, based on immunocompromised mice, are particularly successful in mimicking advanced, metastatic melanoma as their diminished ability to mount an effective immune response allows the growth of human melanomas and the expression of malignant properties (Zaidi *et al.* 2008). It is commonly accepted that the function of cell adhesion molecules, and most of the intervenients in cancer formation and spreading, is profoundly influenced by the extracellular environment. Therefore, melanoma invasion should be examined under more physiological

conditions, namely using xenografts models, which are able to provide a history sequence and provide a more physiological microenvironment for human cells (van Starveren *et al*. 2009).

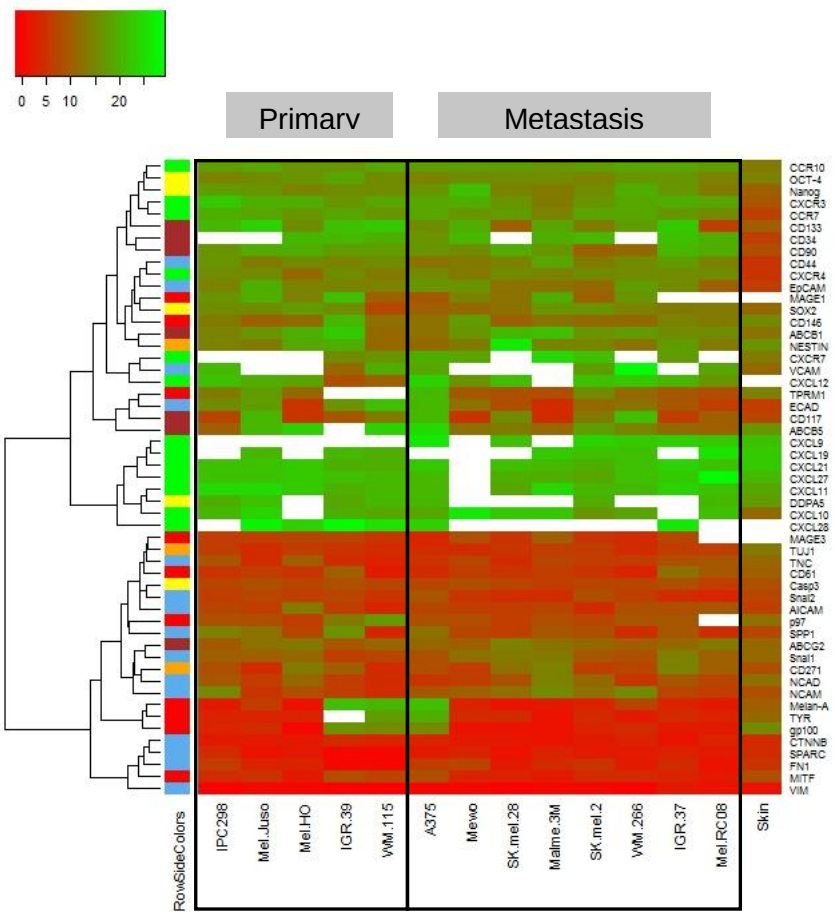

Figure 32. Gene expression in human melanoma cell lines of all tested genes. Relative gene expression is is presented in a heatmap with the ΔCts calculated using RRN18S, PGK1, ACTB, RPL13A and B2M as housekeeping genes. Red represent genes that are more expressed than green. Genes that were not amplified are shown in white.

A comparative analysis of global gene expression has been performed elsewhere between human melanoma cell lines with different metastatic capacity and the xenografts obtained by their subcutaneous injection into immunocompromised mice, demonstrating extensive differential expression between both models (Xi *et al.* 2008). These variations can be due to selection of determined subpopulations with different tumorigenic capacity or to the effect of the different microenvironment within the nude mouse.

In this study we used an athymic nude mice model to perform the xenografts. These mice are not severely immunocompromised, they lack T cells but the B cells, dendritic cells and granulocytes are all relatively intact, and there is a compensatory increase in both natural killer (NK)-cell activity and tumoricidal macrophages in these mice. Then, it is expectable that, by the time we removed the tumors, they have already escaped immune surveillance and cell killing by the immune cells.

Analysing collectively all the data regarding the xenotransplants (i.e., WM115 vs WM115-CX-SC and WM115-CX-IM), we can appreciate significant changes both at protein and gene level.

The ABCB1+ subpopulation increased in both cell lines (Table 20) although this increase was not seen at the gene level (Figure 27). Regarding the SP, there was an increase in both cell lines although being more pronounced on WM-115-CX-IM (Table 20). This increase might be related to the increase in ABCG2 gene expression as this is the only transporter whose expression increases significantly in WM-115-X-IM. Furthermore, the parental cell line did not have a CD90+ subpopulation which appeared in both cell lines (Table 21, concomitant with an increased gene expression, Figure 27). Regarding CD117, although its gene expression was increased in both cell lines (Figure 27), only in WM-115-CX-SC showed a CD117+ subpopulation (Table 21). CD133 was highly overexpressed in both cell lines although this

was not seen at the protein level as no CD133+ subpopulation was detected (Table 21, Figure 27). As for gene expression of pluripotency stem cell markers, there is a slight increase in the gene expression of OCT-4, NANOG, SOX-2 and caspase-3 in WM-115-CX-IM. Concerning EMT marker, there was a slight decrease in the percentage of the N-cadherin+ subpopulation found in WM-115-CX-SC. As for E-cadherin, a small subpopulation was found in both cell lines, although no gene expression was detected (Table 23, Figure 31). Regarding the gene expression of the cell adhesion molecules, EpCAM slightly increased in both cell lines and VCAM was highly increased while NCAM and AlCAM were slightly overexpressed only in WM-115-CX-IM (Figure 20).

In summary, the cell lines stablished after transplantation are different from the parental cell lines, having increased levels of CSC markers, pluripotency stem markers and EMT markers (specially adhesion molecules). Furthermore, slight different patterns can be found depending on the injection site.

Conclusions

Conclusions

1. Flow cytometry and real-time PCR allow the characterisation of human melanoma cell lines established from different origins (primary or metastatic tumor) reflecting the heterogeneity of human melanoma.

2. With the markers studied we could not find a correlation between the pattern of expression and the origin of the cell line (primary or metastatic tumor).

3. The selective pressure exerted by the athymic nude mice microenvironment produced important variations in the gene and protein expression profiles of the human melanoma cell lines transplanted. The variations obtained depend on the location of cell inoculation (subcutaneous or intramuscular).

References

- Achour, L., Labbé-Jullié, C., Scott, M. G. H. & Marullo, S. An escort for GPCRs: implications for regulation of receptor density at the cell surface. Trends Pharmacol. Sci. 29, 528–535 (2008).

- Akasaka, K. et al. Loss of class III beta-tubulin induced by histone deacetylation is associated with chemosensitivity to paclitaxel in malignant melanoma cells. J. Invest. Dermatol. 129, 1516–1526 (2009).

- Al Dhaybi, R., Sartelet, H., Powell, J. & Kokta, V. Expression of CD133+ cancer stem cells in childhood malignant melanoma and its correlation with metastasis. Mod. Pathol. 23, 376–380 (2010).

- Alexeev, V. & Yoon, K. Distinctive role of the cKit receptor tyrosine kinase signaling in mammalian melanocytes. J. Invest. Dermatol. 126, 1102–1110 (2006).

- Allen, S. J., Crown, S. E. & Handel, T. M. Chemokine:Receptor Structure, Interactions, and Antagonism. Annu. Rev. Immunol. 25, 787–820 (2007).

- Bai, X., Chen, J. D., Yang, a G., Torti, F. & Chen, S. Y. Genetic co-inactivation of macrophage- and T-tropic HIV-1 chemokine coreceptors CCR-5 and CXCR-4 by intrakines. Gene Ther. 5, 984–994 (1998).

- Bao, B. et al. Targeting CSCs within the tumor microenvironment for cancer therapy: a potential role of mesenchymal stem cells. Expert Opin. Ther. Targets 16, 1041–1054 (2012).

- Becker, J. C. et al. Mouse models for melanoma: A personal perspective. Exp. Dermatol. 19, 157–164 (2010).

- Ben-Baruch, A. Organ selectivity in metastasis: regulation by chemokines and their receptors. Clin. Exp. Metastasis 25, 345–356 (2008).

- Bertrand, Y., Demeule, M., Michaud-Levesque, J. & Béliveau, R. Melanotransferrin induces human melanoma SK-Mel-28 cell invasion in vivo. Biochem. Biophys. Res. Commun. 353, 418–423 (2007).

- Boiko, A. D. et al. Human melanoma-initiating cells express neural crest nerve growth factor receptor CD271. Nature 466, 133–137 (2010).

- Bongiorno, M. R., Doukaki, S., Malleo, F. & Aricò, M. Identification of progenitor cancer stem cell in lentigo maligna melanoma. Dermatol. Ther. 21 Suppl 1, S1–5 (2008).

- Borroni, E. M., Mantovani, A., Locati, M. & Bonecchi, R. Chemokine receptors intracellular trafficking. Pharmacol. Ther. 127, 1–8 (2010).

- Bradley, J. E., Ramirez, G. & Hagood, J. S. Roles and regulation of Thy-1, a context-dependent modulator of cell phenotype. BioFactors 35, 258–265 (2009).

- Brooke, G., Tong, H., Levesque, J.-P. & Atkinson, K. Molecular trafficking mechanisms of multipotent mesenchymal stem cells derived from human bone marrow and placenta. Stem Cells Dev. 17, 929–940 (2008).

- Bunting, K. D., Zhou, S., Lu, T. & Sorrentino, B. P. Enforced P-glycoprotein pump function in murine bone marrow cells results in expansion of side population stem cells in vitro and repopulating cells in vivo. Blood 96, 902–909 (2000).

- Burns, J. M. et al. A novel chemokine receptor for SDF-1 and I-TAC involved in cell survival, cell adhesion, and tumor development. J. Exp. Med. 203, 2201–2213 (2006).

- Carlisle, A. J., Lyttle, C. a, Carlisle, R. Y. & Maris, J. M. CXCR4 expression heterogeneity in neuroblastoma cells due to ligand-independent regulation. Mol. Cancer 8, 126 (2009).

- Casado, J. G. et al. Expression of adhesion molecules and ligands for activating and costimulatory receptors involved in cell-mediated cytotoxicity in a large panel of human melanoma cell lines. Cancer Immunol. Immunother. 58, 1517–1526 (2009).

- Chambers, A. F., Groom, A. C. & MacDonald, I. C. Dissemination and growth of cancer cells in metastatic sites. Nat. Rev. Cancer 2, 563–572 (2002).

- Charpentier, M. & Martin, S. Interplay of Stem Cell Characteristics, EMT, and Microtentacles in Circulating Breast Tumor Cells. Cancers (Basel). 5, 1545–1565 (2013).

- Chartrain, M. et al. Melanoma Chemotherapy Leads to the Selection of ABCB5-Expressing Cells. PLoS One 7, e36762 (2012).

- Chen, K. G., Valencia, J. C., Gillet, J.-P., Hearing, V. J. & Gottesman, M. M. Involvement of ABC transporters in melanogenesis and the development of multidrug resistance of melanoma. Pigment Cell Melanoma Res. 22, 740–749 (2009).

- Civenni, G. et al. Human CD271-positive melanoma stem cells associated with metastasis establish tumor heterogeneity and long-term growth. Cancer Res. 71, 3098–3109 (2011).

- Cronin, P. A, Wang, J. H. & Redmond, H. P. Hypoxia increases the metastatic ability of breast cancer cells via upregulation of CXCR4. BMC Cancer 10, 225 (2010).

- Cyster, J. G. Chemokines and Cell Migration in Secondary Lymphoid Organs. Science. 286, 2098–2102 (1999).

- Derveaux, S., Vandesompele, J. & Hellemans, J. How to do successful gene expression analysis using real-time PCR. Methods 50, 227–230 (2010).

- Dong, C. & Wu, G. Regulation of anterograde transport of adrenergic and angiotensin II receptors by Rab2 and Rab6 GTPases. Cell. Signal. 19, 2388–2399 (2007).

- Dou, J. et al. Identifying tumor stem-like cells in mouse melanoma cell lines by analyzing the characteristics of side population cells. Cell Biol. Int. 33, 807–815 (2009).

- Drake, M. T., Shenoy, S. K. & Lefkowitz, R. J. Trafficking of G protein-coupled receptors. Circ. Res. 99, 570–582 (2006).

- Du, J. et al. MLANA/MART1 and SILV/PMEL17/GP100 are transcriptionally regulated by MITF in melanocytes and melanoma. Am. J. Pathol. 163, 333–343 (2003).

- Essner, R., Lee, J. H., Wanek, L. a, Itakura, H. & Morton, D. L. Contemporary surgical treatment of advanced-stage melanoma. Arch Surg 139, 961–967 (2004).

- Fang, D. et al. A tumorigenic subpopulation with stem cell properties in melanomas. Cancer Res. 65, 9328–9337 (2005).

- Ferlay J, Soerjomataram I, Ervik M, Dikshit R, Eser S, Mathers C, Rebelo M, Parkin DM, Forman D, Bray, F. GLOBOCAN 2012 v1.0, Cancer Incidence and Mortality Worldwide: IARC CancerBase No. 11 [Internet]. Lyon, France: International Agency for Research on Cancer; 2013. at <http://globocan.iarc.fr>

- Finger, E. C. & Giaccia, A. J. Hypoxia, inflammation, and the tumor microenvironment in metastatic disease. Cancer Metastasis Rev. 29, 285–293 (2010).

- Frank, N. Y. et al. ABCB5-mediated doxorubicin transport and chemoresistance in human malignant melanoma. Cancer Res. 65, 4320–4333 (2005).

- Frank, N. Y. et al. VEGFR-1 expressed by malignant melanoma-initiating cells is required for tumor growth. Cancer Res. 71, 1474–1485 (2011).

- Fukunaga-Kalabis, M. et al. Tenascin-C promotes melanoma progression by maintaining the ABCB5-positive side population. Oncogene 29, 6115–6124 (2010).

- Garbe, C., Eigentler, T. K., Keilholz, U., Hauschild, a. & Kirkwood, J. M. Systematic Review of Medical Treatment in Melanoma: Current Status and Future Prospects. Oncologist 16, 5–24 (2011).

- Gil-Benso, R. et al. Characterization of a new human melanoma cell line with CD133 expression. Hum. Cell 25, 61–67 (2012).

- Gillet, J.-P., Varma, S. & Gottesman, M. M. The clinical relevance of cancer cell lines. J. Natl. Cancer Inst. 105, 452–458 (2013).

- Gottesman, M. M., Fojo, T. & Bates, S. E. Multidrug resistance in cancer: role of ATP-dependent Transporters. Nat. Rev. Cancer 2, 48–58 (2002).

- Grichnik, J. M. et al. Melanoma, a tumor based on a mutant stem cell? J. Invest. Dermatol. 126, 142–153 (2006).

- Haass, N. K., Smalley, K. S. M., Li, L. & Herlyn, M. Adhesion, migration and communication in melanocytes and melanoma. Pigment cell Res. 18, 150–159 (2005).

- Hadnagy, A., Gaboury, L., Beaulieu, R. & Balicki, D. SP analysis may be used to identify cancer stem cell populations. Exp. Cell Res. 312, 3701–3710 (2006).

- Hammock, L. et al. Chromogenic in situ hybridization analysis of melastatin mRNA expression in melanomas from American Joint Committee on Cancer stage I and II patients with recurrent melanoma. J. Cutan. Pathol. 33, 599–607 (2006).

- Hatina, J., Fernandes, M. I., Hoffmann, M. J. and Zeimet, A. G. Cancer Stem Cells – Basic Biological Properties and Experimental Approaches. eLS (2003)

- Hearing, V. J. Determination of Melanin Synthetic Pathways. J. Invest. Dermatol. 131, E1-E8 (2011).

- Hieken, T. J. et al. Beta3 integrin expression in melanoma predicts subsequent metastasis. J. Surg. Res. 63, 169–173 (1996).

- Higgins, C. F. ABC transporters: physiology, structure and mechanism--an overview. Res. Microbiol. 152, 205–210 (2001).

- Kakinuma, T. & Hwang, S. T. Chemokines, chemokine receptors, and cancer metastasis. J. Leukoc. Biol. 79, 639–651 (2006).
- Kawada, K. et al. Pivotal Role of CXCR3 in Melanoma Cell Metastasis to Lymph Nodes Pivotal Role of CXCR3 in Melanoma Cell Metastasis to Lymph Nodes. 4010–4017 (2004).
- Keshet, G. I. et al. MDR1 expression identifies human melanoma stem cells. Biochem. Biophys. Res. Commun. 368, 930–936 (2008).
- Kim, M. et al. CXCR4 signaling regulates metastasis of chemoresistant melanoma cells by a lymphatic metastatic niche. Cancer Res. 70, 10411–10421 (2010).
- Kim, S.-W. et al. Cytoplasmic trapping of CXCR4 in hepatocellular carcinoma cell lines. Cancer Res. Treat. 40, 53–61 (2008).
- Klein, W. M. et al. Increased expression of stem cell markers in malignant melanoma. Mod. Pathol. 20, 102–107 (2007).
- Kong, D. & Yamori, T. JFCR39, a panel of 39 human cancer cell lines, and its application in the discovery and development of anticancer drugs. Bioorg. Med. Chem. 20, 1947–1951 (2012).
- Krementz, E. T. et al. Regional chemotherapy for melanoma. A 35-year experience. Ann Surg 220, 520–525 (1994).
- Kulbe, H., Levinson, N. R., Balkwill, F. & Wilson, J. L. The chemokine network in cancer--much more than directing cell movement. Int. J. Dev. Biol. 48, 489–496 (2004).
- Kuphal, S., Bauer, R. & Bosserhoff, A.-K. Integrin signaling in malignant melanoma. Cancer Metastasis Rev. 24, 195–222 (2005).

- Lagarkova, M. A., Volchkov, P. Y., Lyakisheva, A. V, Philonenko, E. S. & Kiselev, S. L. Diverse epigenetic profile of novel human embryonic stem cell lines report. Cell Cycle 5, 416–420 (2006).

- Larue, L. & Beermann, F. Cutaneous melanoma in genetically modified animals. Pigment Cell Res. 20, 485–497 (2007).

- Lázár-Molnár, E., Hegyesi, H., Tóth, S. & Falus, a. Autocrine and paracrine regulation by cytokines and growth factors in melanoma. Cytokine 12, 547–554 (2000).

- Lee, N., Barthel, S. R. & Schatton, T. Melanoma stem cells and metastasis: mimicking hematopoietic cell trafficking? Lab. Invest. 94, 13–30 (2014).

- Li, F. Z., Dhillon, A. S., Anderson, R. L., McArthur, G. & Ferrao, P. T. Phenotype Switching in Melanoma: Implications for Progression and Therapy. Front. Oncol. 5, 1–7 (2015).

- Longo-Imedio, M. I., Longo, N., Treviño, I., Lázaro, P. & Sánchez-Mateos, P. Clinical significance of CXCR3 and CXCR4 expression in primary melanoma. Int. J. Cancer 117, 861–865 (2005).

- Lu, J.-W. et al. Overexpression of Thy1/CD90 in human hepatocellular carcinoma is associated with HBV infection and poor prognosis. Acta Histochem. 113, 833–838 (2011).

- Ludwig, A, Ehlert, J. E., Flad, H. D. & Brandt, E. Identification of distinct surface-expressed and intracellular CXC-chemokine receptor 2 glycoforms in neutrophils: N-glycosylation is essential for maintenance of receptor surface expression. J. Immunol. 165, 1044–1052 (2000).

- Meijer, J., Zeelenberg, I. S., Sipos, B. & Roos, E. The CXCR5 chemokine receptor is expressed by carcinoma cells and promotes growth of colon carcinoma in the liver. Cancer Res. 66, 9576–9582 (2006).

- Miettinen, M. & Lasota, J. KIT (CD117): a review on expression in normal and neoplastic tissues, and mutations and their clinicopathologic correlation. Appl. Immunohistochem. Mol. Morphol. 13, 205–220 (2005).

- Mihic-Probst, D. et al. Consistent expression of the stem cell renewal factor BMI-1 in primary and metastatic melanoma. Int. J. Cancer 121, 1764–1770 (2007).

- Mocellin, S., Rossi, C. R. & Marincola, F. M. Quantitative real-time PCR in cancer research. Arch. Immunol. Ther. Exp. 51, 301–313 (2003).

- Monteagudo, C., Martin, J. M., Jorda, E. & Llombart-Bosch, a. CXCR3 chemokine receptor immunoreactivity in primary cutaneous malignant melanoma: correlation with clinicopathological prognostic factors. J. Clin. Pathol. 60, 596–599 (2007).

- Monteagudo, C. et al. CCL27-CCR10 and CXCL12-CXCR4 chemokine ligand-receptor mRNA expression ratio: new predictive factors of tumor progression in cutaneous malignant melanoma. Clin. Exp. Metastasis 29, 625–637 (2012).

- Monzani, E. et al. Melanoma contains CD133 and ABCG2 positive cells with enhanced tumourigenic potential. Eur. J. Cancer 43, 935–946 (2007).

- Müller, A et al. Involvement of chemokine receptors in breast cancer metastasis. Nature 410, 50–56 (2001).
- Murakami, T., Cardones, A. R. & Hwang, S. T. Chemokine receptors and melanoma metastasis. J. Dermatol. Sci. 36, 71–78 (2004).
- Na, I.-K. et al. Nuclear expression of CXCR4 in tumor cells of non-small cell lung cancer is correlated with lymph node metastasis. Hum. Pathol. 39, 1751–1755 (2008).
- Notohamiprodjo, M. et al. CCR10 is expressed in cutaneous T-cell lymphoma. Int. J. Cancer 115, 641–647 (2005).
- Nowell, P. The clonal evolution of tumor cell populations. Science. 194, 23–28 (1976).
- O'Connor, J. E. et al. The relevance of flow cytometry for biochemical analysis. IUBMB Life 51, 231–239 (2001).
- Onai, N. et al. Pivotal role of CCL25 (TECK)-CCR9 in the formation of gut cryptopatches and consequent appearance of intestinal intraepithelial T lymphocytes. Int. Immunol. 14, 687–694 (2002).
- Parmiani, G. et al. Immunotherapy of melanoma. Semin. Cancer Biol. 13, 391–400 (2003).
- Perego, M. et al. Heterogeneous phenotype of human melanoma cells with in vitro and in vivo features of tumor-initiating cells. J. Invest. Dermatol. 130, 1877–1886 (2010).
- Piras, F. et al. The stem cell marker nestin predicts poor prognosis in human melanoma. Oncol. Rep. 23, 17–24 (2009).

- Proksch, E., Brandner, J. M. & Jensen, J.-M. The skin: an indispensable barrier. Exp. Dermatol. 17, 1063–1072 (2008).
- Rapanotti, M. C. et al. Melanoma-associated markers expression in blood: MUC-18 is associated with advanced stages in melanoma patients. Br. J. Dermatol. 160, 338–344 (2009).
- Refaeli, Y., Bhoumik, A., Roop, D. R. & Ronai, Z. a. Melanoma-initiating cells: a compass needed. EMBO Rep. 10, 965–972 (2009).
- Rege, T. A & Hagood, J. S. Thy-1 as a regulator of cell-cell and cell-matrix interactions in axon regeneration, apoptosis, adhesion, migration, cancer, and fibrosis. FASEB J. 20, 1045–1054 (2006).
- Reya, T., Morrison, S. J., Clarke, M. F. & Weissman, I. L. Stem cells, cancer, and cancer stem cells. Nature 414, 105–111 (2001).
- Richmond, A., Yang, J. & Su, Y. The good and the bad of chemokines/chemokine receptors in melanoma. Pigment Cell Melanoma Res. 22, 175–186 (2009).
- Robinson, J. et al. The European searchable tumour line database. Cancer Immunol. Immunother. 58, 1501–1506 (2009).
- Robledo, M. M. et al. Expression of functional chemokine receptors CXCR3 and CXCR4 on human melanoma cells. J. Biol. Chem. 276, 45098–45105 (2001).
- Sabatino, M. et al. Conservation of Genetic Alterations in Recurrent Melanoma Supports the Melanoma Stem Cell Hypothesis. Cancer Res. 68, 122–131 (2008).

- Sarkadi, B., Homolya, L., Szakács, G. & Váradi, A. Human multidrug resistance ABCB and ABCG transporters: participation in a chemoimmunity defense system. Physiol. Rev. 86, 1179–1236 (2006).

- Satyamoorthy, K., Muyrers, J., Meier, F., Patel, D. & Herlyn, M. Mel-CAM-specific genetic suppressor elements inhibit melanoma growth and invasion through loss of gap junctional communication. Oncogene 20, 4676–4684 (2001).

- Schaeuble, K. et al. Ubiquitylation of the chemokine receptor CCR7 enables efficient receptor recycling and cell migration. J. Cell Sci. 4463-4474 (2012).

- Scharenberg, C. W., Harkey, M. a. & Torok-Storb, B. The ABCG2 transporter is an efficient Hoechst 33342 efflux pump and is preferentially expressed by immature human hematopoietic progenitors. Blood 99, 507–512 (2002).

- Schatton, T. et al. Identification of cells initiating human melanomas. Nature 451, 345–349 (2008).

- Schmidt, P. et al. Eradication of melanomas by targeted elimination of a minor subset of tumor cells. Proc. Natl. Acad. Sci. U. S. A. 108, 2474–2479 (2011).

- Shimizu, S., Brown, M., Sengupta, R., Penfold, M. E. & Meucci, O. CXCR7 protein expression in human adult brain and differentiated neurons. PLoS One 6, e20680 (2011).

- Shoemaker, R. H. The NCI60 human tumour cell line anticancer drug screen. Nat. Rev. Cancer 6, 813–823 (2006).

- Shuff, J. H., Siker, M. L., Daly, M. D. & Schultz, C. J. Role of Radiation Therapy in Cutaneous Melanoma. Clin. Plast. Surg. 37, 147–160 (2010).
- Simonetti, O. et al. Potential role of CCL27 and CCR10 expression in melanoma progression and immune escape. Eur. J. Cancer 42, 1181–1187 (2006).
- Smith, L. M., Nesterova, A., Alley, S. C., Torgov, M. Y. & Carter, P. J. Potent cytotoxicity of an auristatin-containing antibody-drug conjugate targeting melanoma cells expressing melanotransferrin/p97. Mol. Cancer Ther. 5, 1474–1482 (2006).
- Speetjens, F. M. et al. Nuclear localization of CXCR4 determines prognosis for colorectal cancer patients. Cancer Microenviron. 2, 1–7 (2009).
- Steeg, P. S. Tumor metastasis: mechanistic insights and clinical challenges. Nat. Med. 12, 895–904 (2006).
- Sun, X. et al. CXCL12 / CXCR4 / CXCR7 chemokine axis and cancer progression. Cancer Metastasis Rev. 29, 709–722 (2010).
- Tan, C. M., Brady, A. E., Nickols, H. H., Wang, Q. & Limbird, L. E. Membrane trafficking of G protein-coupled receptors. Annu. Rev. Pharmacol. Toxicol. 44, 559–609 (2004).
- True, L. D. et al. CD90/THY1 is overexpressed in prostate cancer-associated fibroblasts and could serve as a cancer biomarker. Mod. Pathol. 23, 1346–1356 (2010).
- Urosevic, M., Braun, B., Willers, J., Burg, G. & Dummer, R. Expression of melanoma-associated antigens in melanoma cell cultures. Exp. Dermatol. 14, 491–497 (2005).

- van Staveren, W. C. G. et al. Human cancer cell lines: Experimental models for cancer cells in situ? For cancer stem cells? Biochim. Biophys. Acta - Rev. Cancer 1795, 92–103 (2009).

- Vandercappellen, J., Van Damme, J. & Struyf, S. The role of CXC chemokines and their receptors in cancer. Cancer Lett. 267, 226–244 (2008).

- Vandesompele, J. et al. Accurate normalization of real-time quantitative RT-PCR data by geometric averaging of multiple internal control genes. Genome Biol. 3, research0034 (2002).

- Visvader, J. E. & Lindeman, G. J. Cancer stem cells in solid tumours: accumulating evidence and unresolved questions. Nat. Rev. Cancer 8, 755–768 (2008).

- Weinstein, D., Leininger, J., Hamby, C. & Safai, B. Diagnostic and Prognostic Biomarkers in Melanoma. Journal of clinica and aesthetic dermatology. 7, 13–24 (2014).

- Winnepenninckx, Véronique ; De Vos, Rita; Stas, Marguerite; van den Oord, J. J. New Phenotypical and Ultrastructural Findings in Spindle Cell (Desmoplastic/Neurotropic) Melanoma. Appl. Immunohistochem. Mol. Morphol. 11, 319–325 (2003).

- Woodman, S. E. & Davies, M. a. Targeting KIT in melanoma: a paradigm of molecular medicine and targeted therapeutics. Biochem. Pharmacol. 80, 568–574 (2010).

- Yasuoka, H. et al. Cytoplasmic CXCR4 expression in breast cancer: induction by nitric oxide and correlation with lymph node metastasis and poor prognosis. BMC Cancer 8, 340 (2008).

- Zabierowski, S. E. & Herlyn, M. Learning the ABCs of melanoma-initiating cells. Cancer Cell 13, 185–187 (2008a).

- Zabierowski, S. E. & Herlyn, M. Melanoma Stem Cells: The Dark Seed of Melanoma. J. Clin. Oncol. 26, 2890–2894 (2008b).

- Zaidi, M. R., Day, C.-P. & Merlino, G. From UVs to Metastases: Modeling Melanoma Initiation and Progression in the Mouse. J. Invest. Dermatol. 128, 2381–2391 (2008).

- Zhao, S., Guo, Y., Sheng, Q. & Shyr, Y. Advanced Heat Map and Clustering Analysis Using Heatmap3 (2014).

- Zimmerer, R. M. et al. Functional features of cancer stem cells in melanoma cell lines. Cancer Cell Int. 13, 78 (2013).

Resumen

Introducción

El **melanoma** es el tipo de cáncer de piel más agresivo. Ocurre en los melanocitos, células productoras de melanina ubicadas en la capa inferior de la epidermis, en la piel. El melanoma puede propagarse a través del tejido creciendo en áreas cercanas. Cuando las células tumorales se separan del tumor primario y viajan a través del sistema linfático o de la sangre para otras partes del cuerpo donde se establecen y empiezan a formar un tumor metastásico, se denomina **metástasis**. La metástasis generalizada es la principal causa de muerte en el melanoma.

Los cánceres surgen a través de la adquisición de mutaciones que suprimen la senescencia y promueven la división celular, pero hay distintos modelos para explicar el crecimiento del tumor. El modelo clonal o estocástico afirma que se producen cambios (epi)genéticos en todas las células tumorales al largo del tiempo, y que hay una selección natural gradual de las células más aptas y más agresivas. El **modelo de las células madre tumorales** sugiere que sólo una subpoblación de células dentro del tumor, las células madre tumorales, o en el caso del melanoma, las células iniciadores del melanoma, tienen la capacidad de regenerarse y mantener un tumor *in vivo*. La mayor parte de la población de células tumorales es heterogénea, no comparte estas propiedades y carece de la capacidad de ser tumorigénicos.

Un proceso importante para la progresión del melanoma y la ocurrencia de metástasis es la **transición epitelio-mesenquica**. Este proceso se caracteriza por la pérdida de adhesión celular, la represión en la expresión de E-cadherina resultando en el aumento de la movilidad celular.

En el melanoma la metástasis ocurre preferencialmente hacia el cerebro, pulmón, hígado y piel. Esta selectividad de la metástasis por determinados órganos viene determinada por consideraciones anatómicas de flujo

sanguíneo, por propiedades intrínsecas de las células tumorales y por propiedades intrínsecas del órgano diana. La interacción **quimiocina-receptor** puede inducir señales que no solo actúen sobre la movilidad celular hacia un gradiente, sino que las quimiocinas pueden jugar papeles alternativos sobre la adhesión de las células tumorales, la invasión, la supervivencia, el crecimiento tumoral y la angiogénesis.

El melanoma es un tumor heterogéneo a nivel genético, morfológico y antigénico. Las **líneas celulares** muestran células con distinta morfología incluyendo formas ovales pequeñas, fusiformes, poligonales planas y grandes con formas dendríticas. La expresión antigénica es también muy heterogénea, pudiendo distinguirse subpoblaciones celulares de distinto tamaño con distintos marcadores antigénicos. Esta expresión puede ser dinámica, variando con la superficie de cultivo celular, cambios de medio, densidad celular y duración del cultivo. Otro modelo comúnmente usado en el estudio del melanoma es un **modelo animal de xenotransplante**. En este modelo, muestras humanas de melanoma (provenientes de pacientes o de líneas celulares) son trasplantadas en ratones atímicos inmunodeficientes que, al tener un sistema inmunitario defectuoso, permiten el crecimiento de las células tumorales y la expresión de sus propiedades.

Hipótesis y Objetivos

El melanoma cutáneo humano es una neoplasia altamente heterogénea compuesta por subpoblaciones de células tumorales con fenotipos moleculares y biológicos distintos. Estas distintas subpoblaciones son la base de una complejidad biológica que incluye los fenómenos de auto-renovación, diferenciación, iniciación tumoral, progresión y resistencia a terapia.

En este trabajo se plantean las siguientes **hipótesis**:

La utilización de líneas celulares de melanoma humano permite determinar la heterogeneidad intra- e inter-tumoral mediante la cuantificación de las proteínas que intervienen en los procesos anteriormente mencionados utilizando técnicas cuantitativas de citometría de flujo y PCR-cuantitativa en líneas celulares procedentes del tumor primario o de la metástasis.

El xenotransplante de las líneas celulares a ratones atímicos inmunodeficientes permite establecer las subpoblaciones celulares y variaciones de expresión génica que se seleccionen preferentemente en los tumores, cuando estos se desarrollan en ratones dentro de un microambiente más similar al que existía en el paciente afectado.

En este marco, se proponen los siguientes **objetivos**:

- Caracterizar fenotípica y funcionalmente, mediante análisis citómico y cuantificación de la expresión génica, los antígenos de melanoma, marcadores de células madre tumorales, de pluripotencia y del proceso de transición epitelio mesenquina, en distintas líneas celulares de melanoma humano, obtenidas a partir de melanomas primarios y de metástasis.

- Caracterizar fenotípica y funcionalmente, mediante análisis citómico y cuantificación de la expresión génica, los sistemas formados por los receptores de quimiocinas CXCR3, CXCR4, CXCR7, CCR7 y CCR10 y respectivas quimiocinas ligando, en distintas líneas celulares de melanoma humano, obtenidas a partir de melanomas primarios y de metástasis.

- Comprender las variaciones fenotípicas y de expresión génica que se seleccionan preferentemente en los tumores, cuando estos se desarrollan en ratones sobre la presión del microambiente.

- Correlacionar los resultados obtenidos con el origen del melanoma, primario o metástasis.

Metodología

1. Muestras biológicas

- *Líneas celulares de melanoma humano:* MeWo, A-375, SK-MEL-2, SK-MEL-28, Malme-3M (ATCC); WM-266, WM-115 (ECACC); Mel-HO, Mel-Juso, IPC-298, IGR37, IGR39 (DSMZ) y Mel-RC08 (Departamento de Patología, Universitad de Valencia). WM-115, Mel-HO, Mel-Juso, IPC-298 y IGR39 son líneas establecidas a partir de tumores primarios mientras que MeWo, A-375, SK-MEL-2, SK-MEL-28, Malme-3M, WM-266, IGR37 y Mel-RC08 son líneas establecidas a partir de tumores primarios.

- *Xenotransplantes (de WM-115 y WM-266) y sus líneas derivadas.*

2. Cuantificación de proteínas por citometría de flujo:

- Caracterización inmunofenotipica por citometría de flujo de antígenos de melanoma, marcadores de células madre tumorales, característicos de la transición epitelio-mesenquima y de quimiocinas y sus receptores (Tabla 2A y 2B).

- Análisis de la *side population*.

3. Cuantificación de la expresión génica, por PCR cuantitativa:

- Aislamiento y control de calidad del ARN aislado de las líneas celulares.

- Cuantificación de los distintos genes listados (Tabla 5).

4. Análisis estadístico:

- El análisis estadístico de las cuantificaciones de proteína por citometría de flujo se hijo con test t de student.

- Los datos de expresión génica se refieren a ΔCts y se presentan en heatmaps producidos con el programa R (package Heatmap3).

- La correlación entre los datos de cuantificación de proteína y de expresión génica se realizaron con Graphpad prism usando la correlación de Spearman.

Resultados

Se han caracterizado 13 líneas de melanoma humano, 5 con origen primario y 8 con origen en metástasis de distintas localizaciones (piel, cerebro, nódulos linfáticos y pulmón).

Hemos encontrado un perfil de expresión de antígenos de melanoma, marcadores de células madre tumorales, característicos de la transición epitelio-mesénquima y de quimiocinas muy heterogéneo. Además, analizando el perfil de todos los genes cuantificados es perceptible que no hay un patrón específico de expresión génica que caracterice y distinga las células primarias de las metastáticas. Al revés, se puede apreciar la variabilidad y heterogeneidad que existe entre las distintas líneas estudiadas.

Con relación al sistema quimiocinas-receptor, comprobamos que la expresión de receptores es intracelular y no ocurre en la superficie de las células. Verificamos también que los niveles de expresión de los receptores de quimiocinas y sus ligandos sufren variaciones dinámicas tras la xenotrasplantación, que son distintas dependiendo del origen de la línea trasplantada. Sin embargo, no se ha detectad la expresión de superficie de los receptores de quimiocinas, como esperado.

Analizando colectivamente los datos relativos al xenotransplante (i.e., WM115 vs WM115-CX-SC and WM115-CX-IM), se pueden apreciar importantes cambios a nivel de proteína y de expresión génica. La subpoblación ABCB1+ ha incrementado en ambas las líneas y con relación a la SP se produjo un aumento en ambas las líneas, más significativo en WM-115-CX-IM (Table 20). Este se puede deber a un gran aumento en la expresión génica de ABCG2. Además, la línea parental no tenía una subpoblación CD90+ que apareció en las dos líneas trasplantadas. De igual forma se produjo un aumento de la expresión génica de CD117 y CD133 (Table 21, Figure 27). También se produjeron aumentos en la expresión de genes de pluripotencia y característicos de la transición epitélio-mesenquima (en concreto de algunas moléculas de adhesión). Los patrones de expresión génica fueron distintos dependiendo del local de inoculación de las células en el ratón (subcutáneo o intramuscular).

Conclusiones

- Las técnicas cuantitativas de citometría de flujo y de PCR en tiempo real permitieron caracterizar el perfil de expresión de distintos marcadores, a nivel proteico y genético, en distintas líneas celulares de melanoma humano, obtenidas a partir de melanomas primarios y de metástasis, reflejando la heterogeneidad del melanoma humano.

- Los marcadores estudiados no se correlacionan con el origen del tumor (primario o metástasis).

- La presión selectiva de microambiente del ratón produce importantes cambios en los patrones de expresión génica y de proteína, que son distintos dependiendo del local de inoculación de las células en el ratón (subcutáneo o intramuscular).